IMPACTS OF THE DEEPWATER HORIZON OIL SPILL ON REPRODUCTION AND ONTOGENY OF GULF KILLIFISH (FUNDULUS GRANDIS)

A Dissertation

Submitted to the Graduate Faculty of the
Louisiana State University and
Agricultural and Mechanical College
In partial fulfillment of the
Requirements for the degree of
Doctor of Philosophy

in

The Department of Biological Sciences

by
Charles Alexander Brown
B.S., Augusta State University, 2008
M.S., Louisiana State University, 2011
May 2020

ACKNOWLEDGEMENTS

I would first like to thank Dr. Fernando Galvez for accepting me into his lab and taking me under his fin. Under his guidance, I learned a lot about science, planning an experiment, organization, and writing. I also learned a lot about the differences between Americans and Canadians, about hockey (specifically, the Leafs), and that if you know your advisor well enough, you can communicate entire thoughts with a single look. Thank you to my committee members, Drs. Chris Green, Mike Kaller, and Mike Polito for your guidance, direction, and open door policies for quick chats. Thank you to my lab mates, Chelsea Hess (never forget the Summer of 15) and Charles "C2C" Campbell, your help with my projects and willingness to be sounding boards to my ideas are greatly appreciated. Thank you to all of my friends in Biological Sciences, Oceanography, and Renewable Natural Resources.

A very special thanks to my family, who were always eager to listen to what I had been working on and were always a phone call away when I needed to chat. I would like to thank my mom, Delaine, and dad, Charlie, for encouraging my pursuits and putting up with the "strange child" that I was. I would like to thank my sister, Ashley, for teaching me to not be a big dork as a kid. And I would like to thank my grandfather, Charlie, or more commonly known as "Paw", for the continuous love and support throughout all of my pursuits. Lastly, I would like to thank Helen Seder for her love, patience, nights of Bananagrams, general shenanigans, and introducing me to Mac and Chester.

TABLE OF CONTENTS

LIST OF TABLES

LIST OF FIGURES

LIST OF ABBREVIATIONS

AHR……..aryl hydrocarbon receptor

AR…….adsorption ratio

ARNT……aryl hydrocarbon nuclear translocator

BPM…….beats per minute

CEWAF……...chemically enhanced water accommodated fraction

CYP1A……cytochrome P450, family 1, member A

DHOS……Deepwater Horizon oil spill

DOSS……..dioctyl sulfosuccinate

DPF……..days post fertilization

ER……...estrogen receptor

ET50…….median time to effect

EVOS…….Exxon Valdez oil spill

GOM……Gulf of Mexico

HEWAF……..high energy water accommodated fraction

HMW…….high molecular weight

K_{OW}……..octanol/water partition coefficient

LC50……..median lethal concentration

LMW……...low molecular weight

MVD……mean volume diameter

NRDA……..Natural Resource Damage Assessment

PAH……...polycyclic aromatic hydrocarbon

PC…….parental control

PE……parental exposed

SCAT……...shoreline cleanup and assessment technique

TCDD……2,3,7,8-tetrachlorodibenzodioxin

TDD…….total droplet density

WAF……..water accommodated fraction of oil

WB……..whole body

XRE……..xenobiotic response element

ABSTRACT

On April 20, 2010, the Deepwater Horizon oil spill released an estimated 779 million liters of Macondo-252 crude oil into the Gulf of Mexico, making it the largest marine oil spill in history. Over a thousand kilometers of marshland that many species of fish use as a spawning grounds and nurseries was oiled, exposing breeding adult fish and their offspring to oil. My dissertation investigates the impacts of the Deepwater Horizon oil spill and associated remediation efforts on the reproduction and ontogeny of a sentinel ecotoxicological species, the Gulf killifish (*Fundulus grandis*). Concerns were raised regarding use of freshwater diversion release and application of chemical dispersants for coastal remediation efforts as the effects of their concurrent use on coastal ecosystems had not been investigated. My research found that chemical dispersants become toxic to Gulf killifish during normally benign acute osmotic challenges through disruption of osmoregulatory physiology. Toxicity increases throughout ontogeny, concomitant with development of the gill as an osmoregulatory organ. Next, a novel high throughput methodology was developed to investigate the interaction of crude oil droplets with Gulf killifish embryos and found that binding characteristics of oil droplets to chorions differ based on if they were physically or chemically dispersed, and on chorionic morphology. Assessing binding characteristics of oil droplets to chorions is important in understanding the toxicity of crude oil as toxic components may be transmitted to embryos through direct adsorption of droplets. Lastly, intergenerational effects of oil exposure were investigated through exposure of adult Gulf killifish and their offspring to oil. Oil exposure reduced the reproductive capacity of adult fish and sensitized offspring to additional oil toxicity during embryogenesis. Population level differences were also observed as a population of killifish collected three years following Deepwater Horizon oiling of their habitat possessed increased oil sensitivity compared to a reference population,

suggesting that oil spills continue to impact fish well beyond initial oiling. Overall, these results provide a comprehensive characterization of the damage imposed by the Deepwater Horizon oil spill and provides insight into mechanisms of toxicity that should be considered for future spills.

CHAPTER 1
INTRODUCTION

Scope of Injury Resulting from Oil Spills

Assessment of ecosystem injury resulting from oil spills has only recently garnered attention relative to the long history of reliance on crude oil. In 2018 alone, there was an estimated 5.2 trillion liters of crude oil extracted worldwide and this amount is only expected to increase as energy demand rises (International Association of Oil and Gas Producers, 2019). Oil exploration is being driven into more remote and extreme environments, and associated with this pattern is an increase in the frequency of oil spill disasters. Worldwide, an estimated 3,469 spills of over 159,000 liters have occurred since 1964. Of these, over a 1,000 spills have occurred in the United States and 17 in the Gulf of Mexico (ABSG Consulting Inc., 2016). Each oil spill is unique, with the chemistry of the source crude oil, the geology and environmental conditions at the site of a spill, and other factors dictating the remediation efforts to mitigate resource damage. For instance, the application of chemical dispersants to disrupt surface floating oil slicks is limited by salinity constrains, and other alternatives are regionally contextual, such as the release of fresh water from salinity control structures, when available, under the intention of preventing encroaching oil from reaching sensitive habitats. Prevention of injury to these habitats, such as coastal marshes, is paramount when considering oil spill mitigation strategies. However, these strategies are not always fully successful and may result in the inevitable oiling of ecosystems. Therefore, oil spills are also associated with a program to assess the damage to natural resources.

The Deepwater Horizon Oil Spill

On April 20, 2010, an exploratory well within the Macondo Canyon Block 252 prospect ruptured following the explosion of the Deepwater Horizon oil platform. Over a span of 87 days,

an estimated 779 million liters of Macondo-252 light sweet crude oil was released into the Gulf of Mexico making it the largest marine oil spill in history (Lehr et al., 2010; McNutt et al., 2012; Nixon et al., 2016). Both during the spill and after the well was capped, multiple remediation efforts were performed to limit the amount of oil reaching sensitive coastal habitats: controlled burns of oil slicks provided a rapid and effective method in removing oil slicks from the water surface, although at the cost of toxic soot residue released into the atmosphere; floating booms were deployed adjacent to coastal marsh to limited success and salinity control structures in southern Louisiana were opened to divert fresh water from the Mississippi River to estuaries, albeit at the expense of damaging protracted reductions in regional salinity (< 5 g/L; Deepwater Horizon Natural Resource Damage Assessment Trustees, 2016).

Protection of coastal marshland in Louisiana was paramount, given its important ecological, economical, and societal value (Chesney et al. 2000); however, by the time of final capping on July 15, 2010, the spilt oil had created a visible oil slick of 112,146 km^2 and oiled 2,092 km of shoreline along the northern Gulf of Mexico (GOM) from Texas to Florida (Deepwater Horizon Natural Resource Damage Assessment Trustees, 2016). Approximately 52% of this land was classified as marsh, with the majority of the 19,960 tons of crude oil deposited along the Gulf of Mexico coasts of Louisiana and Mississippi (*for review, see* Lee et al., 2015). Oil contamination here peaked in late June 2010 and was no longer apparent on surface waters by October 2010; however, 507 km of marshland was documented as possessing oil-sediment aggregates two years following the spill (Michel et al., 2013). Oiling of Louisiana marsh sediments was highly variable at nine months after the Deepwater Horizon Oil Spill (DHOS) with total hydrocarbon concentrations ranging from 3,900 mg/kg at a location off the southern coast of the Mississippi River delta (South Pass Spit, LA; 28° 59’ 5” N, 89° 10’ 18” W) to 706,000 mg/kg

off the northeast coast of the Mississippi River delta (Black Hole, LA; 29° 11’ 45” N, 89° 2’ 16” W; Brown-Peterson et al., 2017). Hydrocarbon concentrations were even found to vary up to 10-fold along a 10 m transect of Louisiana marshland, indicating the highly variable contamination to oil (Turner et al., 2014). Contamination of these sediments was found to persist long after initial oiling. Adsorption of oil to organic materials suspended in the water column of coastal environments results in the sedimentation of oil, exposing oil to increasingly anaerobic conditions and ultimately reducing biodegradation rates of complex hydrocarbons (Haritash and Kaushik, 2009; Jonker et al., 2006; McGenity, 2014). Consequently, the continued presence of oil in the marsh environment is likely to contribute to long-term ecological impacts through hydrocarbon sedimentation. Reduced plant biomass and toxicity to embryonic fish was observed when exposed to DHOS oiled sediments long after oil was no longer visible, suggesting that contaminated sediments remained toxic for a long period of time (Dubansky et al., 2013; Silliman et al., 2012). Sediments collected in the following year contained concentrations of oil sufficient to activate biomarkers of oil exposure and elicit toxic effects to embryonic fish under laboratory conditions, indicating the recalcitrance of oil to degradation but continued impacts to aquatic biota (Brown-Peterson et al., 2017; Dubansky et al., 2013). Persistent environmental contamination would subsequently have multi-generational impacts for non-migratory species. Furthermore, impacted ecosystems would likely possess reduced resilience in the face of future natural or anthropogenic disasters. For example, in addition to the deposition of environmentally persistent hydrocarbons, shoreline erosion of saltmarshes impacted the DHOS oil increased by 150% (~ 3.0 m per year) compared to erosion rates at reference sites (0.8 to 1.3 m per year; Silliman et al., 2012), hastening an already rapid loss of coastal habitat.

The salt marshes, wetlands, and delta ecosystems impacted by the DHOS provide considerable ecological services to Gulf of Mexico fisheries, generating an estimated $2.5 billion in commercial and recreational fisheries in 2009 (Waring et al., 2009). These coastal habitats contribute to the regional food web that supports coastal and marine ecosystems (Chesney et al., 2000). Marshlands of the GOM provide excellent spawning and nursery grounds for many species of fish through their large area of habitat and high rate of primary production (Nordlie, 2000; Silliman and Zieman, 2001). Although species utilize the marsh as a spawning ground at different times of the year, peak spawning of many fish species occur during the spring and fall months when marsh productivity is at its highest (Greeley Jr and MacGregor III, 1983; Nordlie, 2000; Silliman and Zieman, 2001), which coincided with the peak oiling of the DHOS in late June of 2010, potentially exposing multiple life stages of fish to crude oil toxicants.

Environmental Injury from Response Efforts

As previously mentioned, different methods were used to protect coastal marshes. Amongst the two most controversial were the application of dispersants and extended release of fresh water into coastal habitats. Chemical dispersants, such as Corexit 9527A and Corexit 9500A (termed hereon solely as Corexit), are a complex mixture of chemicals whose primary purpose is to lower the interfacial tension between oil and water, ultimately allowing for greater slick dispersion with less energy than would otherwise be needed (Landry et al., 2019). The lowering of interfacial tension between the two phases is accomplished through the entrainment of an amphipathic surfactant at the surface of the oil that allows for the polar head of the surfactant to interact with the aqueous phase while the surfactants hydrophobic tails interact with the oil phase. However, Corexit is a marine dispersant (*e.g.* legislated for use at distances greater than 5.5 km from the coast) that has been found to be ineffective in fresh water (Houma ICP Aerial Dispersant

Group, 2010; Landry et al., 2019). This decision also reduced the likelihood that chemically-dispersed oil, which is known to be more toxic than crude oil alone, would impact coastal marsh ecosystems (Kuhl et al., 2013; Landry et al., 2019; Milinkovitch et al., 2011; Ramachandran et al., 2006). Corexit toxicity is generally considered low to marine organisms, although data characterizing Corexit toxicity in fluctuating salinities is limited (George-Ares and Clark, 2000). However, salinity control structures in Louisiana (*i.e.*, Davis Pond, Caernarvon, Bayou Lamouque, West Pointe a la Hache, Violet Siphon, White Ditch, Naomi Siphon, Ostrica Lock, and Bohemia), used to regulate estuarine salinities at the mouth of the Mississippi River, were opened to their near maximum capacity during peak oiling of the DHOS to flush encroaching oil slicks away from marshlands, rapidly reducing coastal water salinities. The diversions at Caernarvon and Davis Pond, which are the two largest structures on the coast, released up to 283,168 liters per second for six weeks, into Barataria Bay and Black Bay / Breton Sound (Deepwater Horizon Natural Resource Damage Assessment Trustees, 2016). While their effectiveness at reducing coastal oiling was considered questionable and the prolonged reduction in salinity (< 5 g/L) devastated populations of economically valuable eastern oyster (*Crassostrea virginica*, Powers et al., 2017; Deepwater Horizon Natural Resource Damage Assessment Trustees, 2016), the confluence of dispersant application and acute reductions in coastal water salinities had not been previously investigated.

Exposure to dispersants or to surfactants alone have been demonstrated to cause toxicity in several aquatic species at sufficiently high concentrations, including Gulf killifish (*Fundulus grandis*, Bodinier et al., 2014; George-Ares and Clark, 2000). This toxicity is believed to occur when surfactants (*e.g.* dioctyl sulfosuccinate [DOSS], the primary surfactant in Corexit) interact with and destabilize the biological membranes of animals (Cserháti et al., 2002; Heerklotz, 2008;

John et al., 2016). Early life-stage exposure to DOSS increased time-to-hatch and decreased hatch success in embryonic killifish and impaired expression of osmoregulatory proteins in larval killifish gills (Bodinier et al., 2014). Furthermore, surfactant exposure to the gills of adult fish results in cellular and tissue damage that may lead to tissue necrosis (Agamy, 2013; Dasgupta et al., 2018; Rosety-Rodríguez et al., 2002). Consequently, gill damage would impair biological processes associated with gill function, such as osmoregulation, making it much less likely that a fish could handle environmental perturbations like osmotic challenges. So, chemical dispersant induced disruptions in osmoregulatory capabilities would have severe physiological consequences on fish resident to salt marshes in the Gulf of Mexico where tidal fluctuations, extreme storm events, and riverine discharge can rapidly alter environmental salinity (Sklar and Browder, 1998; Teal et al., 1986). Given the role of the gill as an osmoregulatory organ, dispersant exposure may disrupt osmoregulatory processes of the gill and compromise the ability of fish to maintain osmotic balance when subjected to variations in environmental salinity (Brown et al., 2019).

Chemical Properties of Oil

A central tenet of oil spill research is that no two oils are identical. Crude oil consists of a heterogeneous mixture of structurally diverse constituents, the concentrations of which vary greatly between different sources of oil and provide diversity in the physical characteristics of different oils (Tissot and Welte, 1984). Crude oil constituents can be classified according to the SARA model as: saturated aliphatic hydrocarbons, aromatic hydrocarbons, resins, and asphaltenes (Leahy and Colwell, 1990), the relative proportions of which are used to characterize oil types. Saturated aliphatic hydrocarbons are composed of chains of single bonds between carbon atoms with the maximum possible number of hydrogen atoms and may exist in gas form at low molecular weights (≤ C4; less than four carbon atoms), in liquid form at medium molecular

weights (C5 – C17), or as waxy solids at high molecular weights (>C18), and possess very low aquatic toxicity compared to other constituents in the oil (Leahy and Colwell, 1990). While straight chained aliphatic constituents are readily biodegradable, branched and non-aromatic polycyclic derivatives, such as sterane and hopane, are resistant to biodegradation (Speight and El-Gendy, 2017). Aromatic hydrocarbons form cyclic, planar structures that are composed of a varying numbers of ring structures, ranging from mono-aromatic benzene to two or more fused ring structures, which are typically termed polycyclic aromatic hydrocarbons (PAHs), and are considered the most toxic component of crude oil (Di Toro et al., 2007; Hodson, 2017). Resins possess aromatic or polar heads with aliphatic tails, and are considered precursors to asphaltenes, which are characterized as possessing large aromatic cores with aliphatic tails and heteroatoms on the edges of the aromatic core (Abdel-Raouf, 2012). Additionally, asphaltene content plays a large role in oil viscosity and density due, in part, to the large size of asphaltene molecules (mean weight of approximately 1,200 Da; Lee et al., 2015). Although they are non-toxic, previous studies have shown that resins and asphaltenes are persistent in aquatic environments due to their low water solubility and interact to form aggregates that stabilize crude oil droplet structure in aqueous media (Mousavi et al., 2016).

Predictions of PAH toxicity is most often made through assessment of their water solubility as this characterization best predicts their bioavailability. The most common method for estimating the water solubility of a PAH is through measurement of its octanol-water coefficient (K_{OW}), which represents the concentration ratio of a molecule dissolved into the *n*-octanol (hydrophobic) phase relative to the water (hydrophilic) phase (Sverdrup et al., 2002). Following the mixing of oil in water, PAHs with log K_{OW} coefficients < 5-6 are readily soluble in water and bioavaiable to aquatic organisms, while hydrophobic PAHs with log K_{OW} coefficients > 5-6

remain associated with oil, but more effectively interact with the lipid portions of biological membranes (Di Toro et al., 2007; Sørensen et al., 2017). In general, low molecular weight (LMW) PAHs with two to three aromatic rings (< C16) are considerably more water soluble than high molecular weight (HMW) PAHs with four or more aromatic rings (> C16), although the log K_{OW} of a PAH, and thus its water solubility, can vary with the degree of alkylation and the presence of polar heteroatoms (Lee et al., 2015; Mackay and Shiu, 1977). These classifications are important when considering the environmental fate of PAHs over time as relative water solubility directly influence rates of biotic and abiotic degradation (Lee et al., 2015).

Light crude oils, such as the Macondo oil released during the DHOS, possess high proportions of soluble PAHs relative to the asphaltene content (Lee et al., 2015). Light crude oils are less viscous and are easily dispersible compared to heavy oils, and the high PAH content in these oils contributes to their acute toxicity to flora and fauna compared to the lower acute toxicity following exposure to spills of heavy oils (Lee et al., 2015). However, the composition of crude oil may change considerably over time due to evaporation, photooxidation, dissolution, emulsification with water, and microbial degradation, collectively referred to as weathering. Following the mixing of oil in water, low and medium molecular weight aliphatic saturated hydrocarbons, soluble monoaromatic hydrocarbons, and LMW PAHs are subject to volatilization and dissolution into the water column, where they may undergo microbial biodegradation (Atlas and Hazen, 2011; Haritash and Kaushik, 2009; Reddy et al., 2012; Speight and El-Gendy, 2017). On the other hand, hydrophobic HMW PAHs associated with the oil phase do not undergo the same natural weathering processes (Hylland, 2006), although slick dispersion into oil droplets enhances the surface area of the oil phase for microbial degradation (Landry et al., 2019). Weathering creates an oil that is dominated by hydrocarbons recalcitrant to degradation and that is

denser and possesses higher concentrations of asphaltenes and HMW PAHs relative to less weathered oils (Forth et al., 2017b; Wong et al., 2015). The entrainment of water into weathered oil through wave action creates an emulsion that is more viscous than the source oil (Wong et al., 2015). Photooxidation of the outer layer encrusts the emulsion forming a highly degradation resistant tar ball that possesses a core of less weathered oil and anthropogenic surfactants, if present during encrustation (*for review*, *see* Beyer et al., 2016; White et al., 2014). This form of crude oil is more environmentally persistent, allowing large masses of oil and surfactant to travel long distances within the water column with little biodegradation (Mendelssohn et al., 2012; White et al., 2014).

Several sources of weathered oils were collected following the DHOS through skimming efforts to remove surface oil slicks and for research purposes. Slick oil was collected on July 29, 2010 at the surface near the well head by several skimmers and transported by barge number CTC02404 (referred to as slick A). Additional slick oil was collected along the mouth of the Mississippi River delta on July 19, 2010 using the U.S. Coast Guard Cutter Juniper (referred to as slick B; BP Gulf Science Data, 2014). By the time of collection, these oil slicks had changed considerably from the source Macondo oil through weathering processes, with slick B being considerably more weathered (85% depletion of select PAH analytes relative to hopane from source Macondo oil) than slick A (68% select PAH depletion; Forth et al., 2017b). However, despite a considerable degree of weathering, both slicks had sufficiently high enough PAH concentrations to elicit toxicity in aquatic organisms (Deepwater Horizon Natural Resource Damage Assessment Trustees, 2016).

Ecological Damage Assessment Following the Deepwater Horizon Oil Spill

Despite the considerable amount of oil spill research, few studies have definitively drawn conclusions on the long-term impacts of any spill. Some of the most comprehensive work emerged in the aftermath of the Exxon Valdez Oil Spill (EVOS). During the EVOS, 42 million liters of North Slope crude oil were spilt on March 24, 1989, contaminating 2,414 km of Alaskan coastline (Exxon Valdez Oil Spill Trustee Council, 1994). Although oiling led to significant acute lethality, the long-term effects were also considered severe. For example, in a first-of-its-kind study, same year class pink salmon (*Oncorhynchus gorbuscha*), exposed to North Slope crude oil as embryos in the laboratory and released into the wild, had reduced over-winter survival. These data suggested that transient oil exposure during sensitive life stages can reduce organismal fitness (Bue et al., 1996; Short, 2017). Additional research demonstrated the environmental persistence of Exxon Valdez oil in oxygen and nutrient poor conditions, highlighting the potential for continuous PAH exposure decades after initial oiling (Li and Boufadel, 2010; Short et al., 2007). These studies, and others, provided the framework for potential ecotoxicological pathways during the DHOS (Short, 2017).

In response to the Exxon Valdez oil spill, the Oil Pollution Act of 1990 was established to address oil spill prevention, response, and reparations to shareholders of navigable waters, shorelines, and economic zones of the United States (Deepwater Horizon Natural Resource Damage Assessment Trustees, 2016). The Oil Pollution Act establishes a set of procedures for assessing the damage and loss of natural resources resulting from oil spill contamination. These procedures include conducting a natural resource damage assessment (NRDA) to characterize the impacts of an oil spill and remediation efforts on affected species and habitats and to ultimately assign a dollar amount required for compensation of these natural resources (Deepwater Horizon

Natural Resource Damage Assessment Trustees, 2016). Field observations of oil concentration in the water, sediment, and biota are used to assess the spatial and temporal extent of oil contamination, and laboratory toxicity assays are used to assess species sensitivity. Shoreline cleanup and assessment technique (SCAT) surveys are performed to assess the extent of oiling within marsh regions. Oil responders also perform visual surveys to enumerate instances of oiled wildlife and spill-associated mortalities, and collect tissue, water, and sediment samples for evidence of contaminant exposure (Deepwater Horizon Natural Resource Damage Assessment Trustees, 2016).

In order to investigate impacts of the DHOS in a laboratory setting protocols were developed and standardized within the NRDA program that would mimic the way oil-in-water mixtures, also referred to as water accommodated fractions (WAFs), would be formed in the field. These protocols included the generation of high-energy WAFs (HEWAFs) created by blending together oil and water at high speeds that would mimic the mixing of oil through wave action and the development of protocols for generating chemically enhanced WAF (CEWAFs) created through the application of the chemical dispersant, Corexit, to the surface of the medium-energy mixing oil-water interface that would mimic the areal application of Corexit to surface slicks (Deepwater Horizon Natural Resource Damage Assessment Trustees, 2016). These methods allowed for the mixing of oil in water by dispersing oil into droplets entrained within the water column to mimic the composition that was found in the environment. Laboratory toxicity testing was performed through traditional toxicity bioassays where organisms were exposed to a wide range of concentrations of oiled sediment and water to develop dose response curves and determine effective concentrations for numerous aquatic biota under different exposure scenarios. Thus, slick A and slick B oils were used in conjunction to these WAF generation methodologies

to perform laboratory toxicity assays on biota representative of the GOM, ultimately contributing to the body of research used to estimate the $18.7 billion in damage caused by the DHOS (U.S. Department of Justice, 2015). Although this research included characterizing the behavior, fate, transport, and effects of oil in aquatic environments, additional research needs were identified by the scientific community in building upon and advancing this body of knowledge. These additional research needs included investigating the biological effects of chemical dispersants at varying salinities, investigating the behavior of physically and chemically dispersed DHOS oil, and investigating population sensitivities of fish to fresh and weathered DHOS oil (Forth et al., 2017a; Landry et al., 2019; Deepwater Horizon Natural Resource Damage Assessment Trustees, 2016).

The Toxicity of Polycyclic Aromatic Hydrocarbons

The exposure of aquatic organisms to hydrocarbons such as PAHs may result in toxic effects that can be dependent or independent of aryl hydrocarbon receptor (AHR)-mediated mechanisms (Geier et al., 2018; Incardona, 2017; Meador and Nahrgang, 2019). According to the narcosis model of toxicity, monoaromatic and 2-ring PAHs may disrupt cellular membranes and cause extreme cellular stress (Lin and Tjeerdema, 2008). The disruption of cellular processes may produce an effect like that observed in over-anesthetized organisms at lower concentrations and may be lethal at increased concentrations (Dupuis and Ucán-Marín, 2015). Similarly, exposure to LMW PAHs may disrupt cardiac function through disruption of excitation-contraction coupling in cardiomyocytes, resulting in bradycardia and irregular heart rates (Brette et al., 2014; Heuer et al., 2018; Incardona, 2017; Incardona et al., 2004; Incardona et al., 2014; Khursigara et al., 2017; Philibert et al., 2019; Sørhus et al., 2016). These arrhythmias may influence blood flow dynamics that, in turn, influence maturation of the heart during embryonic cardiac development (Hove et al.,

2003). Arrhythmias, in the form of bradycardia, would also result in a reduction of shear-strain stress in developing vasculature, preventing mechanically induced cardiac remodeling and hormonal stimulation of angiogenesis (Burggren, 2005; Hove et al., 2003).

In general, HMW PAH toxicity is mediated by activation of the AHR (Incardona et al., 2006; Incardona et al., 2011). Cardiotoxicity can also occur through AHR-mediated disruption in cardiac morphogenesis. Activation of the AHR pathway via HMW PAHs or dioxins such as, 2,3,7,8-tetrachlorodibenzodioxin (TCDD), leads to cardiomyocyte toxicity, ultimately disrupting development of the epicardium and leading to cardiac edema, tube heart, and phenotypes associated with reduced blood circulation in embryonic zebrafish (*Danio rerio*; Hofsteen et al., 2013; Incardona et al., 2006; Incardona et al., 2011; Scott et al., 2011; Sørhus et al., 2016), and mummichog (*Fundulus heteroclitus*; Clark et al., 2010; *for review, see* Incardona, 2017). Transcriptional evidence suggests that PAH exposure can induce AHR-independent and AHR-mediated disruption in calcium cycling in cardiomyocytes (Incardona, 2017; Sørhus et al., 2016), and these results were also observed in early life stage mahi-mahi (*Coryphaena hippurus*) exposed to CEWAF (Greer et al., 2019). The presence of pericardial edema is indicative of severe cardiac impairment and may serve as an indication of heart failure (Incardona et al., 2004; Jones and Braun, 2011).

Exposure to HMW PAHs have been shown to cause gross morphological development in early life-stage teleosts through AHR-mediated disruptions of neural crest cell migration in mummichog (Bozinovic et al., 2013), false kelpfish (*Sebasticus marmoratus*; He et al., 2011), and zebrafish (De Soysa et al., 2012; Yelick and Schilling, 2002) and through disruptions in skeletal ossification in medaka (*Oryzias latipes*; Dong et al., 2011; Seemann et al., 2015) and zebrafish (Xiong et al., 2008). Consequently, fish larvae having undergone PAH-induced

dysmorphogenesis typically hatch out with morphological abnormalities such as jaw malformations and spinal deformities (*e.g.* curvature) and have been documented in Atlantic cod (*Gadus morhua*; Hansen et al., 2019) and Atlantic haddock (*Melanogrammus aeglefinus*; Sørhus et al., 2016) that would directly impact prey capture and locomotory capabilities (Chollett et al., 2014).

Upon ligand binding, the AHR heterodimerizes with the aryl hydrocarbon nuclear translocator (ARNT), which binds to xenobiotic response elements (XREs, also known as dioxin response elements and AHR response elements) for several genes associated with Phase I and II enzymes involved in xenobiotic metabolism, such as those in the cytochrome P450 superfamily (Denison and Nagy, 2003; Hahn, 1998). Because multiple gene duplication events for the AHR occurred within a wide range of teleost families, there are species differences in which paralog of AHR mediates hydrocarbon toxicity (*for review, see* Hahn and Hestermann, 2008). Specifically, it is the AHR1 isolog, AHR2, that mediates PAH toxicity in both zebrafish and *Fundulus sp.*, although PAHs may bind to AHR1, which is the ortholog to the mammalian AHR, in *Fundulus sp.* without any resulting toxicity (Billiard et al., 2007; Billiard et al., 2006; Clark et al., 2010; Karchner et al., 1999). Increased transcription of CYP1A, a target of AHR activation, was observed in Gulf killifish exposed to weathered south Louisiana crude in a laboratory setting (Pilcher et al., 2014), confirming the activation of the pathway observed in field-caught fish from oiled earlier field sites (Dubansky et al., 2013; Whitehead et al., 2012).

The oxidation of HMW PAHs by CYP1A increases xenobiotic reactivity and serves as the first of two phases in xenobiotic metabolism, with the second phase consisting of the conjugation of the xenobiotic radical by a cofactor to facilitate transportation and elimination of the xenobiotic adduct (Forman et al., 2009; Lewis et al., 1998). Chronic exposure of PAHs at sublethal

concentrations can also decrease survivability by negatively impacting other long-term aspects of organismal fitness. This response may be a consequence of the continued increased expression of CYP1A in the face of chronic HMW PAH exposure, resulting in the constant generation of metabolites with a greater bioreactivity than their parent compounds (Hahn and Hestermann, 2008). CYP1A may oxidize benzo-α-pyrene (BaP) via a two-step oxidation process into an intermediate metabolite, BaP-7,8-dihydrodiol-9,10-epoxide, which has been shown to be more toxic and carcinogenic than the parent compound by forming mutagenic DNA adducts (Ericson and Balk, 2000).

Impaired reproduction has also been observed in adult teleosts exposed to sublethal concentrations of PAHs, which may negatively impact recruitment through reductions in egg output and egg quality through endocrine disruption (Hahn and Hestermann, 2008; Lee et al., 2015). This disruption is likely a result of crosstalk between the AHR and estrogen receptor (ER) pathways, although the exact mechanism of PAH influence on reproductive impairment remains to be elucidated. One mechanism suggests that AHR pathway activation interferes with the estrogen receptor (ER) binding to genomic estrogen response elements (Hahn and Hestermann, 2008). XREs have been located on the gene that encodes for aromatase CYP19, an enzyme that converts androgens to estrogens, indicating the potential role for CYP19 gene regulation by PAHs in some species of teleosts (Cheshenko et al., 2008). Furthermore, CYP1A metabolizes estradiol in fish (Scornaienchi et al., 2010), suggesting that PAH-induced expression of CYP1A through activation of the AHR pathway may play a role in decreased circulating levels of estrogen in fish. Indeed, oil-exposed sheepshead minnows (*Cyprinodon variegatus*) exhibited reduced average egg production and decreased fertilization success relative to control exposed fish (Jasperse et al., 2019), and similar results were observed in zebrafish given oil-dosed feed (Bautista and

Burggren, 2019). Gulf killifish sampled Grand Terre, LA during DHOS oiling exhibited signatures of PAH-induced antiestrogenic effects as demonstrated by decreased transcriptional response of genes associated with reproduction (Whitehead et al., 2012). As such, understanding the effect of PAH exposure to Gulf killifish reproduction would aid in predicting the impact of spawning habitat oiling on the population level.

In addition to reproductive impairment, PAH exposure to reproducing adult fish can convey decreased fitness to their offspring. Gulf killifish displayed down regulation of genes associated with reproductive proteins, zona pellucida and choriongenin, involved in oocyte maturation and development (Whitehead et al., 2012), while other studies have shown that PAHs disrupt vitellogenesis (Bemanian et al., 2004; Brooks et al., 1997; Cheshenko et al., 2008). Furthermore, PAH metabolites may be transferred to oocytes during vitellogenesis (Monteverdi and Giulio, 2000). Elevated basal mitochondrial DNA damage was observed in mummichog embryos collected from a broodstock population sourced from the polluted Elizabeth River, Virginia, indicating the potential for deposition of genotoxic PAH metabolites during oocyte development (Wills et al., 2010). Decreased fitness traits resulting from parental exposure were observed to persist into adulthood as offspring of oil exposed sheepshead minnows demonstrated decreased size and prey capture ability as adults (Jasperse et al., 2019). Parental exposure to crude oil may directly impact on embryonic response and survival. As such, assessing oil toxicity on embryonic fish from an ecotoxicological perspective should consider the effects of parental exposure on progeny.

PAHs within crude oil may impact several different physiological processes and molecular mechanisms within an organism; however, the ability of PAHs to perturb these processes is dependent on their concentration and bioavailability as influenced by their solubility in water.

Following the mixing of oil in water, water soluble PAHs quickly partition into the dissolved phase from droplets until equilibrium is reached between the two phases. As soluble PAHs are depleted from the dissolved phase, their concentrations in water are replenished by PAHs in the droplet phase. Conversely, PAHs with low solubility remain primarily associated with the droplet phase at higher oil loading concentrations but too can dissolve into water following further dilutions of oil-in-water mixtures (Forth et al., 2017a; *for review, see* Landry et al., 2019).

In general, soluble, waterborne LMW PAHs are likely less toxic on a per molar basis than less soluble HMW PAHs, as LC50's based on the critical body burden of a PAH are orders of magnitude lower in HMW PAHs than LMW PAHs (Di Toro et al., 2007). However, PAHs with low log K_{OW} values are considered to have a higher aqueous toxic potential since their increased solubility allows them to saturate the aqueous medium at high concentrations compared to PAHs with high log K_{OW} values (Di Toro et al., 2007). HMW PAHs with low solubility are still believed to possess some potential for toxicity if accumulation occurs through non-aqueous routes of exposure, such as direct adsorption of oil droplets to animals, which would allow lipophilic PAHs to be directly absorbed across membranes, effectively by-passing the aqueous phase (Hansen et al., 2018; Petersen and Kristensen, 1998; Redman et al., 2012; Sørensen et al., 2017). Thus, PAHs sequestered in oil droplets, due to their low solubility, may accumulate by direct chorionic contact bypassing the dissolved phase. Adsorption mediated accumulation of PAHs might be influenced by the size and concentration of adsorbed droplets and interaction time.

Several factors, including the droplet size and physicochemistry (*e.g.* density) of an oil type, play a large role in the residence time of oil droplets in the water column. The dispersal of oil in water is thermodynamically unstable, resulting in the coalescence of oil droplets and eventual separation of oil from the water phase through decreased oil surface tension (Tadros,

2013). The rate at which an oil droplet rises out of the water column is influenced by droplet size and oil density, such that that smaller droplets are more stable in oil-in-water mixtures and that as the density of oil approaches that of water through the weathering process, that droplets entrained within water will stabilize due to negative or neutral buoyancy (Forth et al., 2017a; Wong et al., 2015). Understanding the behaviors of the dissolved and droplet phases over time have important implications when considering WAF toxicity as these two phases exist simultaneously within an oil-in-water mixture, with each phase believed to possess differential toxicities to aquatic organisms.

The Gulf killifish as a Model Organism

Gulf killifish are cyprinids common to the salt marshes and tidal estuaries of the northern GOM and southern Atlantic Ocean of the United States (Nordlie, 2006). They are a non-migratory species with high site fidelity within a relatively small home range (Nelson et al., 2014; Williams et al., 2008). Gulf killifish serve an integral part in the food webs of the salt marsh and estuarine ecosystems by providing energy transfer from lower to higher trophic levels (Baker et al., 2013). Adults can tolerate a wide range of salinities (from 0.5 g/L to 76.1 g/L) and temporary exposure to low dissolved oxygen (Nordlie, 2006), and these large environmental tolerances are necessary as rapid and wide swings in the abiotic factors are common in salt marshes.

Gulf killifish are fractional spawners, repeatedly spawning in late spring and late fall when temperatures range between 19 °C and 24 °C, although spawning will continue at a reduced rate outside of this temperature range (Greeley Jr and MacGregor III, 1983; Nordlie, 2000). Females deposit eggs on the bases of marsh grasses where they are fertilized by males, producing large, optically-clear embryos that remain attached to marsh substrate until hatch (Nordlie, 2000). Embryogenesis for this species occurs over a protracted period of time with hatch occurring

approximately 10-14 days following fertilization at 23 °C but may take upwards of 21 days, after which the probability of embryonic mortality increases and hatch is unlikely (Brown et al., 2011; Perschbacher et al., 1990). The chorions Gulf killifish embryos, like those of their congener species, the mummichog, possess an extrachorionic matrix composed of a jelly coat and projecting chorionic fibrils that protects embryos from physical threats and anchors embryos to substrates and each other for the duration of embryogenesis (Brummett and Dumont, 1981; Riehl and Patzner, 1998). Investigations of Gulf killifish reproduction have characterized fecundity at approximately 0.9 eggs per gram female per day, a low reproductive output compared to other teleost species (Clemment and Stone, 2004; Green et al., 2010; Landry et al., 2007). The decreased fecundity is a tradeoff for the considerable degree of energetic input invested into Gulf killifish oocyte development with mature eggs being larger relative to female size (in grams) compared to those of the majority of other teleost species (Greeley Jr et al., 1991; Kamler, 2005; Patterson et al., 2013), resulting in precocial larvae that possess increased mobility and prey capture ability at hatch relative to altricial larvae (Armstrong and Child, 1965; Crawford and Balon, 1994). The extensive pre-hatch development of killifish larvae can be partially attributed to substantial volume of vitellogenin deposited during oocyte development (Brown et al., 2011; Greeley Jr et al., 1988).

The Impact of the Deepwater Horizon Oil Spill on Gulf killifish

The long-term consequences of oil exposure during early-life stage development on organismal fitness has been well documented and suggest that early life stage exposure to crude oil during spill events may have population level consequences (Hamilton et al., 2016; Hamilton et al., 2017). For example, cardiogenesis was altered in several species of fish embryos briefly exposed to sub-lethal concentrations of PAHs, which resulted in altered heart morphology and

reduced aerobic capacity in post-hatch life stages (zebrafish, Hicken et al., 2011; pink salmon, and Pacific herring, *Clupea pallasi,* Incardona et al., 2015; mahi-mahi, Mager et al., 2014). Exposure to sub-lethal concentrations of PAHs during early life-stage development can also disrupt embryonic morphogenesis, notably through skeletal and craniofacial deformities (*for review, see* Billiard et al., 2007). Indeed, Gulf killifish exposed to historically-oiled sediments from Grand Terre, LA (29° 16'23" N, 89° 56'42 W) a year after the DHOS elicited the differential expression of genes, suggesting the potential for PAH exposure to affect killifish populations across multiple generations (Dubansky et al., 2013). Given the low fecundity of the species and large energy investment in reproduction, reproductive toxicity in spawn-ready adults can severely impair species survival through intergenerational impacts. Reductions in early life-stage fitness, whether it be through parental oil exposure or embryonic exposure, have ecological-wide implications as Gulf killifish are an important trophic relay in its respective food web (Baker et al., 2013; Kneib, 1997).

Numerous populations of killifish from the *Fundulus* genus have been documented as possessing decreased sensitivities to anthropogenic pollution (Clark and Di Giulio, 2012; Oziolor et al., 2018; Oziolor et al., 2014; Oziolor and Matson, 2015; Oziolor et al., 2019; Whitehead et al., 2011; Whitehead et al., 2010; Wills et al., 2009). Recently, populations of Gulf killifish derived from the historically-polluted Houston Shipping Channel have been characterized as possessing reduced sensitivity to organic pollutants (Oziolor et al., 2014). Early life-stage exposure of two of these resistant populations (derived from Vince Bayou, TX [29°43′10″N; 95°13′13″W] and Patrick Bayou, TX [29°43′41.64″N; 95°6′50.51″W]) to organic pollutants such as 3,3′,4,4′,5-pentachlorobiphenyl (PCB 126) or PAHs derived from coal tar did not result in the typical arrythmia and teratogenosis phenotypes nor was chromosomal damage observed (Oziolor et al.,

2014). The perceived resistance is a result of decreased AHR inducibility caused by a deletion in the *AHR* loci, which was an introgressed mummichog haplotype conferring increased tolerance to legacy pollutants (Oziolor et al., 2019). Furthermore, characterization of multiple populations showed a graded pollution resistance correlated to environmental pollution concentrations, suggesting the degree of pollution scales with selective pressure for the resistant *AHR* loci (Oziolor et al., 2019). Although transplantation of mummichog resulted in the introgression of the adaptive phenotype, similar pollution adaptation events appear to have evolved in several populations of mummichog derived from geographically distinct areas with a history of anthropogenic pollution (*for review, see* Whitehead et al., 2017). As such, populations of Gulf killifish native to locations characterized as having heavily oiled sediments from the DHOS may be undergoing directional selective pressures that would favor an adapted phenotype. Use of transcriptional analyses anchored with phenotypic endpoints would subsequently help in elucidating the mechanisms of adaptation. Thus, additional research is needed, specifically in populations of fish undergoing selection events, on intergenerational effects of pollution exposure to better understand the molecular underpinnings that drive population level responses.

Scope of Dissertation

The goal of this dissertation is to better characterize the impacts of the DHOS on Gulf killifish beyond that which was covered under the NRDA program. This dissertation seeks to address those research needs from an aquatic toxicology perspective. Gulf killifish was chosen as a model organism because this species meets two fundamental criteria: 1) Gulf killifish possesses a sensitivity to the toxicants of interest (PAHs) such that exposure would result in a sublethal response, which would manifest in a reduced fitness phenotype; and 2) Gulf killifish response to PAH exposure extends beyond the animal itself to the populational level, potentially causing

repercussions at a community level. Identifying and studying the impacts of the DHOS on a potential keystone organism such as Gulf killifish will provide better insight into downstream food web interactions and potential community level consequences.

Chapter 2 investigates the toxicity of the chemical dispersant, Corexit, to Gulf killifish concomitant with osmotic challenges. The majority of Corexit toxicity research has been performed on a single species life-stage at a static salinity; however, Gulf killifish spend the entirety of their life cycle in an environment subject to salinity fluctuations, warranting the need to investigate life-stage specific sensitivities to Corexit in the face of osmotic challenges. I hypothesized that Corexit due to the amphipathic anionic surfactants within dispersants would interact with biological membrane like the fish gill and impair physiological processes mediated by it, such as osmoregulation. The goal of this chapter was to investigate the osmoregulatory effects and toxicity of Corexit in Gulf killifish. Gulf killifish at the embryonic, larval, juvenile, and adult life stages were exposed to Corexit in water of different salinities to assess the interactive effects of ontogeny and salinity on Corexit toxicity. Corexit was not toxic to embryos except when exposed in hyperosmotic water where it had negligible effects; however, its toxicity to Gulf killifish increased dramatically following hatch, showing its greatest deleterious effects in adults. Corexit tended to increase sodium and chloride burdens in Gulf killifish when exposed in hyperosmotic waters and reduced whole-body and plasma ion concentrations in fish exposed to hypoosmotic waters. However, Corexit exposure at hyperosmotic salinities resulted in an increased differential accumulation of sodium over chloride as Gulf killifish matured. These findings suggest that Corexit may impair gill structure or alter specific components of osmoregulatory function, thus impacting osmoregulation in hyperosmotic and hypoosmotic waters, potentially impairing survival during osmotic challenges. Furthermore, the magnitude of

these impacts continued to increase concomitant with gill ontogeny. This chapter was published in *Comparative Biochemistry and Physiology, Part C* (Brown et al., 2019).

Chapter 3 investigates how dispersed crude oil droplets behave in the water column and how suspended droplets interact with the surface of fish embryos. Despite a vast body of research performed to characterize oiled water toxicity, little research has been performed on investigating the confluence of suspended oil droplet behavior across time and interaction with chorions of embryonic fish. As such, a novel, high-throughput protocol was developed for enumerating and sizing droplets suspended in water as well as adsorbed to killifish chorions, allowing for better characterization of the droplet phase in different preparations of water accommodated fractions and of the interaction of the droplet phase with the chorion. I hypothesized that increases in oil density through weathering and method of oil dispersal would influence the distributions of suspended droplets over time, which in turn would influence droplet binding to Gulf killifish chorions. The degree to which suspended droplet diameter changed over time was dictated by the degree of weathering and means of oil dispersal (*i.e.* HEWAF or CEWAF). Less weathered oil (slick A) exhibited a greater degree of change in mean droplet volume diameter compared to less weathered oil (slick B), and larger droplets progressively dominated HEWAF mixtures compared to the prevalence of smaller droplets in CEWAF mixtures over time. The number of droplets adsorbed to killifish chorions changed greatly throughout the course of observation, indicating a temporal nature of adsorbed droplets to the extrachorionic fibers. Conversely, removal of extrachorionic fibers from the chorion appears to have reduced this characteristic of adsorbed droplets.

Chapter 4 investigates the effects of parental oil exposure on embryo fitness. The salt marshes that line the northern GOM serve as breeding grounds and nurseries for Gulf killifish in

addition to several other commercially important species of fish (Chesney et al. 2000). With the DHOS occurring during peak spawning time for Gulf killifish, breeding adults and their offspring were likely exposed to oil. I hypothesized that parental oil exposure would affect reproductive physiology and may also affect offspring fitness and offspring sensitivity to oil, which is an extension of direct impacts on reproductive physiology. Reproductively-ready adult Gulf killifish with differing pollution-exposure histories and genetic backgrounds were exposed to crude oil to test for population-level differences in oil sensitivity. These populations were derived from a Louisiana marsh heavily oiled during the DHOS (Grand Terre, LA), a population from a historically-polluted U.S. Superfund site (Vince Bayou, TX) contaminated with persistent organic pollutants, including PAHs, where Gulf killifish possess decreased sensitivity to high concentrations of organic pollutants, and two geographic reference sites (*i.e.* a lab bred population derived from Leeville, LA [29°15'24.6"N 90°12'51.3"W] and a field caught population from Gangs Bayou, TX [29°15'23.4"N 94°54'43.3"W]) with no history of contamination. Whereas the Vince Bayou population of Gulf killifish exhibited no reproductive or developmental perturbations resulting from oil exposure at either life stage, reproductive impairment was observed in oil-exposed adult Gulf killifish from the Grand Terre site, and their offspring exhibited increased sensitivity to oil in the form of increased mortality following embryonic oil exposure compared to oil-exposed offspring from parents held in unoiled waters. This suggests that oil exposure to pollution sensitive populations of reproductively-active Gulf killifish during the DHOS likely amplified the impacts of the spill on early life stage development. Furthermore, populations of Gulf killifish affected by the DHOS do not exhibit evidence of pollution resistance.

CHAPTER 2
THE INFLUENCE OF SALINITY ON THE TOXICITY OF COREXIT AT MULTIPLE LIFE STAGES OF GULF KILLIFISH

Introduction

Chemical dispersants are composed of a complex mixture of ionic surfactants and petroleum solvents that lower the interfacial surface tensions of oil and break-up oil slicks into smaller droplets (Atlas and Hazen, 2011; Place et al., 2016). However, of the 19 chemical dispersants available commercially for oil spill remediation (USEPA National Contingency Plan Product List 2018, https://www.epa.gov/sites/production/files/2018-12/documents/schedule.pdf), only Corexit® 9527A and Corexit® 9500A (termed hereon solely as Corexit; Nalco Environmental Solutions LLC) were applied during the 2010 Deepwater Horizon Oil Spill (DHOS; Graham et al., 2011). In total, 7 million liters of Corexit were applied directly to the well head and over 46,000 km^2 of surface waters of the northern Gulf of Mexico between April 22 and July 19, 2010 (Lehr et al., 2010). Regardless of the rapid hydrolysis and photodegradation of the anionic surfactants in the dispersant (Batchu et al., 2014; Campo et al., 2013), dioctyl sulfosuccinate (DOSS), the primary anionic surfactant of Corexit, was found up to 300 km from the nearest site of application (Kujawinski et al., 2011). Even though Corexit was not applied within 4.8 km of land (Fabisiak and Goldstein, 2011), DOSS was found entrained within tar balls on coastal Gulf beaches four years after the DHOS (White et al., 2014). In another case unrelated to the DHOS, urban-derived DOSS from non-point sources was likely transported by stormwater and wastewater discharge into Perdido Bay at the Florida and Alabama border, and was found at

---

This chapter, previously published as Brown, C., Williamson, K., and Galvez, F. "The influence of salinity on the toxicity of Corexit at multiple life stages of Gulf killifish" *Comparative Biochemistry and Physiology, Part C* 221 (2019): 38-48, is reprinted here by permission of Elsevier.

concentrations upwards of 19 µg/L (Hayworth and Clement, 2012) suggesting that surfactants may exist in coastal waters of varying salinity.

The acute toxicity (96-h LC50) of Corexit varies between 25.2 and 354 mg/L for aquatic vertebrates (Bejarano, 2018; George-Ares and Clark, 2000), which brackets the recommended dosage of 261 mg/L for oil spill cleanup during peak oiling in salt water (as referenced in Kuhl et al., 2013). Although the toxicity of several chemical dispersants have been described in freshwater and saltwater teleosts, Corexit toxicity under conditions of fluctuating salinity as observed in estuaries, is not well described (George-Ares and Clark, 2000). Research on the interaction between DOSS and salinity on embryonic Gulf killifish (*Fundulus grandis*) showed an inverse relationship between DOSS concentration and hatch success, mean time to hatch, and total length at hatch (Bodinier et al., 2014). Additionally, DOSS exposure decreased the protein expression of Na^+/K^+-ATPase and cystic fibrosis transmembrane conductance regulator, and decreased mitochondrion-rich cell surface area in Gulf killifish larvae (Bodinier et al., 2014). So, in addition to solubilizing hydrocarbons, it appears that the chemical structure of DOSS allows it to interact and destabilize biological membranes or interact and modify the structure and function of membrane proteins (Cserháti et al., 2002; John et al., 2016; Jones, 1992; Schreier et al., 2000), contributing to the cytotoxic effects of Corexit (Dasgupta and McElroy, 2017). In agreement, chemical dispersants containing anionic surfactants have been shown to increase oxidative stress in fish gills leading to tissue necrosis and death (Agamy, 2013; Dasgupta et al., 2018; Rosety-Rodríguez et al., 2002). Biological functions mediated by the gills, such as osmoregulation, may be particularly vulnerable to chemical dispersants due to the large surface area in direct contact with water.

The goal of the current study was to investigate the effects of Corexit on ion regulation and toxicity concomitant with acute hypo- and hyperosmotic challenges in the Gulf killifish of different life stages. Gulf killifish live in the salt marshes of the northern Gulf of Mexico in salinities ranging from fresh water to full-strength sea water (Nordlie, 2006) but have also been found in hypersaline tidal ponds at 72 g/L (Simpson and Gunter, 1956). Gulf killifish and their congener species can rapidly acclimate to acute osmotic challenges with little physiological perturbation, spending their entire lives in these dynamic salt marshes and restricted to a narrow home range (Able et al., 2012; Guan et al., 2016; Rountree and Able, 2007). Rapid changes in environmental salinity can occur due to the ebb and flow of tides and extreme storms; and seasonal changes due to varying freshwater inputs can change due to rainfall and riverine discharge (Sklar and Browder, 1998; Teal et al., 1986). Their limited movement in the environment makes it likely that their exposure to anthropogenic chemicals will be associated with acute fluctuations in environmental salinity. Furthermore, changes to killifish osmoregulatory capacity, and the mechanisms that support it, occur in post-larval development as the site of osmoregulation shifts from the yolk-sac to the gill (Katoh et al., 2000; Varsamos et al., 2005). As such, the effects of environmental salinity challenges in the face of exposure to a dispersant purported to disrupt osmoregulatory processes are likely to differ in severity as osmoregulatory systems develop. This current study describes the changing sensitivities of maturing Gulf killifish to Corexit in the face of acute salinity challenges.

Materials and Methods

Collection of Adult Brood Stock

The effects of Corexit were assessed in Gulf killifish embryos at the onset of cardiovascular circulation (stage 25 of development; Armstrong and Child, 1965), in larvae

immediately after hatch, in juveniles at four-weeks post hatch, and in adults. The adult Gulf killifish [mean ± SEM (*n*): mass of 10.6 ± 0.5 g (*n=80)*; total length of 9.6 ± 0.2 cm (*n=73*)] were obtained from Cocodrie, LA (29°15'13N, 90°39'46W) and held between 12 and 13 g/L (Instant Ocean salt mix; United Pet Group, Cleveland, OH, USA) in a recirculating system for 12 months prior to use. Salinity (13.0 ± 0.1 g/L (*n=46*); YSI 2030 Pro (YSI Incorporated, Yellow Springs, CO, USA)), temperature (23.7 ± 0.2 °C (*n=46*); YSI 2030 Pro), pH (7.1 ± 0.1 (*n=45*); Ultrabasic Benchtop Meter (Denver Instrument, Bohemia, NY)), nitrogenous waste (total ammonia nitrogen: 0.0 ± 0.0 (*n=48*); nitrite: 0.0 ± 0.0 (*n=48*); and nitrate: 0.1 ± 0.7 (*n=48*); API Test Kits (Mars Fishcare, Chalfont, PA, USA)), and dissolved oxygen concentrations (6.0 ± 0.1 (*n=44*); YSI 2030 Pro) were checked weekly to ensure adequate values.

Procurement of Gulf Killifish Embryos, Larvae, and Juveniles

Field-collected adults were first used as a brood stock to obtain embryos, larvae, and juveniles for Corexit exposures but also served as the adults for Corexit exposures once no longer needed as a brood stock. Gulf killifish embryos and larvae were produced from the eggs of 27 females and the sperm of 8 males. Within 12 min of gamete collection, eggs and sperm were mixed together with 100 mL of 12 g/L sea water to activate gametes. A total of 821 eggs were collected and 802 embryos fertilized yielding a 97% fertilization success. Fertilized embryos were grown on polyurethane foam (Premium Poly Foam, American Excelsior Company; www.americanexcelsior.com) moistened with 12 g/L water as described by (Coulon et al., 2012). Embryos were monitored once daily and dead embryos removed immediately. At 5 days post fertilization (dpf), 320 embryos were transferred to treatment replicates for the embryo exposures. The remaining embryos, which were later used in larval exposures, were kept on moistened polyurethane foam for an additional 10 days and then re-immersed in 12 g/L water at

15 dpf to synchronize hatch for procurement of larvae within minutes of one another for larval Corexit exposures. At 15 dpf, 420 embryos were transferred into petri dishes containing 15 mL of 12 g/L water. Of the 420 embryos, 379 larvae were obtained yielding a 90.2% hatch success. Larvae were transferred to treatment replicates (*n=10*) for the larval toxicity assays.

Spawning was repeated to obtain progeny for juvenile exposures. Gametes from 7 males and 19 females were used for *in vitro fertilization* as described previously. A total of 313 eggs were collected, of which 277 embryos were fertilized yielding an 88% fertilization success. Embryos were grown on moistened polyurethane foam from fertilization until hatch for 15 days, as described before, and then randomly transferred to 17 tanks with water at 12 g/L at 23 °C to induce hatch (*n= ~15*). Of the 277 embryos transferred, 262 larvae were obtained, giving a 94.5% hatch success. These killifish larvae were reared at 12 g/L at 27 °C for 4 weeks until the start of juvenile exposures.

Experimental Design and Start of Corexit Exposures

The effects of Corexit at four different salinities were evaluated in killifish embryos (at 5 dpf), larvae (immediately upon hatch), juvenile fish (four weeks post hatch), and adult fish. Corexit was supplied by Nalco under a chemical-materials-use agreement. Exposure of killifish embryos, larvae, and juvenile fish were conducted in 250 mL of treatment water in glass containers (Pyrex®; Corning Incorporated, New York, NY, USA). Each control and Corexit treatment were performed in quadruplicate. Treatment water at 4, 12, 16, and 20 g/L salinity was made 24 h prior to the start of each assay by mixing reverse osmosis water and a stock of 20 g/L water made from Instant Ocean salt mix. Dilutions for control and Corexit treatment waters from the stock solution were made each 48 h as needed. The salinity of each treatment water was verified with a YSI Pro 2030 probe. Corexit exposures were all performed at a nominal

concentration of 261 mg/L (1 mL / 3.63 L), which corresponded to the recommended concentration during peak Deepwater Horizon oil coverage at approximately 40% (Kuhl et al., 2013).

On the day of each exposure, embryos, larvae, and juvenile killifish were randomly distributed to thirty-two 100 x 15 mm glass petri dishes (Pyrex®) at a density of *n*=10 per replicate, except for control replicates for the juvenile exposures, which were allocated at a density of *n*=5 per replicate. Adult exposures were performed in duplicate (*n*=5 per replicate) for control and Corexit treatment waters for each salinity. Adult Corexit exposures were performed at 4, 12, 16, or 20 g/L salinity at a volume of 25 L containing 261 mg/L Corexit (i.e., 6.8 mL Corexit stock and 25 L water, or 1 mL / 3.68 L). All adult exposures were conducted in glass aquaria. Due to the rapid toxicity of Corexit to adults observed during preliminary exposures (*data not shown*), especially in 4 and 20 g/L water salinities, adult exposures were performed for only 24 h rather than 96 h. Exposures at the other life stages were extended for up to 96 h, during which time, exposure water was replaced completely after 48 h to prevent accumulation of nitrogenous waste.

Water Chemistry

To prevent fouling of analytical equipment with Corexit, salinity, dissolved oxygen (DO), and pH were measured for only control waters from two randomly selected replicates at 0, 48, and 96 h. DO, which ranged between 7.4 and 8 mg/L for all exposures, was measured with a YSI Pro 2030. Salinity was quantified using a RHS-10ATC handheld refractometer (Sinotech, Portland, OR, USA) calibrated to ultra-pure water (Merck Millipore, Burlington, MA, USA), and pH levels were always between pH 7.00 to 8.00 as measured using an Ultra Basic Benchtop Meter. For every salinity, total water ammonia of two randomly selected control water replicates and two randomly selected Corexit replicates were measured. There was no total ammonia in treatment

waters based on routine analyses using a colorimetric assay (Verdouw et al., 1978). Room temperature was recorded at 24, 48, 72, and 96 h of exposure and ranged between 23 and 25 °C.

Exposure Sampling

Following the start of control and Corexit exposures, embryos and larvae were monitored at 24, 48, 72, and 96 h for mortality. Cessation of heart beat over a 15 s period, as monitored using a stereomicroscope, was used as a measure of mortality in embryos. Embryos surviving the 96-h exposure were euthanized in 0.5 g/L MS-222 (Syndel USA, Ferndale, WA, USA. Mortality of larvae was assessed based on their lack of response to an external stimuli and lack of opercular movement for 30 s. At the end of the 96 h exposures, a random subset of 10 larvae from the combined replicates for a treatment for each salinity was sampled for whole-body Na^+ and Cl^-. Ten individuals exposed to the 4 g/L treatment and 10 individuals exposed to the 12 g/L treatment were randomly sampled from the Corexit replicates. The remaining individuals (n=6) exposed to the 20 g/L treatment were randomly sampled from the Corexit replicates. Juvenile fish were monitored for moribundity and mortality at least 3 times daily for 96 h from the start of exposures. Individuals that were inactive and unresponsive to stimuli but continued to display opercular ventilation were classified as moribund, whereas fish that did not respond to stimuli and lacked opercular movements were classified dead. However, moribund individuals were counted as dead for survival analyses. Larvae and juveniles were euthanized with 0.5 g/L MS-222 and rinsed with approximately 50 mL of ultra-pure water before being dried with tissue paper (Kimberly-Clark, Irving, TX, USA). Samples were dried to a constant weight at 100 °C for 24 h. After dehydration, the dry weight of fish was recorded. Furthermore, moribund individuals collected throughout the 96-h exposure and juvenile fish surviving the entire 96 h were analyzed for whole-body Na^+ and Cl^- content. For each salinity, 10 individuals were randomly sampled

from the four control replicates at 96 h. The decision to terminate exposures when fish were moribund was made to ensure adequate sample size for Na^+ and Cl^- analyses when Corexit toxicity was high. The same protocol for determining and sampling moribund individuals was used for adult fish, however, exposures were terminated after only 24 h due to the rapidity of toxicity, as described before. Adult fish were euthanized via cervical dislocation before severing the caudle peduncle to collect blood from the caudal vein using ammonium-heparinized microhematocrit capillary tubes (Fisherbrand, cat. No. 22-362-566). Hematocrit tubes were centrifuged at 13,000 *g* for 120 s, plasma collected and snap frozen in liquid nitrogen, and stored at -80 °C awaiting analyses of Na^+ and Cl^-. Muscle biopsies were taken and weighed following cervical dislocation. Muscle tissues were then dried to a constant weight at 100 °C for 24 h, after which the dry weight of muscle was recorded.

Digestion and Ion Assays

Whole-body digestion of larval and juvenile samples were performed using a method modified from (Prodocimo et al., 2007). The larvae and juvenile samples were digested in 1 N nitric acid (Fisher Scientific, Hampton, NH, USA) at 60 °C for 24 h and intermittently agitated with a vortex at high speed. Particulate matter was removed by centrifugation and the homogenate diluted by at least 14-fold (v:v) in ultrapure water. Plasma Na^+ was measured by flame atomic absorption spectroscopy (Varian AA240FS Atomic Absorption Spectrophotometer; Agilent Technologies, Inc., Santa Clara, CA) and plasma Cl^- was determined using a colorimetric assay protocol modified from the thiocyanate method (Thermo Electron Corporation, Marietta, OH). All assays were performed in duplicate. Plasma Na^+ or Cl^- concentrations were not analyzed for embryo exposures due to the inability to separate the embryo from the chorion without loss of sample.

Estimates of Net Sodium Flux Rate

The influence of Corexit on the change in net Na^+ and Cl^- flux rates were estimated from the changes in whole-body Na^+ and Cl^- in larvae and juveniles or plasma Na^+ and Cl^- in adults over exposure time. For larvae and juveniles, the whole-body ion (Na^+ or Cl^-) concentrations were first converted from ion content per kg dry weight (dw) to ion content per kg wet weight (ww) using equation 1 as follows:

$$\text{WB ion (ww)} = \text{WB ion (dw)} \times (100\text{-}\% \text{ Water Content}) \quad \text{(equation 1)}$$

where WB ion is the mmol of Na^+ or Cl^- in the whole bodies of larvae and juveniles expressed in kg dw units. Expressing whole-body Na^+ and Cl^- per kg wet weight allowed for easier comparison of net flux rates with the published literature, which are most often expressed in per wet weight units. Percent water content was determined by first weighing the fish and then drying at 100 ˚C to a constant dry weight. Percent water content measured for larvae and juveniles in the current study (Table 3) correspond with values reported in literature (~89% water weight for larvae, Farhoudi et al., 2011; Pfeiler and Luna, 1984; Riis-Vestergaard, 1982; ~77% water weight for juveniles, Blaber, 1975; Duff and Fleming, 1972; Ramee et al., 2016).

The change in net Na^+ and Cl^- flux for each fish was calculated using equation 2 as follows:

$$\Delta J_{net}^{ion} = (\text{Ind WB ion} - \bar{x}_{12\ g/L}\ \text{WB ion}) \times \frac{1}{\text{exposure time}} \quad \text{(equation 2)}$$

where, ΔJ_{net}^{ion} is the change (or difference) in the net Na^+ ($\Delta J_{net}^{Na^+}$) or Cl^- ($\Delta J_{net}^{Cl^-}$) flux rate in mmol/kg ww/hour for each individual fish over the exposure time relative to the mean Na^+ content or mean Cl^- content of the 12 g/L control fish. Ind WB ion is the whole-body Na^+ or Cl^- in

mmol/kg ww units, as calculated with equation 1; $\bar{x}_{12\ g/L}$ WB Ion is the mean whole-body Na^+ or Cl^- in mmol/kg ww units of the 12 g/L control treatment; and exposure time was the time fish spent in the toxicity chambers before sampling. The time of collection was used as the exposure time, which extended to as much as 96 h for larvae, and 96 h and 24 h for juveniles and adults, respectively, unless sampled as moribund at an earlier time.

Since plasma Na^+ and Cl^- and not whole-body Na^+ were measured for adult fish, estimated whole-body ion content for each adult was calculated by summing the estimated Na^+ or Cl^- contents of the extracellular and intracellular compartments and dividing by the total weight of the fish in kg. The following assumptions were made: intracellular [Na^+] and [Cl^-] of each fish was set at 10% and 37% of the measured plasma [Na^+] and [Cl^-], respectively; the % water content of adult fish was estimated as 70.8% of the total weight, with 55.4% of the fish weight estimated to be distributed to the intracellular compartment and 28.9% of the weight being distributed to the extracellular compartment (Bentley, 2002; Thorson, 1961). The percent of whole-body water weight derived from (Thorson, 1961) corresponded with percent muscle water weight measured in the current study, which ranged from 71.3% ± 3.3% to 77.3% ± 0.4% in muscle tissue derived from adult fish held in 20 g/L and 12 g/L salinity waters, respectively (Table 3). Once whole-body Na^+ and Cl^- content of adults in mmol/kg ww were measured, the change net ion flux for each fish from the respective mean of the whole-body ion content of fish from the 12 g/L control treatment was calculated using equation 2 as described above.

All procedures are in accordance by the Institutional Animal Care and Use Committee at Louisiana State University.

Statistical Analysis

Median effect time (ET50) was calculated on the standard and log scale with 95% confidence limits using the PROC PROBIT procedure in SAS 9.3 (SAS Institute, Cary NC). Confidence limits were estimated by using t-values adjusted by a heterogeneity factor to correct for overdispersion when applicable. Response slopes, which represent the change in probability of mortality per logarithmic unit of time (h), were calculated to compare mortality rates between salinity and life stage treatments. For ion analysis, outliers greater than 2 standard deviations from the mean were removed and concentrations were checked to ensure normality. Daily survival and Na^+ and Cl^- concentrations in whole-body and plasma were analyzed within salinity treatments using ANOVA by the PROC GLM procedure at each life stage. The Bonferroni *post-hoc* test was used to check for significant differences in survival and in whole-body and plasma Na^+ and Cl^- concentrations between control salinity treatments.

Results

Survival and LT50 Data

Control killifish regardless of life stage showed no deleterious effects of acute salinity transfer from 12 g/L to 4, 12, 16, or 20 g/L, except for one juvenile mortality each when transferred from 12 g/L to 4 or 16 g/L water (Table 1). In comparison, Corexit was acutely toxic to fish, particularly to juveniles and adults transferred to hyperosmotic waters. Embryos were least sensitive to Corexit compared to other life stages, particularly in isosmotic and hypoosmotic waters but were moderately sensitive to the chemical dispersant when transferred to 20 g/L water (Table 1; Figure 1). Corexit toxicity in embryos transferred to 20 g/L water was only evident after 72 hours post transfer (hpt), and survivorship was significantly lower than control at 96 h (68% ± 17% survival; $p < 0.01$). Otherwise, there was only a slight toxicity (i.e., ~2% of total) of Corexit

to killifish embryos transferred to 16 g/L water after 96-h exposure. No ET50 values could be calculated for any embryo treatment based on the limited toxicity.

Table 1. Percent survival (mean ± standard deviation) for *F. grandis* at multiple life stages exposed for 0-96 h to 12 g/L water, or for 0-24 h; 24-48 h; 48-72 h; and 72-96 h to Corexit in 12 g/L water. Moribund juvenile and adult fish were considered dead for these analyses. Asterisks represent significant differences ($p < 0.05$) between control and Corexit-exposed groups within salinities.

Life stage	Time Post-Transfer (h)	Treatment	Salinity			
			4 g/L	12 g/L	16 g/L	20 g/L
Embryo	0 - 96	Controls	100% ± 0%	100% ± 0%	100% ± 0%	100% ± 0%
	0 - 24	+ Corexit	100% ± 0%	100% ± 0%	100% ± 0%	100% ± 0%
	24 - 48	+ Corexit	100% ± 0%	100% ± 0%	100% ± 0%	100% ± 0%
	48 - 72	+ Corexit	100% ± 0%	100% ± 0%	100% ± 0%	93% ± 10%
	72 - 96	+ Corexit	100% ± 0%	100% ± 0%	98% ± 5%	68% ± 17%*
Larvae	0 - 96	Controls	100% ± 0%	100% ± 0%	100% ± 0%	100% ± 0%
	0 - 24	+ Corexit	100% ± 0%	100% ± 0%	100% ± 0%	100% ± 0%
	24 - 48	+ Corexit	60% ± 8%*	88% ± 10%	73% ± 17%	40% ± 22%*
	48 - 72	+ Corexit	53% ± 10%*	75% ± 6%*	45% ± 26%*	33% ± 22%*
	72 - 96	+ Corexit	45% ± 13%*	70% ± 8%*	0% ± 0%*	20% ± 16%*
Juvenile	0 - 96	Controls	95% ± 10%	100% ± 0%	95% ± 10%	100% ± 0%
	0 - 24	+ Corexit	93% ± 5%	100% ± 0%	93% ± 15%	75% ± 26%
	24 - 48	+ Corexit	70% ± 8%*	53% ± 36%	0% ± 0%*	0% ± 0%*
	48 - 72	+ Corexit	65% ± 10%*	28% ± 36%*	0% ± 0%*	0% ± 0%*
	72 - 96	+ Corexit	65% ± 10%*	0% ± 0%*	0% ± 0%*	0% ± 0%*
Adult	0 - 24	Control	100% ± 0%	100% ± 0%	100% ± 0%	100% ± 0%
	0 - 24	+ Corexit	70% ± 14%*	92% ± 12%	0% ± 0%*	0% ± 0%*

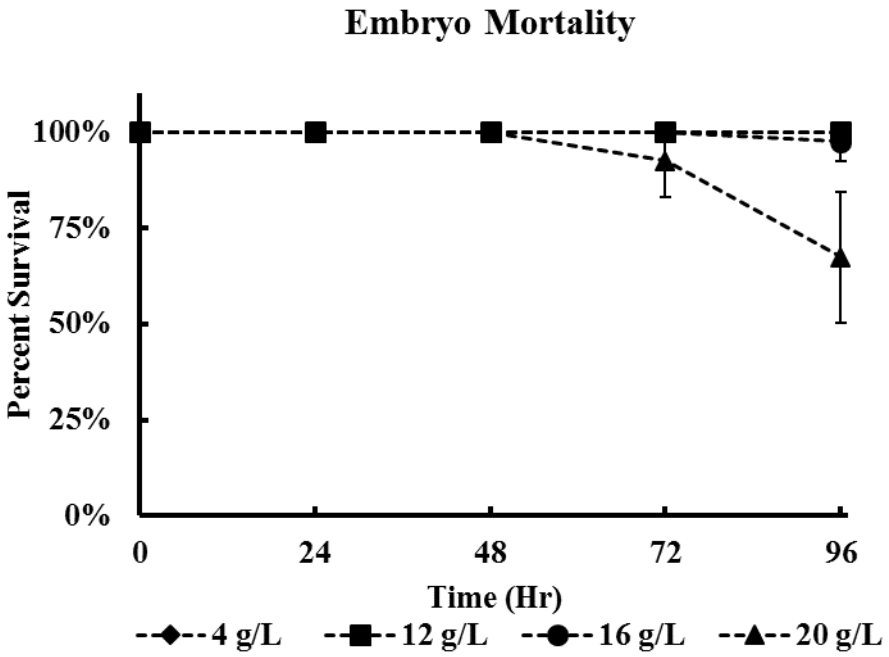

Figure 1. The mean (± standard deviation) percent survival of *F. grandis* embryos at 24, 48, 72, and 96 h during exposure to Corexit in 4, 12, 16, or 20 g/L waters. Mortalities were first noted at 96 h after exposure to Corexit in 16 g/L water and 72 h after exposure to Corexit in 20 g/L water.

Corexit toxicity based on killifish larval mortality was evident as early as between 24-48 hpt, and this toxicity was dependent on water salinity (Table 1). Corexit lethality increased the more the salinity diverged from 12 g/L; however, larvae were most sensitive to dispersant at higher salinities, compared to when exposed in 4 g/L water (Table 1; Figure 2). Corexit was by far the most toxic in 16 and 20 g/L water with survival rates of 0% to 20%, respectively, at 96 hpt, moderately toxic in 4 g/L water (survival of 45% ± 13%), and least toxic in the 12 g/L water (survival of 70% ± 8%; Table 1). Significant reductions in larval survivorship in response to Corexit exposure were first noted by 48 hpt in the 4 and 20 g/L salinities at 60% ± 8% ($p < 0.01$) and 40% ± 22% ($p < 0.01$), respectively; however, significant reductions in survivorship were noted at all salinities by 72 hpt ($p < 0.01$). A similar pattern in ET50 values in larvae with

treatment salinities was observed. Median effect time was most protracted in 12 g/L treatments (131.9 h), however, ET50's decreased by 42% (76.1 h) in 4 g/L treatments and were lowered by 53% (61.3 h) and 59% (53.9 h) in 16 and 20 g/L treatments, respectively, when compared to the ET50 of the 12 g/L and Corexit treatment (Table 2). As such, response slope values followed similar trends to ET50's. The smallest response slope for larvae was observed in the 12 g/L treatment (response slope of -2.95 ± 0.80. Compared to the 12 g/L result, the response slope increased by 8% in 4 g/L water (-3.19 ± 0.61); whereas response slopes increased by 61% (-7.58 ± 1.50) and 31% (-4.28 ± 0.91) in the 16 g/L water and 20 g/L water, respectively (Table 2).

Table 2. The median time to effect (ET50 value) ± 95% confidence intervals (in h) and the response slope (± standard error of the mean) and are provided in brackets for larvae and juvenile *F. grandis* exposed for 96 h to Corexit in 4, 12, 16, or 20 g/L water.

Life stage	Salinity (g/L)	ET50 (95% CI) (h)	Response Slope (± SE)
Larvae	4	76.1 (65.0-94.9)	-3.19 ± 0.61
	12	131.9 (100.0-292.7)	-2.95 ± 0.80
	16*	61.3 (53.3-69.0)	-7.58 ± 1.50
	20*	53.9 (42.2-65.7)	-4.28 ± 0.91
Juvenile	4	120.4 (85.0-359.4)	-1.77 ± 0.53
	12*	52.5 (38.8-63.4)	-6.88 ± 1.87
	16*	27.4 (25.8-29.5)	-24.79 ± 6.71
	20*	26.1 (24.3-27.8)	-18.45 ± 4.82

*Confidence limits were estimated using t-values adjusted by a heterogeneity factor to correct for overdispersion.

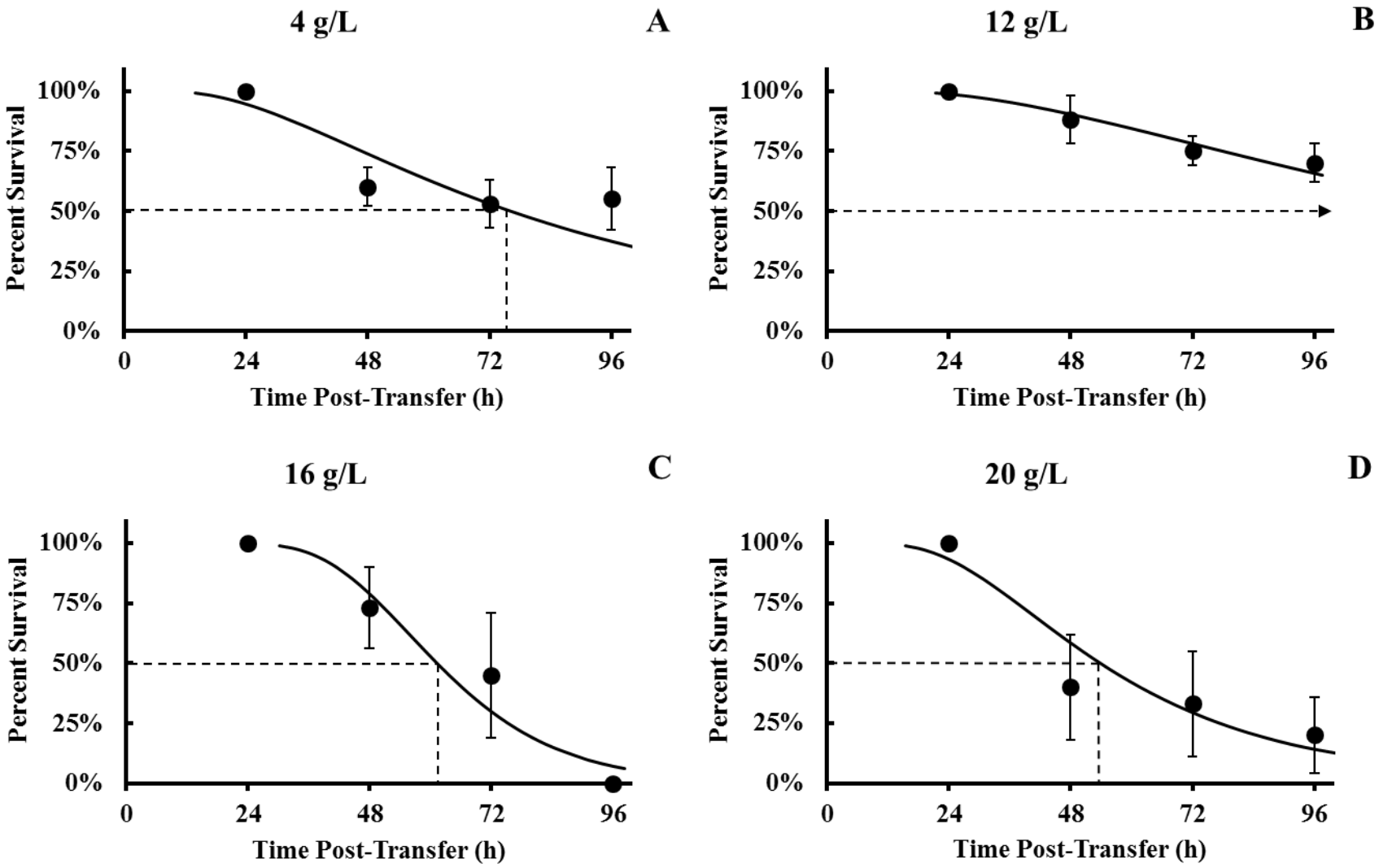

Figure 2. Percent survival (± standard deviation; ●) of larval *F. grandis* larvae during exposure to Corexit in 4 g/L (A), 12 g/L (B), 16 g/L (C), or 20 g/L (D) waters. Solid lines depict modeled percent survival over time and vertical dashed lines depict ET50 values and the open arrow for the 12 g/L exposure only depicts that a calculated ET50 value was beyond the 96-h exposure period

Juvenile mortality to Corexit in the 4, 16, and 20 g/L waters was first noted before 24 hpt (Table 1). Significant reductions in survivorship were first observed by 48 hpt in the 4 (70% ± 8%), 16 (0% ± 0%), and 20 g/L treatments (0% ± 0%; $p < 0.01$). However, survival curves suggest that Corexit killed juvenile fish at 16 g/L and 20 g/L quickly, but is moderately toxic at 12 g/L, and least toxic at 4 g/L (Figure 3), producing much lower ET50 values in hyperosmotic waters compared to the calculated values for larvae (Table 1; Figure 3). Furthermore, the most protracted ET50 and lowest response slope were calculated for juvenile fish exposed to Corexit at 4 g/L (ET50 of 120.4 h, response slope of -1.77 ± 0.53), with the ET50 value decreased by 78% (26.1 h) and response slopes increased by 90% (-18.45 ± 4.82) as water salinity was increased to 20 g/L (Table 2). The correlation between salinity and Corexit toxicity at this life stage is reinforced by the fact 65% ± 10% of juveniles survived at 4 g/L dispersant waters, whereas by 96 h, there were no surviving juveniles in any of the other salinities (Table 1).

Compared to all other killifish life stages, adult killifish were most sensitive to Corexit, with mortality occurring rapidly, particularly in the hyperosmotic waters (i.e., within the first 24 h of exposure; Table 1). Significant reductions in survivorship were observed in adult fish transferred to 4, 16, and 20 g/L salinity waters treated with Corexit by 24 hpt ($p < 0.05$; Table 1). No adult fish survived 24 h of Corexit exposure in 16 g/L and 20 g/L water salinities, whereas, percent survival was 70% ± 14% in 4 g/L water at 24 h. Only one fish was documented as moribund at 24 h with Corexit in 12 g/L water.

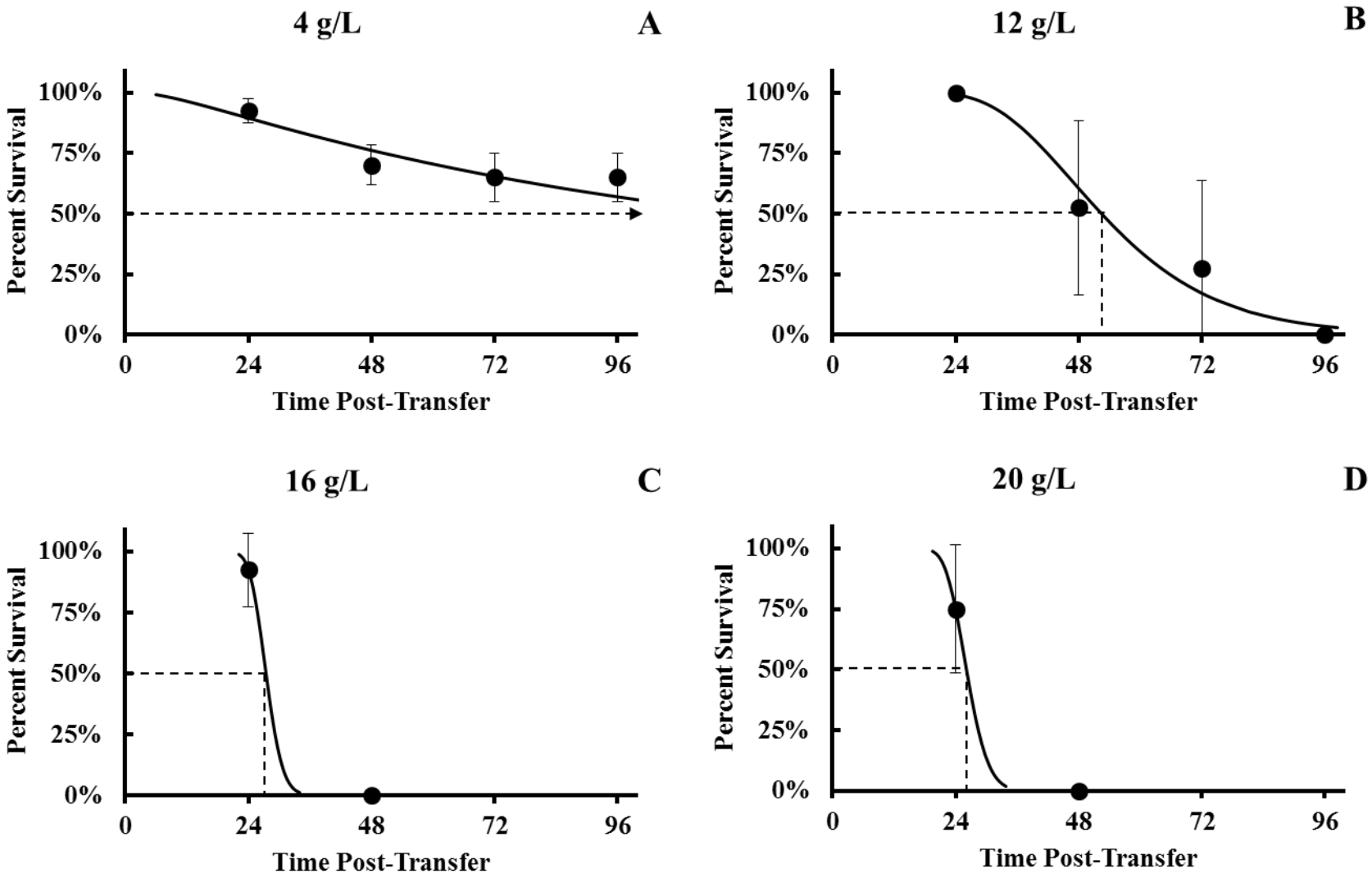

Figure 3. Percent survival (± standard deviation; ●) of juvenile *F. grandis* during exposure to Corexit in 4 g/L (A), 12 g/L (B), 16 g/L (C), or 20 g/L (D) waters. Solid lines depict modeled percent survival over time and vertical dashed lines depict ET50 values and the open arrow for the 4 g/L exposure depicts that a calculated ET50 value was beyond the 96-h exposure period.

Sodium and Chloride Concentrations in Whole-body or Plasma at Multiple Life Stages

No significant differences in larval whole-body sodium concentrations ($[Na^+]$) were detected between control salinities, which ranged from mean values of 226.4 ± 22.6 mmol Na^+/kg dw (n = 8) in the 20 g/L treatment to 274.2 ± 67.3 mmol Na^+/kg dw (n = 9) in the 4 g/L treatment (Figure 4A). Whole-body $[Na^+]$ significantly increased from 226.4 ± 22.6 mmol Na^+/kg dw (n = 8) in larva held in 20 g/L control water to 376.1 ± 56.5 mmol Na^+/kg dw ($p < 0.01$; n= 4) in larva exposed to Corexit, representing a 1.6-fold increase. No significant differences in whole-body chloride concentrations ($[Cl^-]$) were detected between salinity controls, which ranged from mean values of 109.2 ± 10.9 mmol Cl^-/kg dw (n = 8) in the 12 g/L treatment to 148.1 ± 29.0 mmol Cl^-/kg dw (n = 8) in the 20 g/L treatment (Figure 4B). Exposure to Corexit significantly increased whole-body $[Cl^-]$ to 203.8 ± 35.9 mmol Cl^-/kg dw ($p < 0.01$; n= 6) and to 270.2 ± 43.2 mmol Cl^-/kg dw ($p < 0.01$; n= 4) in 12 g/L and 20 g/L treatments, respectively.

No significant difference in juvenile whole-body $[Na^+]$ was detected between control salinities, which ranged from mean values of 109.3 ± 3.7 mmol Na^+/kg dw (n = 10) in the 20 g/L treatment to 120.4 ± 5.0 mmol Na^+/kg dw (n = 9) in the 12 g/L treatment (Figure 4C). Whole-body $[Na^+]$ of 237.0 ± 74.1 mmol Na^+/kg dw ($p < 0.01$; n= 3) and 221.6 ± 29.7 mmol Na^+/kg dw ($p < 0.01$; n= 7) were measured in juvenile fish in 16 g/L and 20 g/L waters with Corexit, respectively. Juvenile whole-body $[Cl^-]$ ranged from mean values of 111.6 ± 2.3 mmol Cl^-/kg dw (n =8) in control 12 g/L treatment to 122.6 ± 2.9 mmol Cl^-/kg dw (n = 10) in the control treatment of 20 g/L, between which significant differences were detected ($p = 0.048$; Figure 4D). Corexit significantly increased whole-body $[Cl^-]$ to 199.9 ± 22.8 mmol Cl^-/kg dw ($p < 0.01$; n= 3) and 190.4 ± 14.1 mmol Cl^-/kg dw ($p < 0.01$; n= 6) in the 16 g/L and 20 g/L waters, respectively.

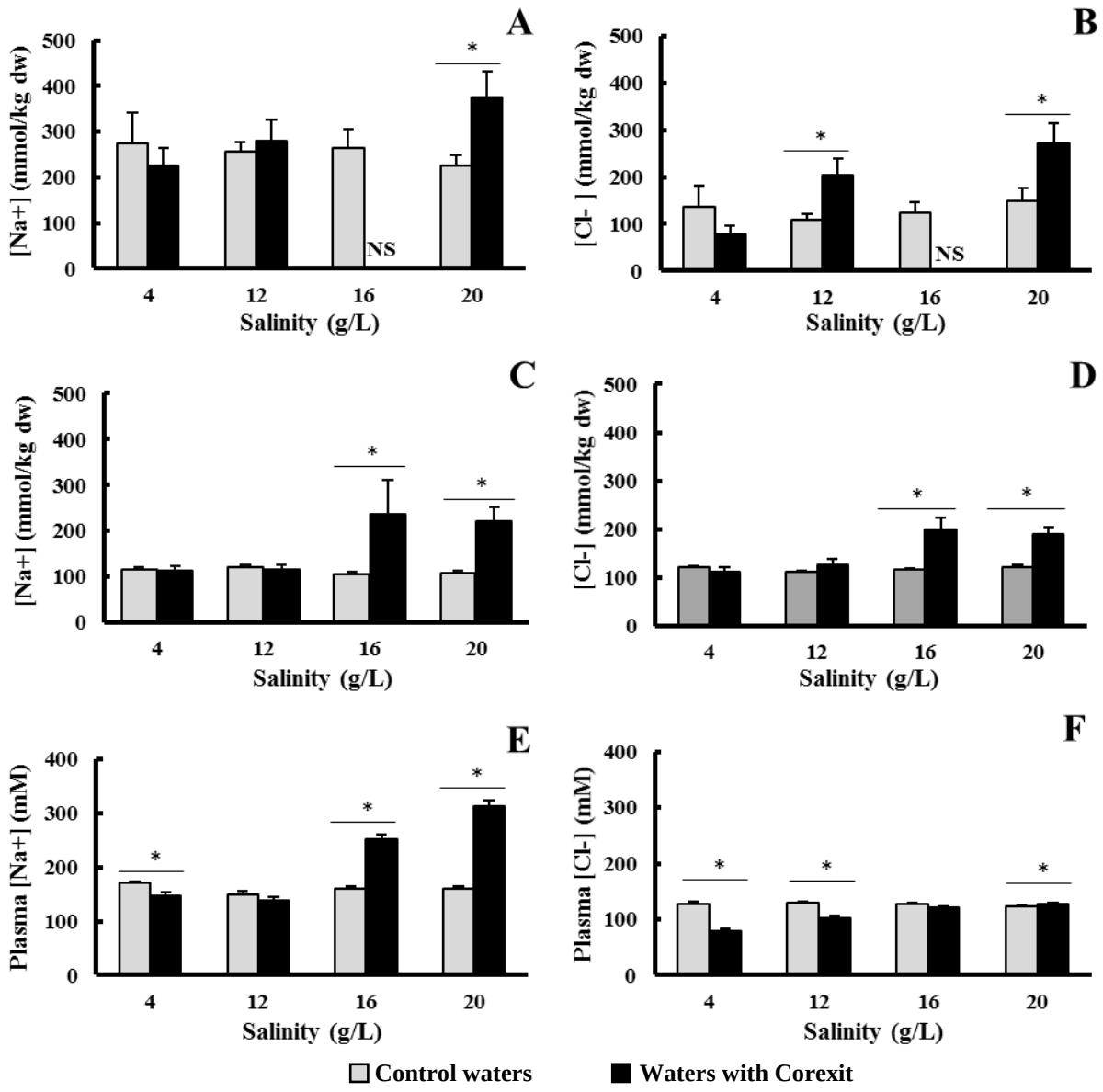

Figure 4. Mean (± standard error of the mean) sodium and chloride concentrations in whole-body larvae (A and B) and juveniles (C and D), or plasma of adult (E and F) Gulf killifish, *F. grandis*, following acute salinity transfers into control waters with no Corexit (□) and waters with Corexit (■). Asterisks represent significant differences ($p < 0.05$) between control and Corexit-exposed groups within salinities. No larvae survived (NS) to the end of the 96-h assay.

Only moribund and not dead fish were sampled for hematological data in the 16 and 20 g/L Corexit treated waters. Plasma [Na^+] ranged from 150.3 ± 6.2 mM Na^+ (n = 9) in the 12 g/L treatment to 170.1 ± 3.2 mM Na^+ (n = 8) in the 4 g/L treatment (Figure 4E). Significant

differences in plasma [Na^+] of adult killifish were detected ($p = 0.03$) between fish in 4 g/L and 12 g/L controls at 170.1 ± 3.16 mM ($n = 8$) and 150.3 ± 6.2 mM ($n = 9$), respectively (Figure 4E). No other significant differences in plasma [Na^+] were detected between control treatments. Exposure to Corexit at 4 g/L produced a significant decrease of 1.2-fold in plasma [Na^+] from 170.1 ± 3.2 mM Na^+ ($n = 8$) to 146.7 ± 7.2 mM Na^+ ($p < 0.01$; $n = 8$), and significant 1.6- and 2-fold increases in plasma [Na^+] were detected in fish transferred to 16 g/L water (251.6 ± 9.1 mM ($p < 0.01$; $n = 3$)) and 20 g/L water (313.8 ± 9.9 mM Na^+ ($p < 0.01$; $n = 8$)) with Corexit (Figure 4E). There was no significant difference in the plasma [Na^+] between adult fish exposed to control water versus those exposed to Corexit at 12 g/L. No significant difference in adult plasma [Cl^-] was detected between control salinities, which ranged from 122.3 ± 3.0 mM Cl^- ($n = 9$) in the 20 g/L treatment to 129.6 ± 2.0 mM Cl^- ($n = 9$) in the 12 g/L treatment (Figure 4F). Corexit significantly decreased plasma [Cl^-] by only 1.6- and 1.3-fold in adults transferred to the 4 g/L (79.5 ± 2.6 mM Cl^- ($p < 0.01$; $n = 9$)) and 12 g/L (101.6 ± 3.8 mM Cl^- ($p < 0.01$; $n = 10$)) treatments; however, a significant increase in plasma [Cl^-] was detected in 20 g/L (130.3 ± 1.8 mM Cl^- ($p = 0.03$; $n = 10$)) treatment fish.

Estimates of Net Ion Flux Rate Impairment by Corexit

Whole-body ion burdens for larvae and juvenile fish and plasma ion concentrations in adult fish were used to estimate the change in net flux rate (ΔJ_{net}^{ion}) in treatment fish compared to the 12 g/L control fish. These estimates allowed an evaluation of the mean net flux rate of Na^+ and Cl^- over the exposure period following salinity transfer with and without Corexit that would have produced the changes in whole-body ion or plasma ion concentrations. The estimates of $\Delta J_{net}^{Na^+}$ and $\Delta J_{net}^{Cl^-}$ of larvae and juveniles transferred from 12 g/L water to 4 g/L, 16 g/L, or 20 g/L were negligible, ranging from -0.09 to 0.07 mmol Na^+/ kg ww/ h (Table 3). Similarly, for adult

fish, change in net Na^+ flux ranged from 0.13 to 0.25 mmol Na^+/ kg ww/ h and the change in net Cl^- flux ranged from -0.03 to -0.15 mmol Cl^-/ kg ww/ h. Collectively, these data support the maintenance of ion balance in fish transferred acutely from 12 g/L to the other three salinities when no Corexit was present in the water.

The influence on Corexit on estimated $\Delta J_{net}^{Na^+}$ rates in killifish was dependent on the life stage and the salinity fish were transferred to. Corexit elicited a large increase in the estimated mean net Na^+ flux rate of 3.60 ± 0.14 mmol Na^+/ kg ww/ h at 20 g/L (*n*=8) over a 24-h exposure period. In comparison, the change in estimated net Na^+ flux rate produced by Corexit in 4 g/L was negligible (-0.05 ± 0.10 mmol Na^+/ kg ww/ h, *n*=8). The greatest impact of Corexit on estimated net Na^+ flux rate in larvae and juveniles was in 20 g/L salinity water, causing an accumulation of Na^+ at rates of 0.73 ± 0.14 (*n*=5) and 0.63 ± 0.26 (*n*=7) mmol Na^+/ kg ww/ h at 20 g/L, respectively, relative to the 12 g/L control fish. Estimated $\Delta J_{net}^{Na^+}$ resulting from Corexit exposure for larval killifish transferred to 4 and 12 g/L treatments suggested overall greater rates of Na^+ accumulation over loss, unlike in juvenile and adult killifish transferred to the same salinities (Table 3).

In comparison, Corexit had its greatest effect on mean $\Delta J_{net}^{Cl^-}$ rates in larvae and juveniles exposed concomitantly with 20 g/L water, showing net accumulation at 0.57 ± 0.09 (*n*=6) and 0.42 ± 0.17 (*n*=6) mmol Cl^- / kg ww/ h (Table 3). However, the opposite was true for adult killifish, where $\Delta J_{net}^{Cl^-}$ was smallest in killifish transferred into the 20 g/L treatment (0.03 ± 0.06 mmol Cl^- / kg ww/ h at 20 g/L, *n*=10), although a net loss of Cl of -1.08 ± 0.09 mmol Cl^- / kg ww/ h (*n*=7) was estimated for fish in 4 g/L.

Discussion

The dispersant Corexit contains amphipathic chemicals that solubilize hydrocarbons to form water/oil emulsions that facilitate oil degradation. Due to their amphipathicity, surfactants at high enough concentrations may disrupt biological membranes by interacting with membrane phospholipids and proteins (Heerklotz, 2008; John et al., 2016; Jones, 1992; Schreier et al., 2000). The gills of sheepshead minnow (*Cyprinodon variegatus*) exposed to Corexit, or solely to its primary surfactant, DOSS, have high levels of reactive oxygen species and reduced antioxidant molecules suggesting oxidative stress (Dasgupta et al., 2018). Increased expression of NOX4, an oxidase responsible for apoptosis-associated ROS production, was observed in Corexit exposed zebrafish (*Danio rerio*) gills (Li et al., 2015). Furthermore, exposure to another anionic surfactant, sodium dodecyl sulfate, results in hyperplasia of the lamellar epithelium of turbot (*Scophthalmus maximus*) gill because of fusion of the secondary epithelia and hemorrhage (Rosety-Rodríguez et al., 2002). Although not measured in the current study, these effects potentially lead to abnormal tissue growth and cytoxicity that produce edema to the primary filaments and the lamellae of the gill, which often result in terminal necrosis and impairment of many of the physiological processes of the gill epithelium, including respiratory and osmotic regulation (Strzyzewska et al., 2016).

Osmoregulation is a particularly critical process in euryhaline fishes due to the differing impacts of fresh water and salt water on organism homeostasis. To test the effects of environmental salinity on Corexit toxicity, the euryhaline Gulf killifish was chosen as the experimental animal model. Gulf killifish can tolerate environmental salinities ranging from fresh water to full-strength sea water and can maintain internal osmotic balance during acute salinity transfer due to the renowned capacity of their transporting epithelia to undergo

Table 3. Estimated ΔJ_{net}^{ion} and percent water content (mean ± standard error of the mean) following exposure of *F. grandis* to Corexit at larval, juvenile, and adult life stages. Calculations for ΔJ_{net}^{ion} were performed as outlined in in Equations 1 and 2. See text for details. Percent water content is reported as whole-body water weight (†) for larval and juvenile fish and as muscle water weight (‡) for adult fish. No larvae survived (NS) to the end of the 96-h assay.

Life stage	Salinity (g/L)	Estimated $\Delta J_{net}^{Na^+}$ (mmol/ kg ww/ h)				Estimated $\Delta J_{net}^{Cl^-}$ (mmol/ kg ww/ h)				Percent Water Content			
		Control		Corexit		Control		Corexit		Control		Corexit	
		Mean ± SEM	n=	Mean ± SEM	n=	Mean ± SEM	n=	Mean ± SEM	n=	Mean ± SEM	n=	Mean ± SEM	n=
Larval	4	-0.03 ± 0.05	7	0.13 ± 0.08	9	-0.02 ± 0.02	5	0.02 ± 0.03	6	86.5% ± 3.8%†	9	77.5% ± 3.4%†	9
	12	0.00 ± 0.05	8	0.09 ± 0.03	10	0.00 ± 0.03	9	0.12 ± 0.02	7	89.2% ± 1.6%†	5	82.2% ± 3.6%†	10
	16	-0.02 ± 0.04	9	NS	0	0.07 ± 0.04	10	NS	0	86.8% ± 2.0%†	8	NS	0
	20	-0.09 ± 0.03	9	0.73 ± 0.14	5	-0.03 ± 0.02	8	0.57 ± 0.09	6	90.8% ± 1.5%†	8	82.5% ± 3.6%†	6
Juvenile	4	-0.03 ± 0.01	10	-0.07 ± 0.05	10	0.00 ± 0.00	10	-0.05 ± 0.05	10	78.4% ± 0.4%†	10	78.8% ± 0.7%†	10
	12	0.00 ± 0.01	9	-0.06 ± 0.03	5	0.00 ± 0.01	10	0.01 ± 0.03	5	77.3% ± 0.4%†	10	78.7% ± 0.6%†	5
	16	-0.03 ± 0.02	9	0.34 ± 0.47	3	0.02 ± 0.01	9	0.14 ± 0.13	3	76.3% ± 0.5%†	9	85.2% ± 1.2%†	2
	20	-0.02 ± 0.01	10	0.63 ± 0.26	7	0.02 ± 0.01	10	0.42 ± 0.17	6	77.1% ± 0.4%†	10	80.0% ± 9.1%†	2
Adult	4	0.28 ± 0.05	8	-0.05 ± 0.10	8	-0.03 ± 0.06	9	-1.08 ± 0.09	7	76.7% ± 0.5%‡	8	77.3% ± 2.1%‡	10
	12	0.00 ± 0.09	9	-0.16 ± 0.08	8	0.00 ± 0.07	9	-0.58 ± 0.08	10	77.3% ± 0.4%‡	9	77.9% ± 0.5%‡	8
	16	0.14 ± 0.06	9	1.61 ± 0.15	3	-0.03 ± 0.04	8	-0.20 ± 0.08	4	77.3% ± 0.3%‡	9	75.1% ± 0.6%‡	5
	20	0.14 ± 0.06	8	3.60 ± 0.14	8	-0.15 ± 0.06	9	0.03 ± 0.06	10	71.3% ± 3.3%‡	10	71.6% ± 3.4%‡	10

physiological adjustments (Evans et al., 2005). Thus, the current study was designed to test the effects of Corexit toxicity to Gulf killifish following acute salinity transfers.

Two separate approaches to study the effects of Corexit on osmoregulation in the Gulf killifish were taken. First, given that osmoregulatory systems develop progressively during ontogeny in *F. grandis* and other euryhaline species (Bodinier et al., 2010; Katoh et al., 2000; Patterson et al., 2012; Perschbacher et al., 1990; Varsamos et al., 2005), we studied the toxicity of Corexit in embryos and larvae when osmoregulatory organs were expected not to be fully developed before first feeding, in juveniles approaching osmoregulatory competence, and in adults when osmoregulatory systems were well established. Based on this ontogenic progression in osmoregulation and the potential of Corexit to interact on biological membranes like the fish gill, Corexit should be least toxic in embryos and most toxic in juveniles or adults. Second, we studied the combined effects of Corexit and salinity transfer to further interrogate the effects of Corexit on fish osmoregulation. It was originally hypothesized that Corexit toxicity would be highest in fish transferred to salinities farthest removed from the isosmotic levels of their extracellular fluids, which is equivalent in osmolality to water of approximately 11 to 12 g/L in salinity (Fritz and Garside, 1974). Thus, impairment of gill function by Corexit in isosmotic conditions might produce a less discernible impact on internal osmolyte balance compared to exposure in hyperosmotic or hypoosmotic salinities when the gills are most taxed with maintenance of internal salt homeostasis.

The early-life stages of animals are typically most sensitive to environmental toxicants relative to more developed late life stages due to high metabolic rates on a per mass basis, the not yet fully expressed xenobiotic metabolism and elimination pathways (Mohammed, 2013), and the large whole-body surface area to volume ratio that allow for increased contact with

environmental toxicants (Kleinow et al., 2008). For instance, many of the toxic components of crude oil are readily absorbed across the skin or gills due to their hydrophobicity of the compound and the large biological membrane surface area of the gill for accumulation (Kleinow et al., 2008). Once absorbed, these compounds produce teratogenic effects that perturb normal organ development and lead to delayed impacts on organismal fitness (Heintz et al., 2000; Hicken et al., 2011). However, with regards to the first experimental objective, the sensitivity to Corexit was low in embryos but increased progressively with fish development as indicated by decreasing percent survival and ET50 values at each progressive life stage (Table 1 and Table 2). The very low sensitivity of Corexit to killifish embryos may be explained in part by the presence of the chorion, which has been shown to protect developing embryos to some aquatic toxicants, such as carbaryl, an insecticide, and thiobencarb, an herbicide (Kashiwada et al., 2008; Villalobos et al., 2000). Since polyethylene glycols less than ≤ 3 kDa in size were found to pass through pores of embryonic fish chorions (0.5-0.7 µm; Pelka et al., 2017; Rawson et al., 2000), DOSS, with a molecular size of 0.45 ≤ kDa, which is approximately 1.5 times larger than the previously mentioned polyethylene glycols, is potentially small enough to pass through chorionic pores of embryonic killifish (1.0-1.5 µm in *F. heteroclitus*; Armstrong and Child, 1965). However, it is possible that negatively-charged N-linked glycoproteins located on the teleost chorion (Lee et al., 2005; Peterson and Martin-Robichaud, 1987) and negatively-charged colloids in the perivitelline fluid (Peterson and Martin-Robichaud, 1986) may inhibit the movement of anionic DOSS into embryonic tissue and limit toxicity.

Despite the potential the chorion may have protected embryos from Corexit toxicity, other factors were likely important. For instance, the sensitivity of larvae to Corexit was low compared to that observed in juveniles and adult killifish despite the predictably high surface

area to volume ratio of larvae but despite the absence of a chorion following hatch. Although larvae may possess physiological mechanisms to protect them from Corexit, their low response to toxicity could also be explained by their incomplete development of target organs. The gills are one such organ that is only rudimentarily developed at hatch and becomes fully functional post hatch (Post and Lee, 1996). As metabolism increases in rapidly-growing fish, the use of gills as an organ for respiration and osmoregulation is necessary. Shortly after hatch, larvae transition out of the yolk-sac stage, initially with respiration occurring cutaneously and ionoregulation occurring primarily in mitochondrion-rich cells located on the yolk-sac (Katoh et al., 2000). Absorption of the yolk-sac and thickening of the skin constrain cutaneous ionoregulatory capabilities of growing larval fish, increasing reliance on the developing gill to meet osmoregulatory demands (*for review see* Brauner and Rombough, 2012). Katoh et al. (2000) observed initial development of gill filaments that corresponded with absorption of the yolk sac in *Fundulus heteroclitus* held at 20 °C at 4 dph. In the current study, larval mortalities began approximately 48 hours after transfer to treatment waters (Table 1), which may correspond with initial development of gill filaments as developmental rates of larvae were potentially accelerated due to holding them at 25 °C. Wilson (1977) also observed increased sensitivity to older generation dispersants in multiple larval marine teleosts transitioning out of the yolk-sac stage. Furthermore, increased Corexit sensitivity at post-larval stages is likely a result of continued maturation of the gill as killifish gills are not fully metamorphosed until between 1 to 4 weeks post hatch (*data not shown*). Thus, it is likely that the gills are the main target organ of Corexit toxicity and that increased gill surface area likely contributes to Corexit sensitivity in fish.

Consistent with reports of strong euryhalinity, no differences in the whole-body Na^+ and Cl^- content of larvae or juvenile killifish exposed in salinities of 4 g/L to 20 g/L in the absence of

dispersant were observed (Figure 4). Similarly, the plasma ion concentrations of adult killifish exposed to the range of salinity treatments remained constant. So, despite differences in the ontogeny of osmoregulation in killifish, the species is euryhaline throughout all life stages tested, even though the gills may not be fully functional for at least a few weeks post hatch. In contrast, dispersant significantly impaired the ability of killifish to maintain osmotic balance following these acute salinity transfers. Assuming that dispersant was disrupting gill integrity or affecting osmoregulatory processes in the gill, we hypothesized that fish would be most sensitive to dispersant in hyperosmotic or hypoosmotic waters and least sensitive to dispersant in isosmotic waters. Furthermore, we expected that Corexit would increase internal salt load in hyperosmotic waters but decrease it in hypoosmotic waters. In fact, as predicted, the tendency of Corexit to impair hypoosmoregulation in hyperosmotic waters and for it to impair hyperosmoregulation in hypoosmotic waters was observed, although these physiological effects of Corexit differed in magnitude amongst life stages.

A reduction in whole-body Na^+ and Cl^- content was observed in control fish transitioning from larval to juvenile life stages (Figure 4 A-D). This may be explained in part by a temporary accumulation of ions in larval stages following hatch and by an increase in percent contribution of somatic tissue to whole-body mass (quantified by percent dry weight) as fish grow and transitioned into later life stages (Guggino, 1980; Rombough, 2007). Ions accumulate from the environment following hatch to meet physiological requirements associated with rapid growth with a concomitant increase in whole-body extracellular fluid (Rombough, 2007). However, the rapid growth observed in fish transitioning from larval to juvenile stages is a result of increasing percentage of structure associated somatic tissue contributing to whole-body weight (Post and Parkinson, 2001; Weatherley et al., 1979; Wuenschel et al., 2006). Thus, the reduction in growth

rate and percent water content at the juvenile stage possibly contributed to the overall reduction in whole-body ion content on a per gram basis. Shearer (1984) noted reductions in whole-body ion composition on a per gram basis in rainbow trout (*Oncorhynchus mykiss*) at post-juvenile stages corresponding to increases in percent whole-body dry weight. As such, the reduction in whole-body ion concentration at the juvenile stage may have resulted in a reduction in whole-body osmolality. A presumed reduction in whole-body osmolality would explain why larvae were least sensitive to Corexit at 12 g/L (Figure 2B) but juveniles were least sensitive at 4 g/L (Figure 3A) as hypoosmotic regulation in hyperosmotic waters (see above) might have contributed to Corexit toxicity.

In general, adult killifish were much more sensitive than were larvae and embryos to the combined effects of dispersant and salinity transfer. Relative to control killifish, adults exposed to dispersant in hyperosmotic waters had higher plasma ion concentrations compared to fish in 16 or 20 g/L water alone, and fish exposed to dispersant in hypoosmotic waters had significantly lower plasma ion levels than salinity controls (Figure 4E and Figure 4F). In hyperosmotic waters, dispersant might impair active salt excretion, enhance passive ion accumulation, or both, collectively leading to the increase in the whole-body and/or plasma concentrations of Na^+ and Cl^- observed. In comparison, dispersant in hypoosmotic waters could impair the mechanisms of active salt accumulation, enhance passive ion loss, or both. With this said, we found that Corexit was most efficacious at disrupting osmotic balance when exposed concomitantly in 20 g/L compared to exposure to 4 g/L; this despite both salinities being approximately 8 g/L from the pre-transfer salinity of 12 g/L, a salinity that approximates the internal osmolality of killifish (Fritz and Garside, 1974). The cause of the greater mortality of adult killifish to Corexit in waters of higher salinity is unclear, however, there is evidence that the dispersant impaired

osmoregulation by more than simply disrupting the integrity of the gill epithelial structure. If Corexit were simply damaging the epithelial structure, ion homeostasis for both Na^+ and Cl^- would likely have been equally impaired, or in fact, plasma Cl^- might have increased more than plasma Na^+ given the higher diffusive gradient of the ion between the hypersosmotic water and the extracellular fluid of killifish. In comparison, there was a much greater differential accumulation of [Na^+] over [Cl^-] in the plasma in the 16 and 20 g/L treatments and a differential loss of plasma [Na^+] over [Cl^-] in 4 g/L, suggesting that mechanisms of Na^+ regulation at the site of the gill were affected by Corexit.

The process of hypoosmoregulation is mediated by extensive remodeling of gill epithelia to support the active secretion of ions. Specifically, an increased presence of leaky tight junctions located between accessory cells and mitochondrion-rich cells in gills facilitates paracellular Na^+ secretion (Hwang et al., 2011), driven by the electrochemical gradient established by the transcellular excretion of Cl^-. Although not measured in the current study, it is possible that Corexit-induced histopathological alterations of gills prevented appropriate gill remodeling that would have allowed for increased Na^+ excretion via leaky tight junctions. Li et al. (2015) observed decreased expression of intercellular tight junction proteins ZO-1, ZO-2, and occludin because of Corexit-induced cytotoxicity in a human bronchial epithelial cell line (BEAS-2B). Consequently, disruption of cytoskeletal proteins associated with cell-cell interactions may have induced reflexive epithelial hyperplasia and lamellar fusion observed in fish gills exposed to anionic surfactants (Rosety-Rodríguez et al., 2002), possibly interfering with the paracellular permeability. These data suggest Corexit may impair Na^+ secretion at leaky paracellular pathways but not affect transcellular Cl^- secretion in mitochondrion-rich cells.

The estimates of change in net flux rates using whole-body and plasma ion concentrations facilitated a more comprehensive understanding of the deleterious effects of Corexit on solute homeostasis. Several major observations were made about the influence of salinity and Corexit on solute balance in Gulf killifish. First, larvae, juvenile, and adult killifish maintained ion balance following acute salinity transfer in the absence of Corexit (Table 3). These data demonstrate an ability of killifish to effectively osmoregulate in the face of fluctuating salinity at all life stages, although this ability appears to improve with development and maturation of the gills (Katoh et al., 2000; Varsamos et al., 2005). Second, Corexit elicited an increase in net Na^+ accumulation in all life stages of killifish in 20 g/L water, although this effect was most pronounced in adults. The rate of Na^+ accumulation in adult fish was estimated at 3.60 mmol Na^+/kg ww/h, which is a 5.7-fold increase in accumulation rate compared to juveniles at the same salinity. Although unidirectional Na^+ flux rates were not measured in this study, the change in net flux was approximately 30% of the unidirectional flux rates of adult *F. heteroclitus* measured at a similar salinity (Prodocimo et al., 2007). This net change in Na^+ flux with Corexit could have been produced by an increase in the unidirectional Na^+ influx, a decrease in the unidirectional Na^+ efflux, or a combination of both. Third, the combined effects of Corexit and salinity transfer on Cl^- balance differed in some key ways to those described previously for Na^+ balance. For instance, whole-body Cl^- and Na^+ burdens increased at similar rates of net flux during the combined exposure to Corexit and 20 g/L water in larvae and juveniles, whereas in adults, estimated Cl^- accumulation was negligible but Na^+ accumulation was very high. In the latter case, net Cl^- balance in adults exposed to saline water was only marginally affected by Corexit. Although exposure of adult killifish to Corexit and 4 g/L water resulted in the largest estimated net change in Cl^- flux (-1.08 mmol Cl^-/kg ww/h) for any life

stage, this change closely resembles net Cl^- flux rates measured in *F. heteroclitus* acutely transferred from brackish to freshwater without instance of mortality, suggesting that Corexit may have had little additional effect (Wood and Laurent, 2003). Similar rates of change in Na^+ balance were estimated for adult killifish exposed to Corexit and 16 g/L salinity (1.61 mmol Na^+/kg ww/h); however, Corexit was more toxic at this salinity, suggesting that rate of Na^+ gain is more disruptive to killifish fitness than Cl^- loss. These data suggest that Corexit has differing impacts on osmoregulation in undeveloped animals than it does in adults.

The degree to which ion balance, and largely, Na^+ balance, is disrupted appears to correlate directly with percent survival over time. However, Corexit was more toxic to juveniles than larvae despite the two life stages possessing similar estimated ΔJ_{net}^{ion} rates at all salinities and the fact that larval killifish likely possessed the highest ionic influx and efflux rates relative to the embryonic and post-larval life stages (Guggino, 1980). Bodinier et al. (2010) observed that larval sea bream (*Sparus aurata*) reared at 25.5 g/L were able to tolerate large fluctuations in internal osmolality from an initial 360 mOsm/kg to a range of 230 to 490 mOsm/kg when subjected to acute salinity challenges of 5 and 39 g/L, respectively, following a 48-h exposure. Thus, despite their capacity to osmoregulate larval killifish may be partially tolerant to fluctuations in internal ion loads, as evident by the fact that larval killifish were able to survive longer than juveniles following exposure to Corexit at corresponding salinities despite experiencing similar estimated ΔJ_{net}^{ion} rates (Table 3). The ability to tolerate large fluctuations in internal osmolarity prior to gill development would be ecologically relevant considering the rapid salinity changes possible in salt marshes.

It should be noted that the salinities utilized in the current study were below the manufacturers' recommendation for its use in full-strength sea water. Salinity greatly influences

the solubility of surfactants, and thus, the functionality of dispersants, as salt decreases the rate of surfactant dissolution into the surrounding aqueous environment (Mackay et al., 1984), becoming less bioavailable (Chandrasekar et al., 2006). Regardless, biological effects of Corexit exposure were still detectible at the salinities utilized in this study and at recommended concentrations. Thus, it is not the intent of the authors to suggest application of Corexit in response to the oil spill could have endangered fish if subjected to acute salinity challenges in tidal marshes. However, the results of the current study provide a more comprehensive understanding of Corexit impacts in a euryhaline fish at different life stages while osmoregulatory systems are in different stages of development.

CHAPTER 3
CHARACTERIZATION OF WEATHERED MACONDO OIL DROPLETS SUSPENDED IN WAF SOLUTIONS AND ADSORBED TO GULF KILLIFISH CHORIONS

Introduction

When oil is dispersed in water (herein referred to as the water accommodated fraction or WAF) by mechanical agitation (e.g., wave action) or chemical dispersion (e.g., Corexit), constituents within the oil will partition to either the dissolved phase or to the particulate (e.g., droplet) phase. The partitioning of individual chemical constituents, such as polyaromatic hydrocarbons (PAH) between phases is dependent, in part, on the concentration and solubility of the specific hydrocarbon and the physicochemical properties of source oil from which it is derived. During the initial dispersal of oil, soluble PAHs; ~log octanol-water partition coefficient (K_{OW} <5-6) may dissolve into the surrounding aqueous medium while low solubility PAHs (~log K_{OW} >5-6) remain primarily associated with oil droplets (Sørensen et al., 2017; Sverdrup et al., 2002). Whereas the dissolved phase is considered highly toxic to aquatic animals due to the bioavailability of soluble PAHs (Di Toro et al., 2007), the degree to which droplets contribute to WAF toxicity is still under debate.

Although the contribution of low solubility PAHs to oil toxicity is likely minimal (Carls et al., 2008; Di Toro et al., 2007; Hansen et al., 2019a; Redman et al., 2017), some studies suggest that droplets may buffer soluble PAH concentrations in the dissolved phase (Landry et al., 2019). Under such a mechanism, PAHs diffuse from the droplet phase to the dissolved phase as components in the oil in the dissolved phase weather through microbial biodegradation, photooxidation, dissolution, and evaporation over time. The diameter and density of oil droplets

in dispersed oil can influence rate of dissolution of PAHs from the droplet to the dissolved phases. Constituents within smaller droplets, with their comparably large surface area to volume ratios, can diffuse more readily into the water column than PAHs found in larger droplets (Landry et al., 2019). Density differences between oil droplets and the aqueous environment surrounding them can also promote droplet vertical migration, with less weathered oils typically possessing lower densities compared to that of water (Tadros, 2013).

Oil droplets may also bind (i.e., adsorb) to animal surfaces during which time PAHs within the droplets could transfer from within the droplet into an animal (Petersen and Kristensen, 1998; Sørensen et al., 2017; Sørhus et al., 2015). This adsorption-mediated accumulation could circumvent the low bioaccumulation potential of PAHs with low water solubility. Because the contribution of PAHs to WAF toxicity would be dependent on their concentrations in the dissolved or droplet phase based on solubility constraints, the two phases would likely exert different toxicity potentials to aquatic organisms. Since PAHs within both the dissolved and droplet phases contribute to the total PAH concentration of a WAF sample but their relative toxicity may vary, it is important to understand the behavior of droplets in WAF solutions (Forth et al., 2017a; Redman et al., 2012; Sørhus et al., 2015). Thus, because a wide variety of droplet sizes and compositions would require extensive trials and replication a need exists for continuous, high-throughput evaluation of both suspended and membrane-adsorbed droplet behavior to better understand the changing toxicity of WAF solutions. Furthermore, recent investigations characterizing the contribution of droplets to WAF toxicity to embryonic fish have shown that the presence of an extrachorionic matrix found on the chorions of some species can limit the degree of droplet-chorion interactions and bioaccumulation (Hansen et al., 2019b; Hansen et al., 2018; Sørensen et al., 2017). The extrachorionic matrix is comprised of

glycoprotein-derived extrachorionic projections and/or a mucopolysaccharide jelly coat on the chorionic surfaces of numerous teleost species that attach their eggs to substrates (Riehl and Patzner, 1998). However, drawing conclusions from multiple species and toxicity endpoints confounds generalizations. Instead, experimental characterization of the extrachorionic matrix in oil droplet adherence within a single-species study design may provide further insights.

The goal of this research was to characterize suspended oil droplet behavior over time and to characterize oil droplet interaction with fish chorions. Three objectives were identified to accomplish this goal: 1) develop a high throughput method to quantify volume diameter and density of oil droplets; 2) apply the method to characterize oil droplet adsorption to embryonic fish chorions; and 3) apply the method to characterize the role of the extrachorionic matrix in adsorption. High energy and chemically enhanced dispersion methods were used to create WAF preparations of two differentially-weathered slick oils collected in the northern Gulf of Mexico during the Deepwater Horizon oil spill (DHOS) by skimmers during July 2010. Following WAF preparation, embryos were exposed over time to the oiled waters, and the water and fish embryos imaged by fluorescent stereomicroscopy to visualize oil droplets. In order to expedite oil droplet analyses in an unbiased manner, a custom macro within FIJI/ImageJ (Schindelin et al., 2012) was used for high-throughput processing and analyses of fluorescent microscopic images of water and fish embryos. While fluorescent imaging has been previously used to quantify oil droplet behavior on animal membranes and suspended in water, this is the first study to our knowledge that utilized a largely automated, high throughput method to quantify both in large volumes of samples. Specifically, we sought to characterize the interaction of oil droplets with Gulf killifish (*Fundulus grandis*) chorions, a species possessing an extrachorionic matrix (Riehl and Patzner, 1998) and known to have encountered DHOS oil (Dubansky et al., 2013).

Materials and Methods

WAF Preparation

Water accommodated fractions (WAF) of Macondo oil collected from the water surface of the northern Gulf of Mexico (GOM) were generated by either mechanical or chemical dispersion, producing a high energy WAF (HEWAF) or a chemically enhanced WAF (CEWAF), respectively, according to protocols developed by Incardona et. al. (2013) and Aurand and Coelho (2005). The two types of oil slicks consisted of oil collected by several skimmers on July 29, 2010 at the surface near the well head and transported by barge number CTC02404 (termed slick A) or collected near the mouth of the Mississippi River delta from the U.S. Coast Guard Cutter Juniper on July 19, 2010 (termed Slick B; BP Gulf Science Data, 2014. Further details on WAF preparation and filtration are described in Forth et al. (2017b). Chemical analyses demonstrated that slick B was considerably more weathered (85% depletion of 50 select PAH analytes [TPAH50] relative to hopane from source oil) than slick A (68% TPAH50 depletion; Forth et al., 2017b). HEWAF preparations were made using slick A and slick B, while CEWAF preparations were made using slick A only since dispersant efficacy is greatly reduced in highly weathered oils, such as slick B (National Research Council, 2005). In brief, all preparations were generated with a loading concentration of 2 g of oil per L of 12 g/L salinity water and diluted to a nominal concentration of 1.12 g of oil per L prior to embryo exposure. HEWAF preparations were first blended (Warring Commercial Blender, CB15) at 15,000 RPM for 30 s followed by a 1-h settling period in 1-L separatory funnels. CEWAF preparations were generated by adding Corexit 9500A to an oiled water mixture at a 1:10 dispersant-to-oil ratio, which was gently vortexed for 18 h and allowed to settle for 6 h.

Characterization of Suspended Oil Droplets in Water

The numerical density (hereafter referred to as density) and mean volume diameter (hereafter referred to as diameter; µm) of suspended oil droplets were assessed over time for HEWAF and CEWAF preparations of slick A oil and the HEWAF preparation of slick B oil. A subsample of each WAF preparation was filtered, and the remainder of each left as unfiltered. Filtered and unfiltered WAF samples were imaged immediately following preparation (0 h) and at 1, 3, 6, and 48 h post preparation by placing them on a glass slide under coverslip and a 3.2 mm by 2.4 mm field of view imaged with a Zeiss SteREO Lumar V12 interfaced with a MRc5 camera at 150-times magnification and 0.25 s exposure under combined bright-field/UV illumination (Ex 450-490 nm / Em LP397 nm). Due to a technical issue (lighting source malfunction), slick A CEWAF was imaged at 5 h and not 6 h following preparation. Suspended oil droplets were analyzed using a macro developed in FIJI/ImageJ (Schindelin et al., 2012; Appendix B-Suspended Droplet Macro) that enhanced droplet image contrast, enumerated droplets, and measured diameter. Accuracy of the method was verified with standard fluorospheres (10 µm diameter; Beckman Coulter Life Sciences), which gave a measured diameter of 10.1 ± 0.1 µm (n = 1,214; see *Image Analysis* below for details).

Collection and Oil Exposures of Fish Embryos

Field-collected Gulf killifish from Cocodrie, LA were used as a broodstock for procurement of embryos by *in vitro* fertilization. Embryos were reared at an ambient temperature of 23 °C at a salinity of 10 g/L prior to and during their use in experiments. Embryos were exposed to WAF between the onset of organogenesis (beginning at stage 19, or approximately at 3 days post fertilization) up to 5 days post fertilization (Armstrong and Child, 1965). In a subsample of embryos, the extrachorionic matrix was mechanically scrubbed from the surface of

the chorion with forceps and a probe (hereafter referred to as “cleaned chorions”), whereas embryos with their matrix intact were referred to as “natural chorions”. Embryos with natural chorions were divided among 5 replicates (n = 25 embryos per replicate) per treatment for unfiltered and filtered WAF exposures. Due to time constraints associated with the chorion cleaning, embryos with cleaned chorions (n = 10) from a single replicate were exposed to unfiltered WAF treatments. Embryos were exposed to 250 mL WAF treatments immediately following settling and held in glass containers on an orbital shaker (29 RPM) for either 3 or 6 h, after which, embryos (n = 10 per treatment) and water samples (*as described above*) were imaged for analyses of density and droplet diameter. For embryo imaging, oil droplets were imaged under UV fluorescent light at 75x magnification. In order to obtain in focus images along the spherical embryo, a series of images at multiple focal planes (12 images at 12 s exposure per image) along the z-axis of the embryo were collected and projected to a composite image using in focus pixels of the 12 slices using extended depth of focus. Only the upper half of each embryo (6.74 ± 0.04 mm^2, n = 120; mean ± SEM) was imaged to avoid semi-obscured quantification of droplets adsorbed to the underside of the embryo. Following imaging, embryos (n = 10 per treatment) were transferred to clean 12 g/L saltwater and were monitored once daily for survival and hatch for up to 21 days post fertilization. Additional embryos (n=115 per treatment, each embryo weighed approximately 4.9 mg) were collected after WAF exposures and held at -20 °C until analysis of total polyaromatic hydrocarbon concentrations for estimates of bioaccumulation (*data not shown*).

Analysis of Oil Droplets on the Fish Chorion

A second macro was developed for FIJI/ImageJ (Schindelin et al., 2012) to account for UV light transmitted through embryonic tissue and to enumerate and size droplets on the surface

of fish embryos (Appendix B-Adsorbed Droplet Macro). Images were reviewed for the presence of autofluorescence from exogenous particulates, were manually removed from the dataset prior to statistical analysis. Oil droplet diameters were binned up to the nearest whole µm to assess the distribution of droplet diameter adhering to the chorion versus droplet diameter in the WAF. Embryo diameters were measured in ImageJ and used to calculate adsorbed droplet count-density per mm^2. Droplet mass was determined by first calculating the volume of an individual droplet for each discreet 1 µm bin for droplets. The mass of each droplet for each oil type was calculated by using equation 3.

$$\text{mass (in g)} = \text{volume (in } \mu m^3) \times \text{ density (in } \frac{g}{cm^3}) \text{ x } 10^{-12} \quad \text{(equation 3)}$$

where the physicochemical density of slick A is 0.98 g/cm^3 and that of slick B is 1.00 g/cm^3 at 16 °C from Forth et al. (2017b). The total droplet mass (in g) of chorion adsorbed droplets binned to a discrete diameter was calculated from the product of the droplet mass (g per droplet) of the specific binned droplet diameters and the count density of that droplet diameter class (refer to Appendix B - Table S1-3). Under the assumption that adsorbed droplet distribution was uniform across the entirety of the chorion, that product was then multiplied by the mean total surface area of embryos used in the current study (13.48 mm^2).

Statistical Analysis

Kernel density (KD) plots were generated in Sigmaplot (v 14) using binned droplets to compare droplet diameter distribution in WAF preparations over time. A common smoothing parameter of 0.5 was selected to compare droplet count-densities across time and WAF type while accurately describing the data without over- or undersmoothing the data (Bowman and Azzalini, 1997). Oil type and WAF preparation methodology (slick A HEWAF and CEWAF,

and slick B HEWAF) were aggregated to produce balanced models. All other statistical analyses were performed using SAS (v9.4) at $\alpha = 0.05$. For experiment 1, a generalized linear model (GLM) fitted by log link and a Poisson distribution was used to detect significant differences in mean droplet diameter over a fixed effect of time for each oil type-WAF aggregate. For experiment 2, a three-way GLM fitted by log link and a Poisson distribution was used to detect significant differences in mean droplet diameter with the following interactive fixed effects: 1) medium (adsorbed to natural chorion, adsorbed to cleaned chorion, or suspended in water); 2) WAF preparations (oil-WAF aggregates of slick A HEWAF, slick A CEWAF, slick B HEWAF); and 3) time (3 or 6 h). A second three-way GLM fitted by log link and a Poisson distribution was used to detect significant differences in adsorbed droplet densities for each oil-WAF aggregate with the following interactive fixed effects: 1) chorion status (natural or cleaned); 2) time (3 or 6 h), and 3) discretely binned droplet diameter (1 – 13 μm). *Post-hoc* analyses were performed using Tukey's HSD.

Results

Experiment 1 – Characterization of Suspended Oil Droplets in WAF Preparations

Water samples taken from WAF preparations and sampled over time showed changes in droplet size and count-density profiles over time that were unique to individual WAF preparations. Kernel density estimations showed that droplet diameter in all WAF preparations followed centralized distributions at 0 h post generation (Figure 5A-C), although the density distribution of droplet diameters from the slick A CEWAF preparation was considerably broader than that of slick A HEWAF and slick B HEWAF preparations. The mean diameter of droplets changed significantly over time in slick A HEWAF (ANOVA, $F_{4,4235}$ 68.56; $p < 0.01$), slick A CEWAF (ANOVA, $F_{4,1910}$ 34.89; $p < 0.01$), and slick B HEWAF (ANOVA, $F_{4,5563}$ 11.29; $p <$

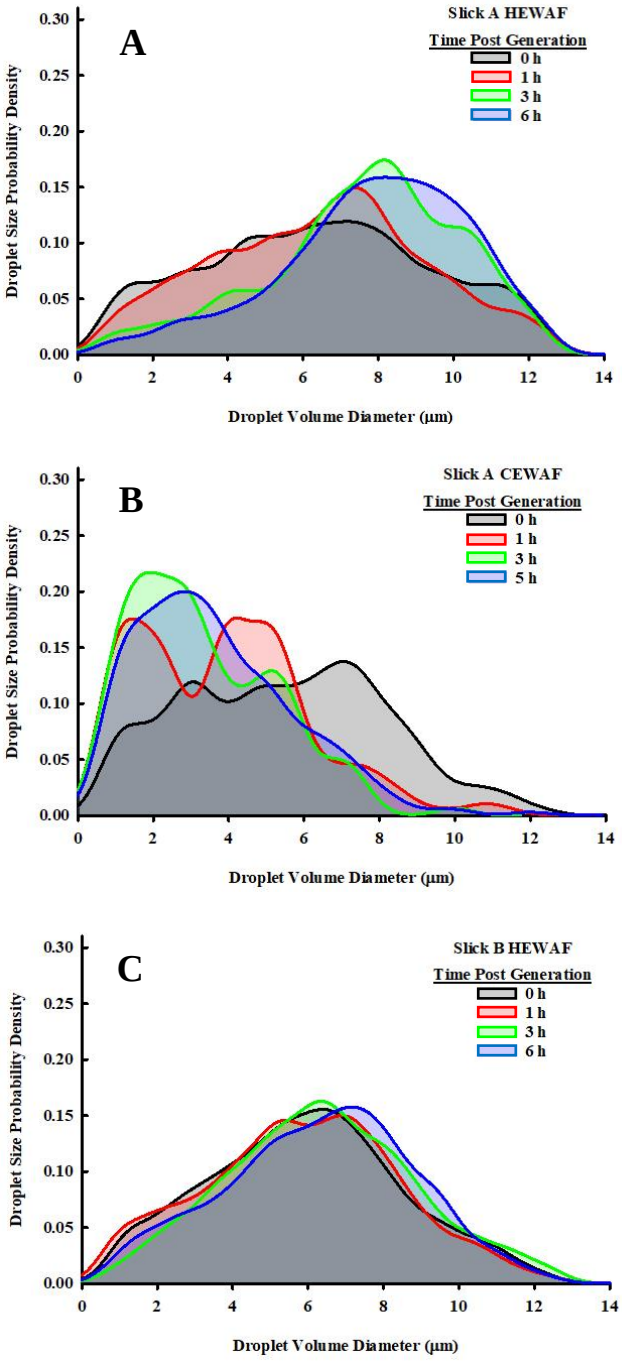

Figure 5. Kernel density plots generated for the probability densities versus droplet volume diameters in water oiled with slick A or slick B oil dispersed mechanically (HEWAF) or chemically Corexit (CEWAF) and visualized using fluorescent microscopy at 0-6 h post generation of WAF.

0.01) preparations (Table 4). Immediately following settling of WAF preparations (0 h), the largest mean droplet diameter was measured in slick A HEWAF preparation at 6.41 ± 0.09 μm (*n* = 1,265) compared to the slick A CEWAF preparation (5.47 ± 0.20 μm; *n* = 183) and slick B HEWAF preparation (5.93 ± 0.06 μm; *n* = 1,774; Table 4). *Post-hoc* analysis determined no significant change in slick A HEWAF droplet diameter by 1-h post generation but significantly increased to 7.58 ± 0.12 μm (*n* = 442; $p < 0.01$) at 3-h post generation, corresponding with the depletion of smaller droplets (diameter ranging from 1 – 5 μm, Figure 5A) at this time point. Slick A HEWAF droplet diameter remained stable past 3 h, but a significant decrease to 7.14 ± 0.17 μm (*n* = 304; $p < 0.01$) was detected at 48-h post generation, likely a result of the depletion of larger droplets (>8 μm; Figure 6).

Slick A CEWAF droplet diameter decreased after 1-h post generation to 3.85 ± 0.16 μm (*n* = 196; $p < 0.01$), when KD plots displayed a bi-modal distribution that was apparent until 3-h post generation, indicating a divergence in distribution of smaller (< 3 μm) and medium (4 – 5 μm) sized droplets (Figure 5B). Past 3 h, droplet diameter distribution was characterized by a higher relative abundance of smaller droplets until 48-h post generation when diameter significantly increased to 4.28 ± 0.08 μm (*n* = 869; $p < 0.01$; Table 4), which appears to be a result of the depletion of small sized droplets at this time point (Figure 6). Droplet diameter and distribution remained relatively stable in slick B HEWAF preparations (Figure 5C), although a small but statistically significant increase in diameter from 5.83 ± 0.08 μm (*n* = 1,020) to 6.36 ± 0.07 μm (*n* = 1,465) was detected at 3-h post generation (Table 4; $p < 0.01$). Droplet diameter and distribution remained stable in slick B HEWAF preparations for up to 48-h post generation.

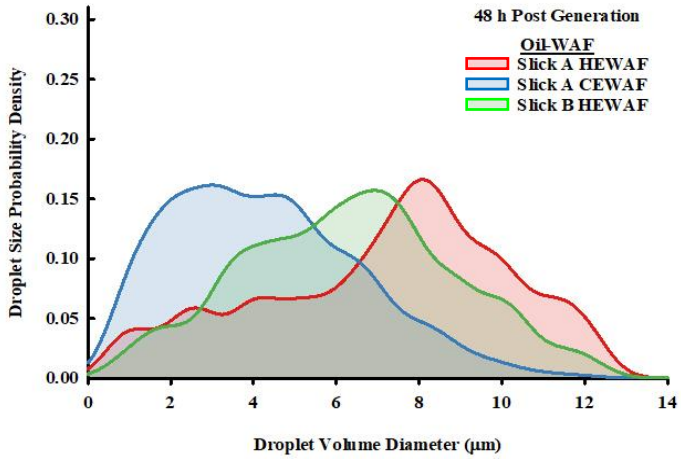

Figure 6. Kernel density plots generated for the probability densities versus droplet volume diameters in water oiled with slick A or slick B oil dispersed mechanically (HEWAF) or chemically with Corexit (CEWAF) and visualized using fluorescent microscopy at 48 h post generation of WAF during experiment 1.

Table 4. Mean diameter of droplets suspended in solution from Experiment 1. Suspended droplet diameter was averaged from a water sample drawn consecutively from a container at the designated times post generation. P-values indicate a significant change, when present, in droplet diameter from the previous time post generation (Tukey's *post-hoc*; $p < 0.05$).

Treatment	Time Post Generation	Total Droplet Count (*n*)	Mean Diameter (µm) ± SEM	*p*-value
Slick A HEWAF	0 h	1,265	6.41 ± 0.09	-
	1 h	733	6.44 ± 0.10	0.99
	3 h	442	7.58 ± 0.12	<0.01
	6 h	1,496	7.89 ± 0.06	0.25
	48 h	304	7.14 ± 0.17	<0.01
Slick A CEWAF	0 h	183	5.47 ± 0.20	-
	1 h	196	3.85 ± 0.16	<0.01
	3 h	126	3.34 ± 0.17	0.12
	5 h	541	3.63 ± 0.09	0.53
	48 h	869	4.28 ± 0.08	<0.01
Slick B HEWAF	0 h	1,774	5.93 ± 0.06	-
	1 h	1,020	5.83 ± 0.08	0.84
	3 h	1,465	6.36 ± 0.07	<0.01
	6 h	956	6.31 ± 0.08	0.99
	48 h	353	6.33 ± 0.14	1.00

Experiment 2 – Characterization of Suspended Droplet-Chorion Interaction
Interaction of Chorions and Suspended Droplets

Droplet adsorption ratios (ARs) were calculated by comparing the densities of adsorbed (mm^{-2}) to suspended droplets (mm^{-2}) categorized in discretely binned (1 µm) droplet diameter (ranging 1 – 13 µm). Slick A HEWAF droplet ARs at 3 h ranged from approximately 2 to 3.5 for droplets sized 1 – 5 µm (Appendix B - Table B1), while larger droplets (>6 µm) sparsely populated natural chorions. However, only 1 µm droplets had an AR greater than 1 by 6 h. Adsorption ratios for cleaned chorions exposed to slick A HEWAF for 3 h follow a similar trend, with preferential binding of droplets less than 5 µm. By 6 h of exposure, only 1 µm droplets existed in a higher proportion adsorbed than suspended. Adsorbed ratios for slick A CEWAF exposures did not exceed 0.45 for any chorion treatment or length of exposure. For slick B HEWAF exposures, ratios followed a similar trend to those observed with slick A CEWAF exposure, never rising over 0.42 despite higher counts of adsorbed and suspended droplets in slick B exposures. Ratios for natural chorions decreased by half for nearly all droplet diameters over time, but ratios for cleaned chorions nearly quadrupled for all droplet diameters over time despite consistent suspended droplet ratios within the 6 h timeframe.

Droplet Attachment over Time

A statistically significant overall interaction between WAF preparation (slick A HEWAF, slick A CEWAF, slick B HEWAF), medium (natural or cleaned chorion, or suspended), and time (3 or 6 h) on droplet mean diameter was detected (three-way GLM; $F_{4,37723}$ 28.10; $p < 0.01$). Statistically significant interactions between chorion status (natural or cleaned), time (3 or 6 h), and discretely binned (1 µm) droplet diameter (ranging 1 – 13 µm) was detected for slick A HEWAF (three-way GLM; $F_{51,468}$ 28.86; $p < 0.01$) and slick B HEWAF (three-way GLM; $F_{51,468}$ 12.17; $p < 0.01$) but not for slick A CEWAF. The diameter of slick A HEWAF droplets adsorbed

to embryos with natural chorions statistically significantly decreased from 4.55 ± 0.02 µm (*n* = 8,085) to 4.24 ± 0.04 µm (*n* = 3,589) between 3 and 6 h of exposure ($p < 0.01$; Tables 5 and 6).

Table 5. Mean diameter of droplets suspended in solution or attached to the chorion from Experiment 2. Suspended droplet diameter was averaged from a water sample while adsorbed droplet diameter was averaged across 10 embryos. See Table 6 for statistical comparisons.

Treatment	Droplet Location	Chorion	Time Post Generation	Total Droplet Count (*n*)	Mean Volume Diameter (µm) ± SEM
Slick A HEWAF	Adsorbed	Natural	3 h	8,085	4.55 ± 0.02
			6 h	3,589	4.24 ± 0.04
		Cleaned	3 h	3,714	4.46 ± 0.04
			6 h	4,360	4.90 ± 0.04
	Suspended		3 h	1,664	8.03 ± 0.06
			6 h	2,078	7.57 ± 0.06
Slick A CEWAF	Adsorbed	Natural	3 h	733	4.59 ± 0.09
			6 h	334	4.79 ± 0.12
		Cleaned	3 h	356	5.20 ± 0.13
			6 h	531	4.94 ± 0.11
	Suspended		3 h	809	4.87 ± 0.09
			6 h	420	3.46 ± 0.12
Slick B HEWAF	Adsorbed	Natural	3 h	2,970	3.69 ± 0.03
			6 h	852	3.89 ± 0.07
		Cleaned	3 h	372	3.52 ± 0.10
			6 h	1,842	4.72 ± 0.06
	Suspended		3 h	2,086	5.39 ± 0.06
			6 h	2,936	6.45 ± 0.05

Table 6. Statistics (Tukey's *post-hoc*; $p < 0.05$) for droplet mean volume diameter in Table 5 from Experiment 2. Rows and columns are formatted as a matrix to display multiple comparisons at and across 3 and 6 h post generation. Significant differences in droplet diameter are bolded and time of data collection are italicized. Comparisons across time between identical WAFs and chorion treatments are indicated by *3x6 h* text within the diagonal column. Contrasts depicting differences in chorion treatment and in WAF type were omitted.

Droplets Adsorbed to Chorion		Droplets Adsorbed to Chorion						Droplets Suspended in Water		
		Slick A HEWAF		Slick A CEWAF		Slick B HEWAF				
		Natural	Cleaned	Natural	Cleaned	Natural	Cleaned	Slick A HEWAF	Slick A CEWAF	Slick B HEWAF
Slick A HEWAF	Natural	<0.01 *3x6h*	0.88 *3h*	1.00 *3h*	-	<0.01 *3h*	-	<0.01 *3h* <0.01 *6h*	-	-
	Cleaned	<0.01 *6h*	<0.01 *3x6h*	-	<0.01 *3h*	-	<0.01 *3h*	<0.01 *3h* <0.01 *6h*	-	-
Slick A CEWAF	Natural	<0.01 *6h*	-	0.99 *3x6h*	<0.01 *3h*	<0.01 *3h*	-	-	0.48 *3h* <0.01 *6h*	-
	Cleaned	-	1.00 *6h*	1.00 *6h*	0.97 *3x6h*	-	<0.01 *3h*	-	0.68 *3h* <0.01 *6h*	-
Slick B HEWAF	Natural	<0.01 *6h*	-	<0.01 *6h*	-	0.38 *3x6h*	0.98 *3h*	-	-	<0.01 *3h* <0.01 *6h*
	Cleaned	-	0.23 *6h*	-	0.86 *6h*	<0.01 *6h*	<0.01 *3x6h*	-	-	<0.01 *3h* <0.01 *6h*

Chorion adsorbed total droplet density (TDD) in slick A HEWAF treatments was measured at 115.1 droplets per mm^2 at 3 h of exposure, corresponding with an adsorbed oil mass of 158.4 ng. By 6 h, TDD decreased to 55.5 per mm^2 and an adsorbed oil mass of 73.8 ng (Table 7). This observation was in agreement with statistically significant decreases from 3 to 6 h in the densities of slick A HEWAF droplets sized 2 to 8 µm adsorbed to natural chorions ($p < 0.01$; Figure 7A and 7D). For embryos with cleaned chorions exposed to slick A HEWAF, despite no statistically significant change in binned diameter droplet density over time, a TDD of 54.43 droplets per mm^2 was measured at 3 h of exposure and increased to 66.96 droplets per mm^2 after 6 h of exposure, which corresponded to an increased adsorbed oil mass of 81.5 ng to 128.4 ng. Additionally, the mean diameter of slick A HEWAF droplets adsorbed to cleaned chorions increased statistically significantly from 4.46 ± 0.04 µm (n = 3,714) to 4.90 ± 0.04 µm (n = 4,360) between 3 and 6 h of exposure ($p < 0.01$; Tables 5 and 6). Overall, embryos exposed to slick A CEWAF had the least number of droplets adsorbed to their chorions regardless of chorion treatment and adsorbed oil mass never exceeded 17.0 ng. In natural chorions, TDD decreased from 10.45 droplets adsorbed per mm^2 at 3 h to 5.16 droplets adsorbed per mm^2 at 6 h (Table 7). Similar TDD measurements were observed adsorbed to cleaned chorions, which increased from 5.02 droplets per mm^2 at 3 h to 8.19 droplets per mm^2 at 6 h. No statistically significant change in *post-hoc* analysis of diameter over time was detected in slick A CEWAF droplets adsorbed to natural (4.59 ± 0.09 µm; n = 733) nor in cleaned (5.20 ± 0.13 µm; n = 356) chorions (Tables 5 and 6), and no significant changes in droplet density over time within chorion treatments were detected (Figure 7B and 7E). For embryos with natural chorions exposed to slick B HEWAF, TDD decreased from 42.81 droplets per mm^2 at 3 h to 13.09 droplets per mm^2 at 6 h (Table 7).

Table 7. Total droplet densities (mm^{-2}) of embryo adsorbed and suspended droplets and total oil mass (μg) adsorbed per embryo. Densities of discrete droplet sizes can be found in Appendix B - Tables B1-3. Sum total oil mass was calculated by equation 1.

WAF	End Point	Medium	Time Post Generation	Total Droplet Density (mm^{-2})	Sum Total Oil Mass (ng) Per Embryo
Slick A HEWAF	Adsorbed Droplet Density*	Natural	3 h	115.06	158.4
			6 h	55.48	73.8
		Cleaned	3 h	54.43	81.5
			6 h	66.96	128.4
	Suspended Droplet Density	Exp 2	3 h	216.67	
			6 h	270.57	
		Exp 1	3 h	57.65	
			6 h	195.12	
Slick A CEWAF	Adsorbed Droplet Density*	Natural	3 h	10.45	17.0
			6 h	5.16	8.3
		Cleaned	3 h	5.02	10.4
			6 h	8.19	15.6
	Suspended Droplet Density	Exp 2	3 h	105.34	
			6 h	54.69	
		Exp 1	3 h	16.43	
			6 h	70.56	
Slick B HEWAF	Adsorbed Droplet Density*	Natural	3 h	42.81	36.7
			6 h	13.09	14.3
		Cleaned	3 h	5.27	3.4
			6 h	28.81	51.9
	Suspended Droplet Density	Exp 2	3 h	271.61	
			6 h	382.29	
		Exp 1	3 h	191.07	
			6 h	124.69	

*Values reported as means. Standard error withheld for clarity. See Figure 3 for error values.

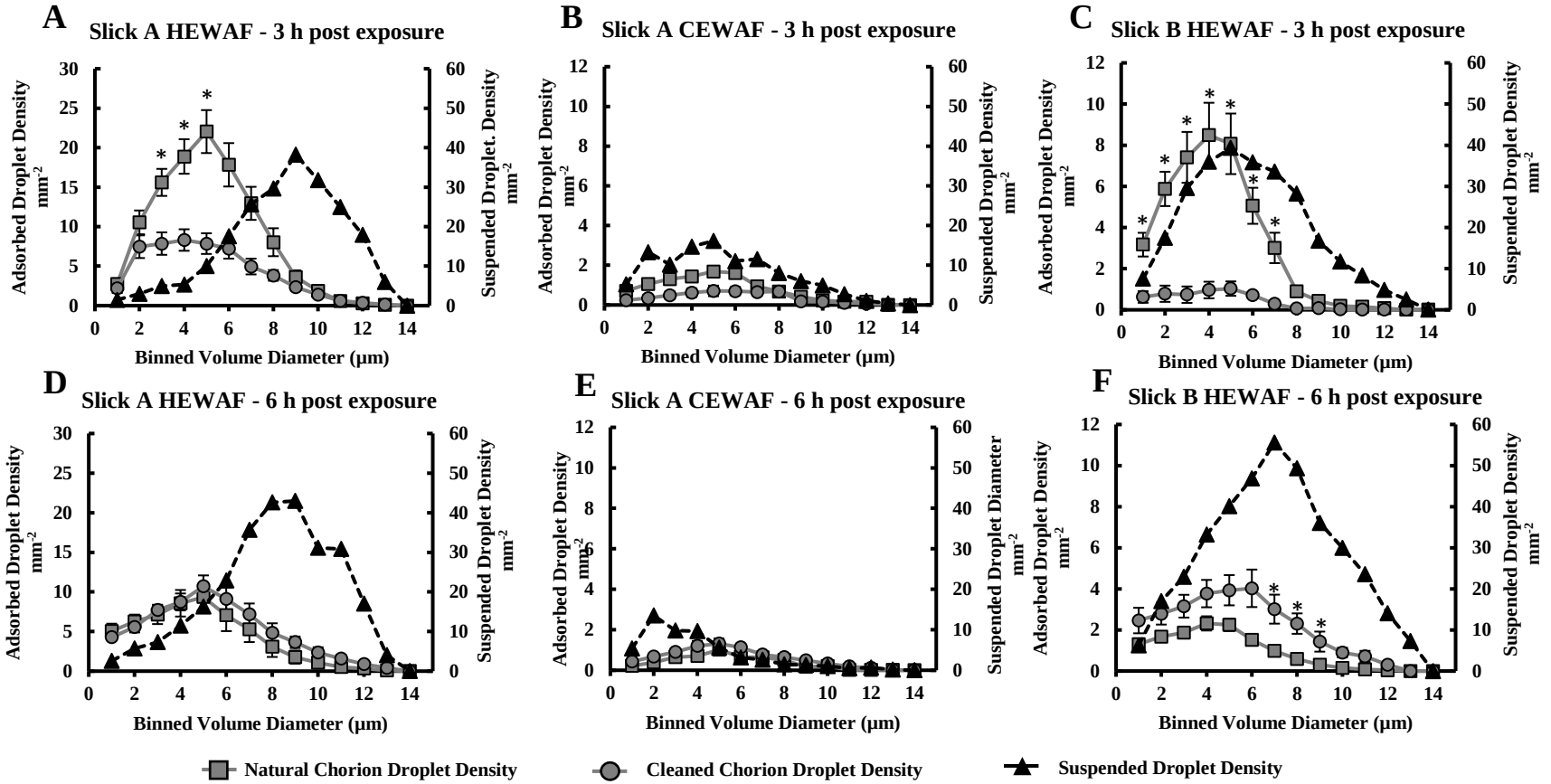

Figure 7. Experiment 2 mean droplet densities (mm^{-2}) adsorbed to natural or cleaned chorions (left-hand y-axis; mean ± SEM) and suspended in WAF preparations (right-hand y-axis; single sample). Stars represent significant differences between adsorbed densities of natural and cleaned chorions (Tukey's *post-hoc*; $p < 0.05$). The first row represents comparisons following 3 h of WAF exposure and the second row represents comparisons following 6 h of WAF exposure. In slick A HEWAF exposures, significantly higher densities of droplets sized 2 to 8 µm were adsorbed to natural chorions at 3 h than at 6 h of exposure, and in slick B HEWAF exposures, significantly higher densities of droplets sized 2 to 7 µm were adsorbed to natural chorions at 3 h than at 6 h of exposure. Significantly higher densities of droplets sized between 1 and 8 µm were detected on cleaned chorions exposed to slick B HEWAF for 6 h than 3 h. No significant differences in binned droplet density between cleaned chorions exposed to slick A HEWAF for 3 or 6 h were detected. No significant difference in binned droplet density was detected for slick A CEWAF exposures across time or chorion treatment.

This decrease corresponded with statistically significant decreases in the densities of slick B HEWAF droplets sized 2 to 7 µm adsorbed to natural chorions ($p < 0.05$; Figure 7C and 7F), ultimately decreasing adsorbed oil mass from 36.7 to 14.3 ng. Conversely, for embryos with cleaned chorions, TDD increased from 5.27 to 28.81 droplets per mm^2 and adsorbed oil mass increased from 4.0 to 51.2 ng. This agreed with statistically significant increases over time in the densities of slick B HEWAF droplets sized 1 – 8 µm adsorbed to cleaned chorions ($p < 0.01$). Continued exposure of natural chorions to slick B HEWAF for 6 h did not statistically significantly change droplet diameter measured at 3 h (3.69 ± 0.03 µm; n = 2,970). However, a statistically significant increase in droplet diameter from 3.52 ± 0.10 µm at 3 h (n = 372) to 4.72 ± 0.06 µm at 6 h (n = 1,842) was detected on cleaned chorions ($p < 0.01$; Tables 5 and 6).

Characterization of Adsorbed Droplets on Natural and Cleaned Chorions

Removal of extrachorionic fibrils (cleaned chorions) prior to exposure to slick A HEWAF for 3 h resulted in statistically significantly lower densities of droplets sized 3 – 7 µm compared to corresponding densities on natural chorions (Figure 7A). As a result, the TDD on cleaned chorions was 2.1-fold lower than the TDD of natural chorions exposed for the same time (Table 7) although droplet diameters were not statistically significantly different. However, by 6 h of exposure, TDD of natural chorions had decreased whereas a slight increase by 6 h was observed on cleaned chorions and statistically significantly larger droplets were adsorbed to cleaned chorions (4.90 ± 0.04 µm; n = 4,360) than to natural chorions (4.24 ± 0.04 µm; n = 3,589; $p < 0.01$; Tables 5 and 6). Statistically significantly larger slick A CEWAF droplets were adsorbed to embryos with cleaned chorions (5.20 ± 0.13 µm; n = 356) than to natural chorions (4.59 ± 0.09 µm; n = 733) at 3 h of exposure ($p < 0.01$; Tables 5 and 6). No statistically

significant differences between droplet densities or diameters adsorbed to natural or cleaned chorions were detected by 6 h of exposure (Figure 7E). Diameters of droplets adsorbed to natural and cleaned chorions were not statistically significantly different for slick B HEWAF exposures (Tables 5 and 6). Statistically significantly higher densities of binned droplets sized 1 – 7 µm were adsorbed to natural chorions over cleaned chorions ($p < 0.05$; Figure 7C), equating to an 8.1-fold higher TDD measured on natural chorions than to cleaned chorions (Table 7). Conversely, after 6 h of exposure, adsorbed slick B HEWAF droplets were statistically significantly larger on cleaned (4.72 ± 0.06 µm; n = 1,842) chorions than compared to natural (3.89 ± 0.07 µm; n = 852) chorions ($p < 0.01$), consistent with a 2.2-fold higher TDD and significantly higher densities of binned droplets sized 7 – 9 µm adsorbed to cleaned over natural chorions.

Discussion

This study demonstrated the use of an alternative-high throughput analysis to characterize the diameter and density of droplets from DHOS oil suspended in water and binding to the chorion of Gulf killifish embryos. Such a method has great potential considering the large numbers of samples needed to appropriately characterize droplet relationships with toxicity. Droplet mean diameters measured in the current study were similar to those observed in Forth et al. (2017a), which ranged from approximately 5 µm in slick B HEWAF preparations to approximately 9 µm in slick A CEWAF preparations immediately following settling. Although several analytical techniques, which include the use of a Coulter Counter, exist for high throughout analysis of droplets suspended in water, most are unable to quantify droplet adherence on animal surfaces. While others have used fluorescence microscopy to visualize oil droplet binding, few have performed much more than semi-quantitative assessments of droplet

adherence (Hansen et al., 2018). Considering the large number of oil droplets both in water following dispersion and the propensity of these droplets to adhere to the fish chorion, the automated approach developed here to process and analyze stereomicroscopic images in a high throughput and unbiased manner provides a method to study oil droplet behavior on biological membranes.

The behavior of the droplet phase in oil-in-water mixtures is obscured by persistent fluctuations in suspended droplet diameter and density throughout time. Droplet dispersal occurs when energy applied to an oil-in-water mixture is sufficient to overcome oil slick viscosity and results in the formation of a thermodynamically unstable mixture of immiscible liquids (Tadros, 2013). As a result, the coalescence of smaller droplets into larger ones is energetically favorable due to reduction in surface tension (Tadros, 2013), although other factors can contribute to coalescence. For instance, despite the same preparation method, an immediate and sustained increase in mean droplet diameter from the slick A HEWAF preparation was observed while mean droplet diameter in the slick B HEWAF preparation changed very little over time (Table 4, Figure 5A, 5C, and Figure 6). Given the same loading concentration and method of production, the divergence in droplet profiles between the two can likely be attributed to differences in source oil viscosity and density. The rate at which droplets rise is described by Stokes' Law, which states that droplet diameter and oil density drive droplet rise velocity. The difference in density (calculated at 16 °C) between 12 g/L salt water used in the current study (0.9989 g/cm^3) and slick A (0.9809 g/cm^3) (Forth et al., 2017b) would have promoted droplet vertical transport and subsequent coalescence, which could have led to the depletion of smaller sized droplets by 3 h (Figure 5A). Conversely, slick B is more weathered (*i.e.* loss of lighter hydrocarbons) than

slick A and possesses a higher density (1.0015 g/cm^3) (Forth et al., 2017b) that stabilizes the oil-in-water mixture (Figure 5C).

Despite similar droplet diameter distributions existing between slick A HEWAF and CEWAF preparations immediately following settling (0 h), suspended smaller diameter droplets (<4 µm) tended to persist longer in the slick A CEWAF preparation than the slick A HEWAF preparation (Table4, Figure 5A and 5B). The addition of chemical dispersant decreases the interfacial tension between oil and water such that more droplets of smaller diameter would have been produced given the same mixing energy (National Research Council, 2005; Gopalan and Katz, 2010; Landry et al., 2019). However, the persistence of small droplets (<4 µm) in CEWAF was unlikely to result from decreased coalescence as research suggests that the entrainment of surfactants in droplets does not create an electrostatic barrier sufficient enough to inhibit coalescence (Sterling Jr et al., 2004). CEWAF preparation requires a 6-h minimum settling time as opposed to a 1-h settling time for HEWAF, and this difference favors the removal of large droplets prior to the 0 h (Forth et al., 2017a). A dominant fraction of small droplets would have experienced reduced collision rates as small droplets are less prone to vertical transport (Landry et al., 2019; Sandoval et al., 2017). Continued monitoring revealed that droplet diameter increased from 6 h to 48 h in slick A CEWAF preparations, suggesting coalescence did occur given enough time, although at a slower rate than what was observed in HEWAF preparations. These results would have a direct impact for biodegradation rates on CEWAF droplets following 6 h as microbes colonize the droplet surface reducing net PAH metabolism as droplet surface area decreases (Landry et al., 2019).

The aqueous toxicity of unfiltered WAF preparations is believed to be primarily driven by dissolved PAH (low K_{OW}) concentrations due to the fact that dissolved PAHs are readily

bioavailable to animals, while, conversely, low solubility heavier PAHs (high K_{OW}) slowly dissolve into the aqueous solution, if at all, due to their hydrophobic nature and are believed to contribute little to aqueous toxicity (Carls et al., 2008; Hansen et al., 2019a; Redman et al., 2017). Eventually the dissolved phase PAH concentration equilibrates with the droplet phase (Faksness et al., 2004; Forth et al., 2017a). In general, low K_{OW} PAHs are believed to be acutely toxic, but are more easily eliminated than heavier and typically alkylated high K_{OW} PAHs, which tend to bioaccumulate and lead to chronic toxicity (Di Toro et al., 2007; Hodson, 2017; Lee et al., 2015; Logan, 2007). Forth et al. (2017a) measured dissolved PAH concentrations of 50 select analytes at 23, 20, and 7 µg/L, which represented 1, 7, and 3% of the total PAH concentration (dissolved and droplet phases) in unfiltered slick A HEWAF, slick A CEWAF, and slick B HEWAF preparations, respectively, indicating that the bulk of the PAH concentration will remain associated with the droplet phase. Thus, oil droplets that are dominated by highly toxic heavy molecular weight and alkylated PAHs will likely contribute little to the dissolved phase toxicity, but may impart toxicity through direct droplet-animal interactions (González-Doncel et al., 2008; Hansen et al., 2018; Petersen and Kristensen, 1998; Sørensen et al., 2017). This suggests that droplets directly adsorbed to Gulf killifish chorions may provide a route for direct uptake high K_{OW} PAHs by effectively bypassing the aqueous phase through direct attachment.

Since oil type and preparation method appear to highly influence droplet adsorption to the chorion we then sought to characterize the interaction between suspended droplets and the chorion. Relative to slick A, fewer slick B droplets adsorbed to natural chorions despite similarly large abundances of suspended droplets of each oil type at 3 h (Appendix B - Table B3, Figure 7C). Given the similarity in WAF preparation methodology, this difference is likely a result of the physicochemical density of slick B approximating that of the aqueous solution, which may

have stabilized suspended droplets and subsequently reduced droplet collision rates with the chorion. Analogous to heavier PAHs, asphaltenes are a class of large molecules recalcitrant to degradation that possess large aromatic cores with numerous polar groups and charged heteroatoms that contribute to the increased viscosity and density of oil concomitant with weathering (Song et al., 2018; Wong et al., 2015). Additional forces on a molecular-level interaction may contribute as well as asphaltenes have been simulated to migrate to the oil/water interface due to their amphipathic nature (Song et al., 2018). This migration effectively creates a film around the droplet that is believed to result in the steric repulsions between droplets and hydrophilic surfaces (Shi et al., 2019). A hydrophilic surface exists on Gulf killifish embryos that possesses an extrachorionic matrix characterized by a hydrophilic jelly coat and extrachorionic fibrils that help to prevent embryo desiccation during periods of tidal emergence (Brummett and Dumont, 1981; Morin and Able, 1983; Rizzo et al., 1998; Shu et al., 2015), potentially reducing binding affinity. Like slick B exposures, decreased adsorption of CEWAF droplets to natural chorions, albeit at a much lower extent, was also observed (Figure 7B). While we cannot rule out droplet stabilization due to the small suspended droplet diameter or reduced droplet contact with chorions due to lower numbers of suspended droplets, some evidence suggests that surfactant entrained droplets exhibit reduced binding affinity (Tummons et al., 2019). For example, despite using the same oil type (slick A), the quantity of adsorbed droplets sized 1– 6 µm were approximately 1.9- to 3.5-fold higher than suspended droplets in HEWAF preparations whereas the quantity of adsorbed droplets within the same size range were approximately 6.8- to 12.5-fold lower than suspended droplets in CEWAF preparations. Hansen et al. (2018) observed reduced binding of chemically dispersed droplets compared to mechanically dispersed droplets

to cod chorions, and Sørensen et al. (2014) observed a reduction in binding of chemically dispersed droplets over mechanically dispersed droplets to suspended particulate matter.

The current study observed differences between adsorbed and suspended droplet sizes, which may be a result of changes in droplet diameter following adsorption, preferential binding of smaller droplets, or a combination of both. Data in this study suggest that adsorbed droplet diameter and density are not static but change over time in a manner independent to that of suspended droplets. The largest change in adsorbed droplet profile over time occurred on natural chorions exposed to slick A HEWAF and was generally characterized by a significant decrease in mean droplet diameter and density (Figure 7A and 7D). Conversely, suspended slick A droplet densities increased, particularly in smaller sized droplets, corresponding to a decrease in mean droplet diameter. The density ratios of adsorbed to suspended slick A droplets (Appendix B - Table B1) indicate that the greater prevalence of adsorbed over suspended droplets less than 5 µm at 3 h disappears by 6 h, with only small droplets (< 3 µm) being equally adsorbed and suspended, suggesting large droplet attachment is temporary. As previously mentioned, the wetting layer created by the charged surface of the extrachorionic matrix likely weakened droplet affinity, which would have allowed for post-adsorption movement. Gentle orbital rocking used in the current study to prevent the formation of hypoxic boundary layers in our Gulf killifish embryos may have created sufficient crossflow shear at the chorionic surface to promote post-adsorption droplet coalescence and/or large droplet removal. Large diameter droplets would be subjected to more crossflow shear than smaller droplets and would have been more likely to be re-suspended into the water column (Tummons et al., 2019), resulting in the observed significant decrease in adsorbed droplet diameter over time.

Removal of the extrachorionic matrix resulted in an initially (3 h) decreased adsorbed droplet density compared to natural chorions; however, unlike with natural chorions, the mean diameter and densities of adsorbed droplets increased by 6 h of exposure (Figure 7). Although these phenomena were observed to occur on cleaned chorions exposed to all WAF treatments, significant increases in droplet diameter were noted only in HEWAF treatments. Within the HEWAF treatments, slick A droplets appear to initially attach in greater quantity (sum total oil mass per embryo [ng]; Table 7) compared to slick B droplets, possibly a result of relatively greater mobility of slick A droplets in the water column due to density differences between slick A oil and the aqueous medium. Furthermore, while bulk oil mass adsorbed to cleaned chorions over time increased 1.6-fold in slick A HEWAF treatments and 1.5-fold in slick A CEWAF treatments, a 13-fold increase was observed in slick B HEWAF treatments (Table 7). So, while the stabilization of slick B droplets may have initially reduced collision rates with cleaned chorions at 3 h, droplet stability in the water column would have sustained rate of droplet collision and adsorption to cleaned chorions.

The DHOS made landfall in the salt marshes lining the northern GOM during the peak spawning season of Gulf killifish, where spawn-ready individuals were observed swimming in oiled waters (Whitehead et al., 2012). Oil droplets were likely in contact with chorions of not just killifish, but also with numerous other species with similar early life stage histories (*for species review see* Nordlie, 2006). The importance for investigating the toxicity of adsorbed oil to cleaned chorions can be justified given that oil exposure of reproductively active females significantly reduced transcription of genes associated with production of the chorionic structure, namely zona pellucida, ZP3 and ZP4, and choriogenin proteins, ChgHm and ChgH (Whitehead et al., 2012). Given this molecular signature, oil exposure to adults may have produced impaired

or absent extrachorionic matrices on eggs like those of the cleaned chorions used in the current study. Ultimately, the data from this experiment suggest that the extrachorionic matrix may act as a net in catching suspended droplets during initial exposure, but that these oil droplets are transiently adsorbed. Conversely, a more permanent adsorption appears to occur on cleaned chorions that could contribute to toxicity through potential direct transfer of heavy and alkylated PAHs.

CHAPTER 4
THE REPRODUCTIVE AND DEVELOPMENTAL EFFECTS OF PARENTAL OIL EXPOSURE IN GULF KILLIFISH POPULATIONS WITH DIFFERENT POLLUTION EXPOSURE HISTORIES

Introduction

Exposure to environmental contaminants can lead to impaired teleost health that can persist for multiple generations through various mechanisms, including behavioral alterations, disruptions in reproductive physiology, epigenetic changes, and genotoxicity (Nilsen et al., 2019). Consideration of the long-term impacts of these mechanisms is important when assessing environmental and ecological impacts of human activity. Exposure to acute environmental challenges outside of species tolerance ranges or introduction of anthropogenic derived stressors, such as crude oil exposure, can perturb homeostatic regulation through disruption of physiological systems (Petitjean et al., 2019). Exposure of reproductively active teleosts to polycyclic aromatic hydrocarbons (PAHs), the primary toxic constituent of crude oil, has been demonstrated to impact their offspring fitness via altered egg provisioning (Jasperse et al., 2019), epigenetic alterations (Head et al., 2012; Lewis et al., 2012), maternal deposition of lipophilic toxicants (Romero et al., 2018), and may also reduce offspring ability to attenuate effects of stressors (Knecht et al., 2017). Embryonic oil exposure has been previously documented to result in genotoxicity and development of negative phenotypes, including bradycardia, teratogenesis, and reduced hatch success (De Soysa et al., 2012; Hodson, 2017; Lee et al., 2015; Rotchell et al., 2008). Intergenerational responses to environmental challenges like those imposed by chronically polluted environments may play an important role in shaping wildlife health over long, multi-generational time. Previous research into the Exxon Valdez oil spill demonstrated the environmental persistence of oil in oxygen and nutrient poor conditions, highlighting the

potential for continuous PAH exposure decades after initial oiling (Li and Boufadel, 2010; Short et al., 2007).

Approximately 780 million L of Macondo oil were released into the Gulf of Mexico during the DHOS, with coastal oiling peaking in late June of 2010 (Michel et al., 2013). Of the 2,092 km of shoreline impacted, over 1,000 km of highly productive saltmarsh habitat was oiled (Lee et al., 2015), likely exposing breeding populations of fish and their offspring to oil (Dubansky et al. 2013; Fodrie and Heck 2011; Rooker et al. 2013, *but see* Roth and Baltz 2009; Schaefer et al. 2016). Fish were likely continuously exposed to oil well after surface water oil was no longer present As sediments collected in the year following the DHOS contained concentrations of oil sufficient to activate biomarkers of oil exposure and elicit toxic effects to embryonic fish under laboratory conditions, indicating the environmental persistence of oil contamination due to sedimentation (Brown-Peterson et al., 2017; Dubansky et al., 2013). Consequently, the continued presence of oil in the marsh environment is likely to contribute to long-term ecological impacts through hydrocarbon sedimentation.

One such species exposed to DHOS oiling was the Gulf killifish (*Fundulus grandis*), which is one of the most numerous vertebrate species in the salt marshes of the northern Gulf of Mexico, using spartina as spawning grounds and nurseries for early-life stages (Nordlie, 2003). Gulf killifish also maintain small home ranges within marsh ecosystems and possess high site fidelity, producing distinct populations of killifish with locally adapted phenotypic traits (Williams et al., 2008). Low migration has also led to adaptation to chronic pollution in multiple populations of Gulf killifish found at Superfund sites within the Houston Ship Channel (Oziolor et al., 2014; Oziolor et al., 2019), which have been characterized as possessing high concentrations of persistent organic pollutants in sediments, which include, but are not limited to,

high molecular weight (HMW; > 4 aromatic rings) PAHs, halogenated-PAHs, and heavy metals (Allen, 2015; Josiam, 2015). Similarly, sedimentation of oil resulting from the DHOS likely exposed gulf killifish to PAHs over multiple generations. The recent Deepwater Horizon oil spill (DHOS) provides a unique opportunity to measure possible intergenerational effects of exposure to environmental toxicants in a sentinel vertebrate ecotoxicological model species, the Gulf killifish.

The goal of this research was two-fold. The first is to investigate the effects of oiling on the reproduction and early life stage development of Gulf killifish impacted by the DHOS. The second was to test for differences in intergenerational impacts of crude oil exposure in two pairs of pollution-naïve and pollution-exposed populations from distinct geographic regions, including a pollution-adapted population from the Houston Ship Channel and a recently oiled population from the DHOS-impacted site, Grand Terre, LA. Specifically, this research sought to investigate if perturbations from adult exposures to oil would be transmitted to offspring through maternal or epigenetic effects, and to investigate if sensitivity to intergenerational effects vary between populations because of their long-term history of toxicant exposure. Because these critical reproductive and developmental periods may have been affected by oiling, this chapter seeks to determine if parental oil exposure influenced Gulf killifish reproductive capacity and if the fitness of embryos derived from oil exposed adults is affected.

Materials and Methods

Adult Fish Collection and Holding

Gulf killifish were collected from a site in Grand Terre, LA (29°16'29.9"N 89°56'32.2"W) heavily oiled during the DHOS as determined by shoreline cleanup and

assessment technique (SCAT) surveys performed by oil spill responders (hereafter referred to as LA-DHOS). This represents a contemporarily polluted field site. A population of Gulf killifish originally derived from Leeville, LA (29°15'24.6"N 90°12'51.3"W) but held in laboratory conditions over several generations served as the Louisiana reference population (hereafter referred to as LA-Ref). Gulf killifish with known pollution tolerance was collected from a historically-polluted U.S. Superfund site, Vince Bayou, TX (29°43'10.0"N 95°13'13.8"W) in the Houston Ship Channel (hereafter referred to as Texas-Superfund; TX-SF) and killifish from a reference population near TX-SF was collected from Gangs Bayou, TX (29°15'23.4"N 94°54'43.3"W) (hereafter referred to as Texas-Reference; hereafter referred to as TX-Ref).

Fish were treated for parasites with a 24-h exposure (0.2 mg/L) of Cupramine (Seachem; Madison, GA, USA) and held in quarantine conditions for two weeks before being transferred to the main laboratory holding systems. Fish were acclimated for a minimum of 120 days before exposure to treatment waters. Fish from LA-Ref (n=69), LA-DHOS (n=52), TX-Ref (n=78), and TX-SF (n=74) were divided between control and water-accommodated fraction (WAF) treatments. Fish from LA-Ref, TX-Ref, and TX-SF were further divided in quadruplicate per treatment (control or WAF), and fish from LA-DHOS were divided in triplicate per treatment. Fish were stocked at an approximate ratio of 2 females to 1 male fish per replicate and each replicate was composed of a 60-L static water tank fitted with submerged glass serological pipettes attached to airlines to provide air and prevent stagnation of treatment water. Fish were checked for mortalities and fed to satiation daily, and total ammonia-nitrogen (TAN) of water from two randomly chosen tanks was assessed daily using the API colorimetric assay (Mars Fishcare; Chalfont, PA, USA). Water was analyzed for salinity, temperature, total ammonia-nitrogen (TAN), and the pH from two randomly chosen tanks prior to 50% water renewals (30 L)

every 4 days. For renewal water chemistry, salinity and temperature were measured with a YSI-30 salinity/conductivity meter (YSI Inc., Yellow Spring, OH, USA); ammonia (TAN) was measured using a Hach DR 4000 Spectrophotometer (Hach Co., Loveland, CO, USA) using the salicylate method; and pH was measured with an Accumet Basic AB15 pH meter (Fisher Scientific, Pittsburg, PA, USA).

Adult WAF Exposures

Every 4 days, 800 L of clean and WAF treatment waters were produced to provide 50% water exchange (30 L every 4 days) for thirty 60-L tanks (15 tanks for controls and 15 tanks for WAF exposures). Considering the large volume of WAF needed, the traditional method of producing WAF by high-energy mixing was not feasible. As such, WAF was produced by passing water across oil soaked Siporax filter media using a custom upweller design like that described by Carls, et al., (2000) and by Kennedy and Farrell, (2005). Siporax filter media was soaked either in Macondo Oil surrogate (supplied by BP America Production Company; sample ID: SO-20110802-MPDF-01) or in clean water for 48 h for the WAF and control treatments, respectively. Siporax media were placed in a polyvinyl chloride (PVC) chamber and 12 g/L saltwater was pumped continuously across the media contained within polytetraflourethylene (PTFE)-lined tubing. Water was drawn from the bottom of a 1,000-L PTFE-lined tank to avoid collection of slick oil and deposited at the top. Every 4 days, after the control and WAF was used for tank water replacements, the 1000-L tanks were refilled with 12 g/L water and the process repeated to generate new batches of water as described above.

Gamete Fertilization

Embryos were obtained via *in vitro* fertilization following 40 days of adult broodstock exposure to treatment water. Eggs from females derived from each population-parental treatment were pooled together before sperm was added followed by the addition 12 g/L water to activate gametes. TX-Ref and LA-DHOS were spawned an additional time 8 days later to obtain embryos for additional analyses. Embryos were assessed at 1 h following fertilization to assess water hardening and raising of the fertilization envelopes. Embryos without raised fertilization envelopes were removed from the study prior to initiation of embryo exposures.

Embryonic HEWAF Exposures

For embryo exposures, a high energy water accommodated fraction (HEWAF) was generated based on the protocol described in (Incardona et al., 2013). In short, artificial sea water (ASW) was created by mixing artificial sea salt (Instant Ocean salt mix; United Pet Group, Cleveland, OH, USA) in reverse osmosis (RO) water to a salinity of 12 g/L. An initial loading concentration of 2 g of surrogate Macondo oil per L of ASW was used to generate HEWAF preparations. HEWAF was generated by vortex (15,000 RPM) oil in a Waring CB15 (Waring; Torrington, CT, USA) for 30 seconds. This mixture was transferred to separatory funnels to settle for 1 h before the bottom WAF fraction was drained into a glass beaker. Care was taken to avoid the formation of any slick residue that had formed at the top of the mixture. Undiluted HEWAF was then transferred to a 75-L glass aquarium and the process was repeated until a sufficient volume of WAF volume was produced. The undiluted HEWAF mixture was aliquoted to 1-L glass bottles and held at -20 °C until needed, at which point, aliquots were thawed in darkness as needed. HEWAF was then diluted to 56% with 12 g/L ASW to give a nominal

concentration of 1.12 g oil/L. This process was repeated every 2 days for renewal purposes for up to 21 days during full treatment water renewals.

Water quality was measured prior to treatment water renewal to ensure proper environmental conditions for killifish embryos. Dissolved oxygen (DO; mg/L) and temperature (°C) were measured with a YSI proODO (Xylem; Rye Rook, NY, USA); pH measured using a Denver Instrument UltraBasic UB-10 (Denver Instrument Co.; Denver, CO, USA) meter; salinity was measured with a RHS-10ATC refractometer (Sinotech; Portland, OR, USA); each calibrated prior to use. Water samples taken for TAN analysis were held at -20 °C until the day of analysis. Samples were run on a Thermo-Fisher Multiskan Ascent spectrophotometer (Thermo Fisher Scientific; Waltham, MA, USA) using the salicylate method described by Verdouw et al. (1978).

Embryo Holding

Embryos from control or WAF-exposed parents of each of the four populations (LA-Ref, LA-DHOS, TX-Ref, TX-SF) were exposed to either clean (12 g/L ASW) or HEWAF (1.12 g oil/L) and embryos were checked daily for mortality and hatch. Gulf killifish embryos typically require approximately 12 days to hatch at the experimental holding conditions (25 °C at 12 g/L ASW), but toxicity tests were extended to 21 dpf since hatch beyond this time is unlikely (Brown et al., 2011; Perschbacher et al., 1990). Unhatched embryos were enumerated at the conclusion of a test and the % mortality, % hatch, and % unhatched calculated.

Phenotypic Endpoint Analyses

At seven days post fertilization (dpf), heart rates (BPM) of three-randomly chosen embryos per quadruplicate were recorded by enumerating ventricular contractions for 30 seconds. An additional set of embryos from each quadruplicate (n=3 per replicate, except where

otherwise stated), were imaged 7- 8 dpf with a Zeiss SteREO Lumar V.12. Brightfield images (*n*=12 per population, parental exposure history, embryo exposure combination) were taken at 36x magnification with a 0.8x objective. Images were randomly assigned numbers prior to phenotypic abnormality (PA) assessment to prevent biased evaluation. A sub-set of images (~20% of the total number) were duplicated and their PA scores were compared to those of the originals in order to quantify variation in PA assessment from blind analysis (76% similarity). Embryos were evaluated for the presence of phenotypic abnormalities types adapted from Whitehead et al. (2010), which included abnormal morphological development, cardiac edema, heart deformation, and hemorrhaging. Embryos were assigned a 1 for each of the abnormalities when present or a 0 when absent. A cumulative phenotypic abnormality score, which ranged from 0 (none of the 4 abnormalities present) to 4 (when all 4 abnormalities were present).

PAH Analysis

Unfiltered WAF was collected from randomly selected adult exposure treatments on days 4, 20, 32, and 36 of parental exposure and control water collected on days 4 and 20. Samples were taken following 50% treatment water renewals. For embryo exposures, unfiltered diluted HEWAF (1.12 g oil/L) and control water were collected on days 16 and 18 of exposure. The effect of contemporary weathering on these same batches of HEWAF was assessed by measuring PAH concentrations of a composite sample of all four replicates 48 h after dilution. WAF and HEWAF samples were held at -20 °C following collection and were analyzed at ALS Environmental, where parent PAHs and their alkylated homologs were analyzed using GS-MS (USEPA method 8270C). Although the concentrations of 72 PAH analytes were determined, concentrations of the 23 parent and 27 alkyl homologues referenced in Forth et al., (2017) were

summed to give the total PAH concentration (hereafter referred to as TPAH50; mean ± SD; Table 8).

Statistics

All statistical analyses were performed with SAS v 9.4 at $\alpha = 0.05$ unless otherwise noted. Fisher's Exact Test was used to test for differences between fertilization success of embryos derived from control water or WAF exposed parents within populations. Bonferoni adjustment was applied to account for error inflation for multiple comparisons ($\alpha = 0.0125$). A three-way generalized linear model (GLM 1) fitted by log link and a Poisson distribution was used to detect significant differences in embryonic heart rate with the following interactive effects: 1) population (LA-Ref, LA-DHOS, TX-Ref, TX-SF); 2) parental exposure history (parental control [PC] or parental WAF exposed [PE]); and 3) embryonic exposure (control or HEWAF). A previous model including an interaction with PA score found PA score was not influenced by parental exposure and was omitted for clarity. For each parental treatment (PC or PE), a three-way GLM fitted by log link and a Poisson distribution (GLM 2) was used to detect significant differences in sum total phenotypic abnormality (PA) score with the following interactive effects: 1) population; 2) embryonic exposure; and 3) occurrence within binned PA score (none, medium, or high). For each response variable, a three-way GLM model fitted by logit link and a binomial distribution (GLM 3) was performed to detect significant differences in frequency of hatch, mortality, or non-hatch with the above-mentioned interactive effects for embryonic heart rate analysis. All *post-hoc* analyses were performed using least significant difference (LSD) test.

Results

Parental Exposures

There were no mortalities of adult killifish to control waters during their 40-day exposure. Similarly, adult killifish survival after 40-d exposure to WAF at TPAH50 of 135 ± 70.8 µg/L (mean ± SD; *n* = 2; Table 8 and Figure 8) was 90% ± 3% (mean ± SEM) for LA-Ref, 90% ± 2% for TX-Ref, and 97% ± 1% for TX-SF, whereas it was only 73% ± 1% for WAF-exposed LA-DHOS fish (Figure 9). Mortality of LA-DHOS fish exposed to WAF started on day 8 and survival remained at 73% ± 1% following until conclusion of exposures.

Table 8. Mean water chemistry (± SD) for adult and embryo exposures. Number within parentheses represents the number of data points. Note that adult fish were exposed to control water (PC) or WAF (PE) and embryos exposed to control water or HEWAF.

Life Stage	End Point	Sampling Condition	Treatment	
			Control	WAF/HEWAF
Adult	TPAH50 (µg/L)	0 h (fresh)	2.1 ± 0.5 (2)	135.0 ± 70.8 (2)
	Salinity (g/L)	-	12.2 ± 0.3 (11)	12.2 ± 0.3 (11)
	Temperature (°C)	-	21.1 ± 0.7 (11)	21.4 ± 0.6 (11)
	TAN (mg/L)	-	0.2 ± 0.2 (10)	0.1 ± 0.1 (10)
	pH	-	8.3 ± 0.2 (10)	8.2 ± 0.3 (10)
Embryo	TPAH50 (µg/L)	0 h (fresh)	0.0 ± 0.0 (2)	220.4 ± 50.0 (4)
		0 h + 48 h (weathered)	0.0 ± 0.0 (2)	123.7 ± 5.6 (4)
	Salinity (g/L)	PC	12.8 ± 0.6 (40)	12.6 ± 0.6 (38)
		PE	12.7 ± 0.6 (53)	12.6 ± 0.6 (60)
	Temperature (°C)	PC	22.3 ± 0.7 (40)	22.3 ± 0.6 (38)
		PE	22.5 ± 0.6 (53)	22.4 ± 0.6 (58)
	TAN (mg/L)	PC	0.1 ± 0.1 (23)	0.0 ± 0.1 (26)
		PE	0.1 ± 0.1 (34)	0.0 ± 0.1 (41)
	pH	PC	7.9 ± 0.1 (40)	7.8 ± 0.1 (38)
		PE	7.9 ± 0.1 (53)	7.8 ± 0.1 (60)

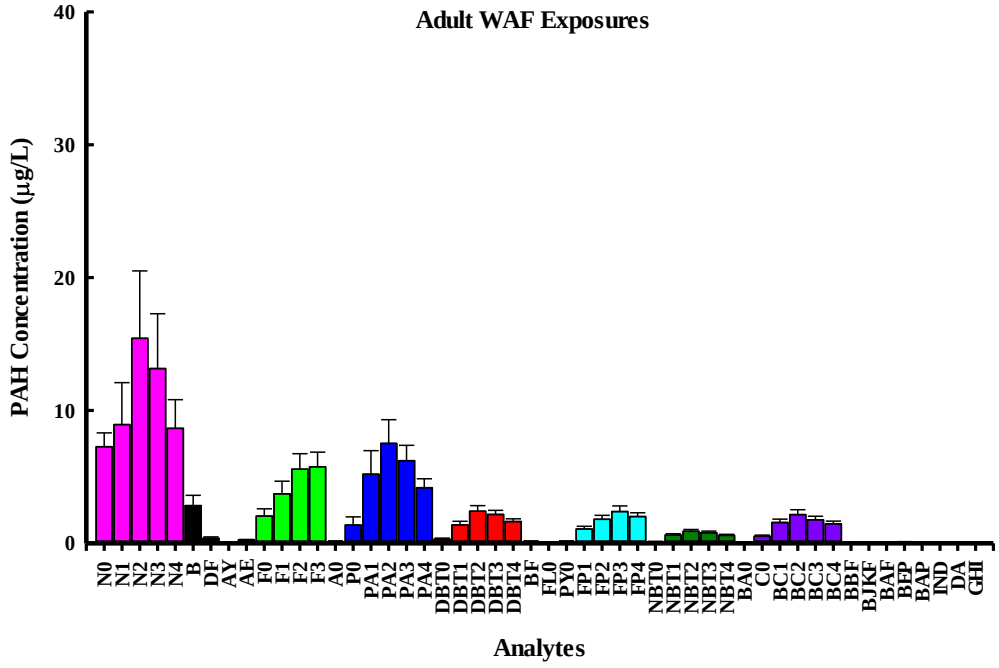

Figure 8. Mean (± SEM) TPAH50 concentrations (µg/L) for adult WAF exposures.

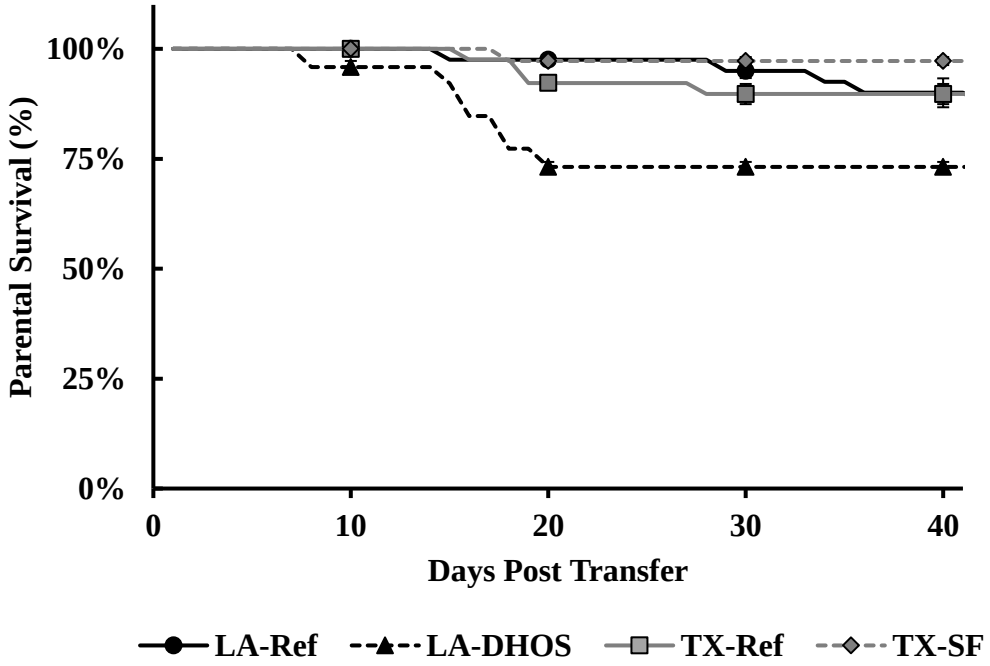

Figure 9. Mean (± SEM) survival of adults (n=9-10 per quadruplicate for LA-Ref, TX-Ref, and TX-SF populations and per triplicate for LA-DHOS) exposed to WAF for up to 40 days. No mortalities occurred in control conditions over 40 days.

Reproductive Endpoints

The number of eggs produced per female in control-exposed populations ranged from 54.4 eggs per female in the LA-Ref population to 18.4 eggs per female in the TX-SF population at day 40 (Figure 10A). The number of eggs produced per female exposed to WAF for 40 days increased relative to their control counterparts and ranged from 51.5 eggs per female in the TX-Ref population to 78.9 eggs per female in the TX-SF population. The increase in egg production was 11% increase in LA-Ref, 26% in LA-DHOS, 28% in TX-Ref, and 77% in TX-SF (Figure 10A). The fertilization success of embryos derived from control-exposed parents ranged from 85% in LA-Ref population to 94% in LA-DHOS, TX-Ref, and TX-SF (Figure 10B). Parental WAF exposure statistically significantly reduced embryonic fertilization success of gametes from LA-Ref to 26% ($X^2 = 434.30$, $p < 0.0125$), LA-DHOS to 31% ($X^2 = 382.71$, $p < 0.01$), and TX-Ref to 30% ($X^2 = 430.27$, $p < 0.01$) parents relative to those derived from control parents. Fertilization success of gametes derived from WAF-exposed TX-SF measured at 94% of their control counterparts, which were not statistically significantly different from another.

Embryo Exposures - Heart Rates

The mean heart rates of PC embryos reared in control water ranged from 107 ± 2 bpm (mean ± SEM; TX-SF) to 118 ± 2 bpm (LA-DHOS), and from 97 ± 2 bpm (LA-DHOS) to 124 ± 3 bpm (TX-Ref) for PE embryos reared in control water (Figure 11). Mean heart rates of embryos reared in HEWAF (fresh HEWAF TPAH50 of 220.4 ± 50.0 µg/L (n = 4) and 48-h weathered HEWAF TPAH50 of 123.7 ± 5.6 µg/L; mean ± SD; n = 4; Table 8 and Figure 8) ranged from 87 ± 2 bpm (TX-Ref) to 104 ± 3 bpm (TX-SF) from PC treatments, and from 76 ± 2 bpm (LA-Ref) to 107 ± 1 bpm (TX-SF) for PE treatments. Although no three-way interaction

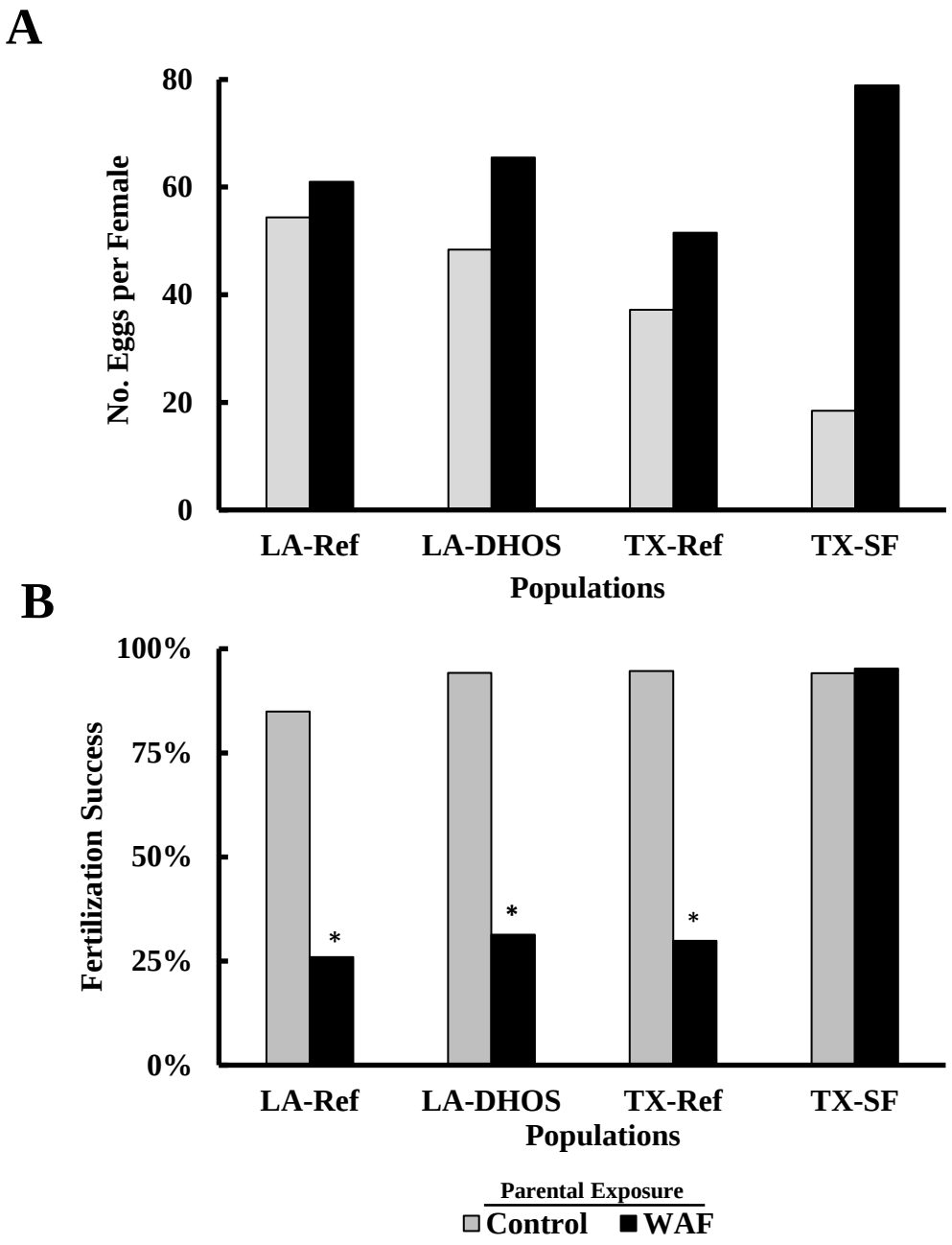

Figure 10. (A) Number of eggs produced per female, and (B) the fertilization success of those eggs following 40 days of exposure to control water (gray bars) or to WAF (black bars). Adult killifish were exposed to treatment water for 40 days prior to *in vitro* fertilization. Fertilization was performed by mass spawning where the total number of eggs were counted at the end of the spawn and then divided by the number of females who gave eggs. Stars in panel (B) represent significant difference in fertilization success of eggs derived from control or WAF exposed parents from a given population (Fisher's Exact Test).

was detected between killifish population, parental exposure history, and embryo exposure, a two-way interaction between population and parental exposure history was detected (two-way GLM 1; $F_{3,159}$ 7.14; $p < 0.01$) and a two-way interaction between population and embryo exposure history was detected (two-way GLM 1; $F_{3,159}$ 30.21; $p < 0.01$). Regardless of parental exposure history, HEWAF exposure during embryogenesis statistically significantly reduced the heart rates of embryos from the LA-Ref, LA-DHOS, and TX-Ref populations (LSD $p < 0.01$; Figure 12). HEWAF exposure during embryogenesis did not significantly decrease mean heart rates in the PE-derived TX-SF embryos. The control embryos from PC parents had statistically similar heart rates.

Louisiana-DHOS embryos derived from WAF exposed parents (PE) and reared in control water possessed statistically significantly lower mean heart rate at 97 ± 2 bpm than the mean heart rate of their PC counterparts (118 ± 2 bpm) reared in control water (LSD $p < 0.01$; Figure 11). Conversely, the mean heart rate of PE TX-Ref embryos reared in control waters (124 ± 3 bpm) was statistically significantly higher than the mean heart rate of their PC counterparts (115 ± 2 bpm; LSD $p < 0.01$). Parental exposure history did not statistically significantly affect the heart rates LA-Ref or TX-SF embryos reared in control waters. Within their respective parental exposure histories, LA-Ref and LA-DHOS embryos reared in control water possessed statistically similar heart rates. In control water exposures, a statistically significantly higher heart rate was detected in PE TX-Ref embryos (124 ± 3 bpm) over heart rates of TX-SF embryos (102 ± 1 bpm; LSD $p < 0.01$). Exposure of PE LA-Ref and PE LA-DHOS embryos to HEWAF resulted in the lowest recorded mean heart rates across all HEWAF exposures at 88 ± 3 bpm and 85 ± 4 bpm, respectively. The responses of embryonic heart rate to parental exposure history and embryo treatment exposure were statistically similar between LA-DHOS and their LA-Ref

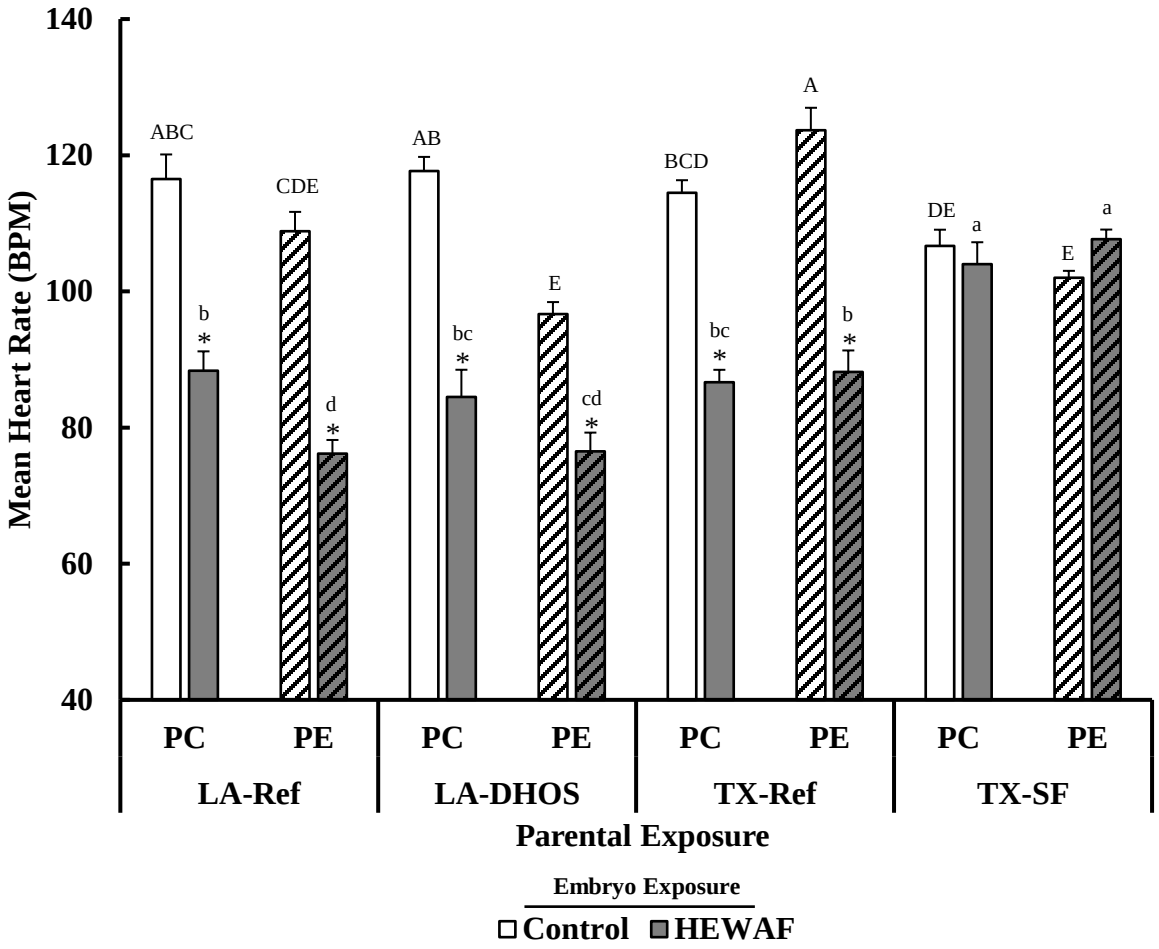

Figure 11. Mean heart rates (± SEM) of embryos exposed to control or HEWAF for 7 days. Solid bars represent heart rates of embryos derived from parental control (PC) treatments and patterned bars represent heart rates of embryos derived from parental exposed (PE) treatments. In both cases, the white bars, whether open or patterned, are control-exposed embryos, and dark bars, whether open or patterned, are WAF exposed embryos. Stars (*) represent significant differences between heart rates of embryos exposed to control or HEWAF treatments within population and parental treatment, and upper (PC) and lower (PE) case letters represent significant differences between heart rates of embryos within embryonic exposure treatment (Control or HEWAF) across all populations and parental treatments (LSD, $\alpha < 0.05$). No significant interaction between parental treatment, population, and embryo treatment was detected.

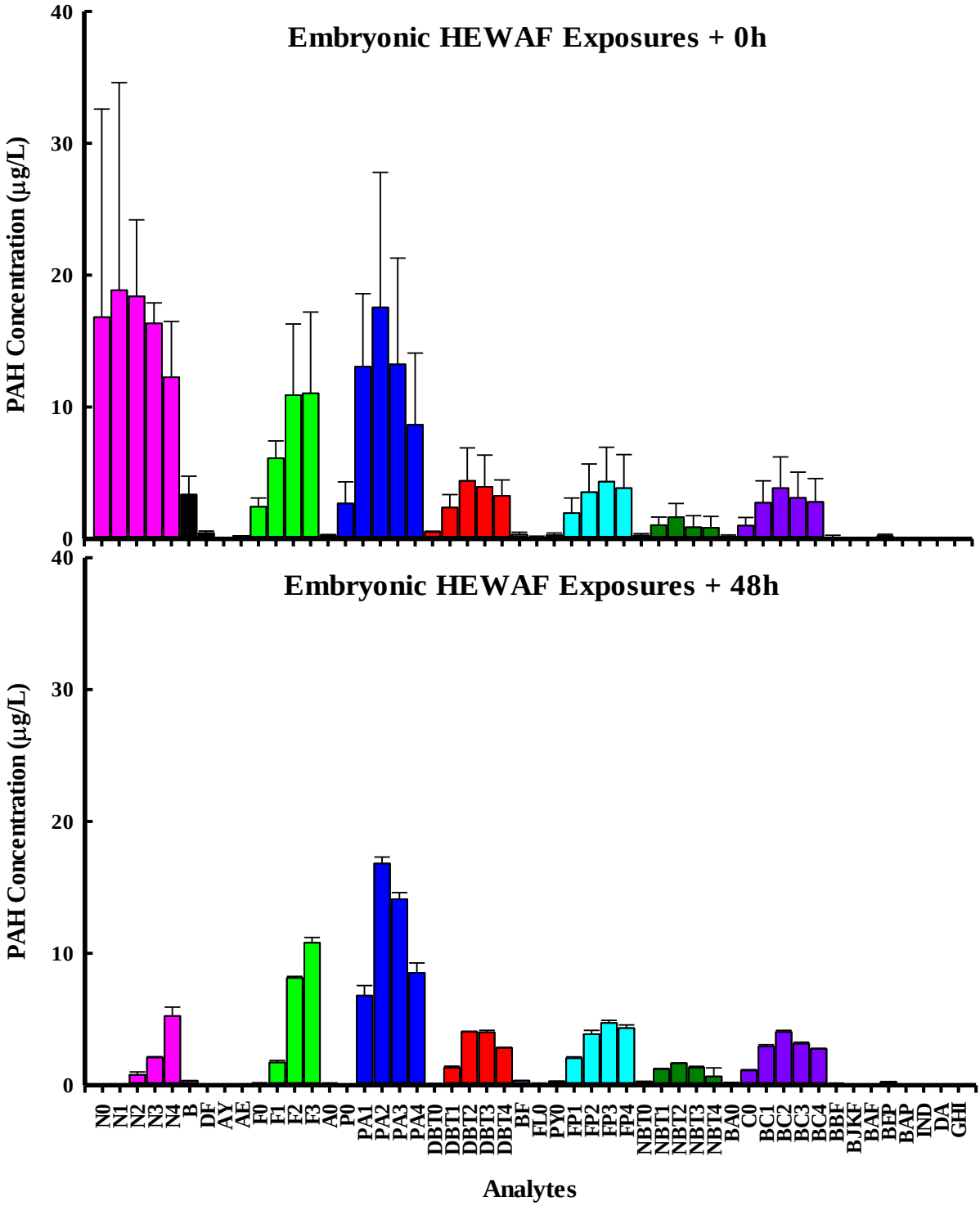

Figure 12. Mean (± SEM) TPAH50 concentrations (µg/L) for embryo HEWAF exposures.

counterparts, although this was not the case between the two TX populations. With the exception of PE TX-Ref control embryos possessing a statistically significantly higher mean heart rate of 124 ± 3 bpm compared to PE LA-Ref control embryos with a heart rate of 109 ± 3 bpm (LSD $p < 0.01$), little difference was noted in embryonic heart rates in response to parental exposure history and embryonic HEWAF exposure of the LA-Ref and TX-Ref populations. Embryonic heart rates differed in response to parental exposure history and embryonic HEWAF exposure between the LA-DHOS and TX-SF populations. Parental control (PC) derived LA-DHOS embryos reared in control water possessed a statistically significantly higher mean heart rate at 118 ± 2 bpm than that of PC TX-SF embryos (107 ± 2 bpm) reared in control water (LSD $p < 0.01$). Additionally, HEWAF exposure statistically significantly reduced mean heart rates of PC and PE LA-DHOS embryos from control values to 85 ± 4 bpm and 77 ± 3 bpm (LSD $p < 0.01$), respectively, whereas the mean heart rates of PC and PE TX-SF embryos exposed to HEWAF did not differ from control heart rates.

Embryo Exposures - Phenotypic Abnormality Analysis

A statistically significant overall interaction between population (LA-Ref, LA-DHOS, TX-Ref, and TX-SF), embryo exposure (control or HEWAF), and occurrence within binned PA score (none, medium, or high) was detected for PC-derived embryos (GLM 2; X^2 262.65, $p < 0.01$) and for PE-derived embryos (GLM 2; X^2 221.37, $p < 0.01$; Table 9). No instances of 'high' PA scores were observed in embryos exposed to control treatment waters, regardless of parental exposure history (Table 9). However, exposure to HEWAF increased the percentage of embryos with 'medium' or 'high' PA scores within all populations. A statistically significantly higher percentage of embryos from all PC treatments but only TX-SF from PE treatments, were observed to have 'no' PA score compared to a 'high' sum PA score when reared in control water

(Table 9; LSD $p < 0.01$). Within the PC treatment, HEWAF exposure resulted in statistically significant increases in percentage of embryos with 'medium' PA scores over 'no' PA score in LA-DHOS embryos (LSD $p < 0.01$); and a statistically significant increase in percentage of LA-Ref, LA-DHOS, and TX-Ref embryos with 'high' PA scores over 'no' PA score (LSD $p < 0.01$). Of these populations, LA-Ref embryos exhibited the highest occurrence of a 'high' sum PA score following HEWAF exposure in both PC (75% ± 16% occurrence; mean ± SEM) and PE treatments at (67% ± 19% occurrence). The lowest occurrence of a 'high' sum PA score following embryonic HEWAF exposure was noted in TX-SF embryos at 0% regardless of parental exposure history. A moderate percentage of PC TX-SF embryos exhibited a 'medium' PA score of 42% ± 8% occurrence following HEWAF exposure and was not statistically significantly different than the percentage of PC TX-SF embryos with 'no' PA score (58% ± 8% occurrence). However, PE TX-SF embryos exposed to HEWAF exhibited a statistically significantly lower percent occurrence of a 'medium' PA score at 25% ± 8% compared to 'no' PA score at 75% ± 8% occurrence (LSD $p < 0.01$).

Embryo Exposures – Fate by 21-Days Post Fertilization

Embryonic fate as represented by percentage can be found in Figure 13 and the starting numbers of embryos and number of embryos that hatched, died, or failed to hatch (non-hatch) used to generate Figure 13 can be found in Table 10. A statistically significant overall interaction between population (LA-Ref, LA-DHOS, TX-Ref, and TX-SF), parental exposure (PC or PE), and embryo exposure (control or HEWAF) was detected on frequency of hatch (GLM; X^2 88.70, $p < 0.01$). Exposure of PC embryos to HEWAF during embryogenesis statistically significantly reduced hatch success relative to control water exposed embryos (LA-DHOS – 55% ± 8% to 18% ± 18%; TX-Ref – 50% ± 23% to 23% ± 10%; mean ± SEM; LSD $p < 0.01$), whereas HEWAF

Table 9. Distribution of embryo total phenotypic abnormality (PA) scores for embryos exposed to control or HEWAF. Individual embryos were assigned a PA score based on accumulated abnormalities of hemorrhaging, cardiac edema, abnormal development, and tube heart at 7 days post fertilization. Stars (*) represent significant difference from the absence (None) of a PA score and lettered superscripts represent significant differences within PA score and parental treatment (LSD, $\alpha < 0.05$). No significant effect of parental exposure on PA score was detected.

Parental Treatment	Population	Embryo Treatment	Sum PA Score		
			None	Medium	High
Parental Control	LA-Ref	Control	83% ± 10%^{ab}	17% ± 10%*^{b}	0%*^{a}
		HEWAF	0%^{d}	25% ± 16%*^{bc}	75% ± 16%*^{b}
	LA-DHOS	Control	67% ± 24%^{bc}	33% ± 24%*^{b}	0%*^{a}
		HEWAF	0%^{d}	33% ± 16%*^{ab}	67% ± 16%*^{b}
	TX-Ref	Control	83% ± 10%^{a}	17% ± 10%*^{bc}	0%*^{a}
		HEWAF	17% ± 10%^{cd}	33% ± 14%^{ab}	50% ± 10%*^{b}
	TX-SF	Control	92% ± 8%^{ab}	8% ± 8%*^{d}	0%*^{a}
		HEWAF	58% ± 8%^{ab}	42% ± 8%^{ab}	0%*^{a}
Parental Exposed	LA-Ref	Control	83% ± 17%^{ab}	17% ± 17%*^{a}	0%*^{b}
		HEWAF	0%^{c}	33% ± 19%^{a}	67% ± 19%*^{a}
	LA-DHOS	Control	50% ± 35%^{bc}	50% ± 35%^{a}	0%^{ab}
		HEWAF	0%^{bc}	50% ± 35%^{a}	50% ± 35%^{ab}
	TX-Ref	Control	92% ± 8%^{a}	8% ± 8%*^{a}	0%*^{ab}
		HEWAF	0%^{c}	67% ± 24%*^{a}	33% ± 24%^{b}
	TX-SF	Control	92% ± 8%^{a}	8% ± 8%*^{a}	0%*^{b}
		HEWAF	75% ± 8%^{a}	25% ± 8%*^{a}	0%*^{b}

exposure increased hatch success in PC TX-SF embryos from 33% ± 0% in control waters to 75% ± 8% (Figure 13A). Within the PE treatment, embryonic HEWAF exposure statistically significantly reduced hatch success from 58% ± 8% to 27% ± 1% in TX-Ref only (LSD $p <$ 0.01). No interaction was detected between parental and embryonic exposure on LA-Ref, TX-Ref, or TX-SF hatch success. Parental exposure (PE) to WAF statistically significantly reduced hatch success to 25% ± 0% in LA-DHOS embryos reared in control water (LSD $p < 0.01$), although this same effect was not observed in embryos reared in HEWAF. No other statistically significant differences in hatch success was observed between the two reference populations with respect to interactions of parental exposure history or embryonic treatment. Although no difference between the hatch success of PC LA-DHOS and PC TX-SF embryos reared in clean water was detected, statistically significantly higher hatch success was detected in PE-derived TX-SF embryos (64% ± 1%) over PE derived LA-DHOS (25% ± 0%) embryos following exposure to either control water or HEWAF (LSD $p < 0.01$).

A statistically significant overall interaction between population (LA-Ref, LA-DHOS, TX-Ref, and TX-SF), parental exposure (PC or PE), and embryo exposure (control or HEWAF) was detected on frequency of mortality (GLM; X^2 57.48, $p < 0.01$). A statistically significant interaction between adult exposure history and embryonic exposure on embryonic mortality was detected for the LA-Ref and LA-DHOS populations (LSD $p < 0.01$), but not for the TX-Ref and TX-SF populations (Figure 13B). Embryonic mortality was generally low in the Texas populations regardless of parental exposure history or embryonic exposure, which, at its highest, had a frequency of 14% ± 8% (mean ± SEM) in the PE TX-Ref population exposed to HEWAF.

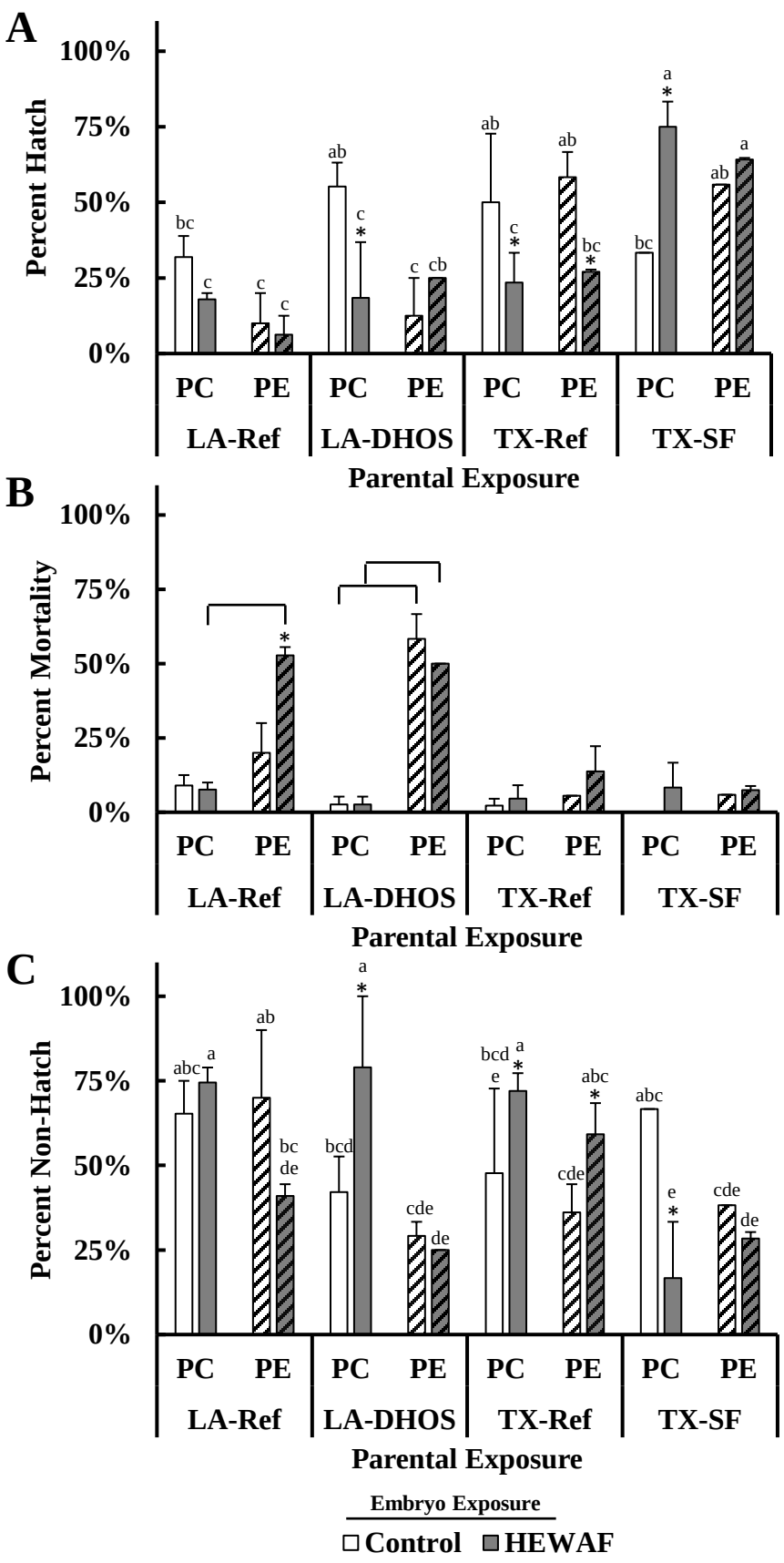

Figure 13. Embryonic fate (mean percent ± SEM) hatch (A), mortality (B), and Non-hatch (C)) of embryos exposed to control or HEWAF treatments for up to 21 days post fertilization. Solid bars represent fates of embryos derived from parental control (PC) treatments and patterned bars represent fates of embryos derived from parental exposed (PE) treatments. Stars (*) represent pairwise significant differences between fates of embryos exposed to control or WAF treatment waters and letters represent significant differences between population, parental exposure, and embryonic exposure. Due to absence of population effect on percent mortality, bars represent significant differences between fates of embryos derived from PC or PE treatments (LSD, $\alpha < 0.05$). Starting counts of embryos and counts for hatch, mortality, and non-hatch can be found in Table 10.

Table 10. Starting counts of embryos and counts for hatch, mortality, and non-hatch by 21 days post fertilization.

Parental History	Population	Embryo Exposure Treatment	Starting Embryo Number	Embryonic Fate Total Count of Occurrence		
				Hatch	Mortality	Non-Hatch
Parental Control	LA-Ref	Control	34	11	3	20
		HEWAF	39	7	3	29
	LA-DHOS	Control	38	21	1	16
		HEWAF	39	7	1	31
	TX-Ref	Control	44	22	1	21
		HEWAF	43	10	2	31
	TX-SF	Control	12	4	0	8
		HEWAF	12	9	1	2
Parental Exposed	LA-Ref	Control	20	2	2	14
		HEWAF	17	1	9	7
	LA-DHOS	Control	7	1	4	2
		HEWAF	8	2	4	2
	TX-Ref	Control	36	21	2	13
		HEWAF	37	10	5	22
	TX-SF	Control	68	38	4	26
		HEWAF	67	43	5	19

Parental WAF exposure (PE) statistically significantly increased mortality in LA-Ref embryos reared in HEWAF to 53% ± 3% over those reared in control water (20% ± 10%; LSD $p < 0.01$). Additionally, percent mortality was statistically significantly higher in PE LA-Ref embryos exposed to HEWAF than PC LA-Ref embryos exposed to HEWAF at 8% ± 2% (LSD $p < 0.01$). Statistically significantly higher mortalities were observed in PE LA-DHOS embryos reared in control or HEWAF treatment waters at 58% ± 8% and 50% ± 0% mortality, respectively, over their PC counterparts (LSD $p < 0.01$).

A statistically significant overall interaction between population (LA-Ref, LA-DHOS, TX-Ref, and TX-SF), parental exposure (PC or PE), and embryo exposure (control or HEWAF) was detected on frequency of embryos that failed to hatch (non-hatch; GLM; X^2 57.48, LSD $p < 0.01$). Statistically significant increases to 79% ± 21% (mean ± SEM) and 72% ± 5% in percent non-hatch were observed in PC LA-DHOS and PC TX-Ref populations, respectively, reared in HEWAF compared to those reared in control water (Figure 13C; LSD $p < 0.01$). Conversely, percent non-hatch for PC TX-SF embryos statistically significantly decreased from 67% ± 0% for embryos reared in control waters to 17% ± 17% for embryos reared in HEWAF (LSD $p < 0.01$). Parental WAF exposure statistically significantly decreased percent non-hatch in LA-Ref (41% ± 3%) and LA-DHOS (25% ± 0%) embryos exposed to HEWAF (LSD $p < 0.01$), although this was likely influenced by an increase in percent mortalities observed in the PE treatments at 53% ± 3% and 50% ± 0% mortality, respectively. Similarly, for embryos reared in clean water percent non-hatch was statistically significantly lower in PE LA-DHOS embryos (29% ± 4%) compared to PE LA-Ref embryos (70% ± 20%; LSD $p < 0.01$), which can also be attributed in part to increased mortality in PE LA-DHOS embryos (58% ± 8%). Statistically significantly

higher percent non-hatch was observed in both PC and PE TX-Ref embryos reared in HEWAF at 72% ± 5% and 59% ± 9%, respectively, compared to their TX-SF counterparts (LSD $p < 0.01$).

Different responses were noted between LA-Ref and TX-Ref embryos reared in control water in response to parental exposure history, as a significantly higher percent non-hatch was detected in PE LA-Ref embryos at 70% ± 20% (mean ± SEM) compared to TX-Ref embryos at 36% ± 8% (LSD $p < 0.01$). Percent non-hatch was statistically significantly higher in HEWAF exposed PC LA-DHOS embryos compared to HEWAF exposed PC TX-SF embryos (LSD $p < 0.01$); however, no differences were detected between control exposed PC LA-DHOS and PC TX-SF embryos. Percent non-hatch was similar between PE LA-DHOS embryos and PE TX-SF embryos regardless of embryonic treatment exposure; although, the observed for PE LA-DHOS embryos can be attributed to increased mortality.

Discussion

This study demonstrated that populations of Gulf killifish that encountered habitat oiling during the DHOS were sensitive to PAHs. Reproductive impairment was observed in adult Gulf killifish from sensitive populations exposed to sublethal concentrations of crude oil (TPAH50 concentration of 135 ± 70.8 µg/L; mean ± SD). These effects were manifest in reduced fertilization successes following the 40-d WAF exposure and may have occurred due to reduction in gamete quality (Sundt and Björkblom, 2011), maternal deposition of PAHs and their metabolites into eggs (Romero et al., 2018), or epigenetic alterations (Bautista and Burggren, 2019; Best et al., 2018). Induction of the aryl hydrocarbon receptor (AHR) has been previously shown to suppress genes associated with vitellogenin production (Bugel et al., 2013). Gulf killifish sampled at Grand Terre, LA following the DHOS showed similar decreased transcription of vitellogenin proteins in addition to decreased transcription of chorionic proteins,

zona pellucida (ZP3 and ZP4) and choriogenin (ChgHm and ChgH; Whitehead et al., 2012), confirming reproductive impairment through activation of the AHR pathway by Macondo oil. Furthermore, male killifish collected in 2011 from previously oiled sites in Bay Jimmy, LA exhibited statistically significant reductions in testes size and germinal epithelium thickness, corresponding with elevated concentrations of PAHs in sediments and suggesting the potential for continued reproductive impairment in oiled sites after initial DHOS oiling (Carr et al., 2018). The current study also found that parental oil exposure increased the number of eggs produced per female when compared to parental control water exposure. This is potentially explained through a hormetic effect on fish egg production caused by exposure to sublethal concentrations of PAHs, which has been observed in sheepshead minnows (*Cyprinodon variegatus*; Jasperse et al., 2019; *for review, see* Calabrese and Mattson, 2017), suggesting that parental oil exposure did not impair fecundity in female Gulf killifish but may have reduced gamete quality of either male or female fish.

HEWAF exposure (TPAH50 concentration of 220.4 ± 50.0 μg/L; mean ± SD) to the LA-Ref, LA-DHOS, and TX-Ref populations of embryonic Gulf killifish resulted in a suite of deleterious phenotypes consistent with early life stage PAH exposure. Statistically significant reductions in embryonic heart rates at 7 dpf were observed in these populations following HEWAF exposure. Reductions in embryonic heart rates occurs following exposure to tricyclic PAHs (Incardona et al., 2004). Tricyclic PAHs reduce heart rates by inhibiting cardiomyocyte repolarization by inhibiting the outward movement of potassium that occurs at the end of excitation-contraction coupling (Brette et al., 2014). Furthermore, specific tricyclics, such as phenanthrene, can also reduce intracellular calcium concentrations (Brette et al., 2017). Gulf killifish embryos in the current study were exposed to concentrations of phenanthrene (2.7 μg /L)

enough to cause bradycardia in HEWAF exposures. Statistically significant increases in PA scores were also observed following embryonic HEWAF exposure, although these phenotypes likely manifested through AHR-mediated processes induced by HMW PAHs. In the current study, phenotypic abnormality (PA) scores were noted through occurrence of abnormal morphological development, cardiac edema, heart deformation, and hemorrhaging. Previous studies have shown that Macondo oil exposure impaired neural crest cell migration and differentiation in the head region of zebrafish (*Danio rerio*), leading to abnormal formation of the cranium (De Soysa et al., 2012). However, other PA scores observed in the current study were likely associated with PAH induced cardiac toxicity. Mummichog, a closely-related congener species to Gulf killifish (*Fundulus heteroclitus*), embryos exposed to PAHs exhibited a strong correlation ($R^2 = 0.82$) between severity of bradycardia and development of phenotypic abnormalities in individual embryos (Bozinovic et al., 2013). AHR-mediated cardiotoxicity can impair development of the heart, leading to formation of 'tube heart' and reduced peripheral circulation (De Soysa et al., 2012; Incardona, 2017), subsequently reducing cardiac contractility and leading to pericardial edema and hemorrhaging in trunk peripheries (De Soysa et al., 2012). Taken together, these developmental perturbations likely contributed to the decreased hatch success observed in embryos from sensitive populations exposed to HEWAF in the current study.

This study also demonstrated decreased sensitivity of the TX-SF (Vince Bayou, TX) population to surrogate Macondo oil. Parental WAF exposure did not result in decreased fertilization success and embryos did not exhibit the suite of oil exposure phenotypes (*e.g.* bradycardia, increased PA score, reduced hatch success) characterized in the other populations following HEWAF exposure. This perceived resistance to PAH toxicity is attributed to a

population-wide ingression of an *AHR* locus containing deletions that reduces AHR sensitivity to halogenated aromatic hydrocarbons and PAHs (Oziolor et al., 2014; Oziolor et al., 2019). Although desensitization to PAHs has been previously characterized for the TX-SF population, to my knowledge this is the first study to characterize their reproductive physiology. Reduced egg production in TX-SF females (18.4 eggs per female) held in clean water was observed relative to other populations reared in clean water (LA-Ref – 54.4 eggs per female, LA-DHOS – 48.4 eggs per female, and TX-Ref – 37.2 eggs per female). Similar reductions in fecundity have been observed in a pollution-resistant population of mummichog from Newark Bay, NJ, which exhibited reduced 17β-estradiol sensitivity relative to a reference population (Bugel et al., 2014). However, female TX-SF Gulf killifish held in WAF treatments for 40 d produced 4.3-fold more eggs than female TX-SF fish held in control conditions without impairment to fertilization success, and hatch success was statistically significantly higher for embryos reared in HEWAF compared to those reared in control water, suggesting that PAH exposure may contribute a 'rescuing' effect to reproductive and developmental physiologies in the TX-SF population. Investigations into the molecular underpinnings behind this 'rescue' effect would aid in better understanding the cost of pollution resistance in this population of killifish.

This study demonstrated that parental exposure (PE) to crude oil resulted in intergenerational effects in the form reduced offspring fitness (*e.g.* hatch and mortality). Exposure of PC derived embryos to HEWAF statistically significantly reduced hatch success likely as a result of the developmental perturbations discussed above and exposure of PE-derived LA embryos to HEWAF resulted in a statistically significant increase in mortality. Previously mentioned impacts on reproductive impairment (*e.g.* maternal deposition of PAHs or their metabolites, epigenetic changes, or reduced egg quality) may have increased embryo sensitivity

to HEWAF exposure (Corrales et al., 2014; Petitjean et al., 2019). However, increases in embryonic sensitivities were not equal across populations, suggesting that population level differences exist in both transgenerational effects and embryonic sensitivity. Gulf killifish derived from the contemporarily oiled Grand Terre, LA (LA-DHOS) appeared to be the most sensitive to the intergenerational effects of oil, which is in line with the hypothesis that a recently-oiled population will show a different intergenerational response to oiling from the reference population (LA-Ref). This suggests that recent oiling from DHOS confers increased sensitivity or susceptibility to intergenerational effects on both overall embryo fitness and sensitivity to additional oiling. Multigenerational parental exposures may have resulted in genotoxicity or aneugenic or clastogenic events that caused gamete chromosomal aberrations (Baršienė et al., 2012; Rotchell et al., 2008). Alternatively, heritable epigenetic changes in LA-DHOS fish may be the dominant mechanism impacting overall adult reproductive and developmental health in response to oil exposure (Bautista and Burggren, 2019).

The salt marshes that line the northern Gulf of Mexico serve as breeding grounds and nurseries for Gulf killifish in addition to several other commercially important species of fish (Chesney et al., 2000) and with the DHOS occurring during peak spawning time for Gulf killifish, breeding adults and their offspring were likely exposed to oil (Dubansky et al., 2013; Fodrie and Heck 2011; Rooker et al. 2013 *but see* Roth and Baltz 2009; Whitehead et al., 2012). The current study demonstrated that surrogate Macondo oil impacts Gulf killifish reproduction, early life stage development, and can lead to intergenerational sensitization to oil exposure. The use of multiple populations with differing genetic backgrounds in the current study has highlighted the need in considering population history and the historical selective pressures of those populations. The unique oiling response of LA-DHOS fish compared to other populations,

suggesting that long-term exposure to oiled sediments caused heritable changes in oil sensitivity, although the underpinnings of those changes require additional investigation.

CHAPTER 5
CONCLUSION

On April 20, 2010, an exploratory well within the Macondo Canyon Block 252 prospect ruptured following the explosion of the Deepwater Horizon oil platform. Over a span of 87 days, an estimated 779 million liters of Macondo-252 light sweet crude oil was released into the Gulf of Mexico making it the largest marine oil spill in history (Lehr et al., 2010; McNutt et al., 2012; Nixon et al., 2016). Both during the spill and after the well was capped, multiple remediation efforts were performed to limit the amount of oil reaching sensitive coastal habitats. Due to a lack of research on their concomitant use, the two most controversial remediation efforts were the application of approximately 7 million liters of the chemical dispersant, Corexit, to enhance slick dispersion (Lehr et al., 2010); and opening of salinity control structures to allow fresh water from the Mississippi River to prevent encroaching surface oil slicks from making landfall (Deepwater Horizon Natural Resource Damage Assessment Trustees, 2016). Despite these efforts, over a 1,000 km of marshland was oiled (Lee et al., 2015). The salt marshes, wetlands, and delta ecosystems impacted by the Deepwater Horizon oil spill (DHOS) provide excellent spawning and nursery grounds for many Gulf of Mexico (GOM) species of fish through their large area of habitat and high rate of primary production (Nordlie, 2000; Silliman and Zieman, 2001). The results of my dissertation provide a comprehensive characterization of the damage imposed by the DHOS and provides insights into mechanisms of toxicity that should be considered for future spills.

In chapter 2, I investigated Corexit toxicity concomitant with acute hypo- and hyperosmoregulatory salinity challenges in Gulf killifish (*Fundulus grandis*) at multiple life stages. The salinities used in this experiment were bracketed by salinities commonly encountered

by fish in northern GOM saltmarshes that range from fresh to full strength sea water (Nordlie, 2006; Sklar and Browder, 1998). However, rapid fluctuations in salinity are known to occur in saltmarshes following the ebb and flow of tides, extreme storm events, or from increased riverine discharge, which occurred following the DHOS as salinity control structures were opened to full capacity to prevent the encroaching floating oil slicks from making landfall (Deepwater Horizon Natural Resource Damage Assessment Trustees, 2016). Although Corexit application was legislated for applications greater than 5.5 km from the coastline, evidence suggests that saltmarsh fish may have been exposed to Corexit or to surfactants contained within it that are purported to interact with fish gills (Deepwater Horizon Natural Resource Damage Assessment Trustees, 2016; Houma ICP Aerial Dispersant Group, 2010; White et al., 2014). I found that Corexit exposure was acutely toxic to adult Gulf killifish in the face of acute salinity challenges and that it compromised the ability of ability to mitigate physiological perturbations during acute salinity challenges. Ion body burden increased in hyperosmotic exposures and decreased in hyposmotic exposures, suggesting that Corexit exposure impairs osmoregulation in fish, likely at the site of the gill. In agreement with this finding, I found that Corexit toxicity increased concomitant with maturation of the gill throughout ontogeny. The understanding of mechanisms that lead to osmotic perturbations could be improved by investigating potential histopathology of the gill following exposure to Corexit. Potentially, Corexit disrupts paracellular sodium excretion and cellular machinery associated with chloride balance in fish exposed to hyperosmotic waters or may inhibit epithelial remodeling at the site of the gill in hypoosmotic waters.

In chapter 3, I characterized the behavior of crude oil droplets suspended in water and the interaction of oil droplets with Gulf killifish chorions. A novel high throughput method was developed that allowed for unbiased analysis of a large volume of samples associated with

droplets suspended in water and adsorbed to Gulf killifish chorions. Mechanical dispersion of oil results in higher densities of suspended droplets than chemical dispersion and that chorionic morphology influences densities of adsorbed oil droplets. Chemical analysis of unfiltered dispersed oil mixtures considers both water soluble toxic polycyclic aromatic hydrocarbons (PAHs) in the dissolved phase and non-soluble PAHs enriched in the particulate (droplet) phases in determination of total PAH concentrations. Basing toxicity estimates on total PAH concentrations can underestimate oil toxicity given that toxicity is associated with dissolved phase PAHs and not droplets (Di Toro et al., 2007; Hansen et al., 2019; Redman et al., 2017). Thus, it is important to consider the contribution of oil droplets to toxicity as droplets are thought to act as a reservoir to the dissolved phase (Landry et al., 2019) and serve as a route of direct transfer of PAHs when interacting with biological membranes (Petersen and Kristensen, 1998; Sørensen et al., 2017; Sørhus et al., 2015). Investigations into PAH bioaccumulation following exposure of embryonic fish to the water-soluble fraction of oil or to unfiltered dispersed oil solutions (dissolved and particulate phases) linked with analysis of droplet interaction with embryonic fish chorions would strengthen the understanding of oiled water toxicity.

In chapter 4, I investigated the intergenerational effects of oil exposure on multiple populations of Gulf killifish. This species spends the entirety of their lifecycle within small home ranges in GOM saltmarshes, using these marshes as spawning grounds and nurseries (Nordlie, 2000; Williams et al., 2008). Exposure of breeding Gulf killifish to oil impaired reproduction and increased the sensitivity of offspring to subsequent oil exposures, suggesting the impacts of habitat oiling on early life stage development of Gulf killifish may have been worse than what previous studies investigating solely early life stage toxicity had determined. A population of Gulf killifish collected from a habitat several years after it was heavily oiled during the DHOS

(Grand Terre, LA [29° 16’23” N, 89° 56’42 W]) demonstrated increased sensitivity to the effects of oiling compared to a reference population, which suggest that the impacts of habitat oiling are persistent and may decrease organismal fitness on a population level well beyond initial oiling. Investigations into the transcriptional underpinnings associated with reproductive impairment and sensitization of offspring would clarify the understanding of how oil spills impact ecosystems. This work increases the understanding of the long-term impacts of oil spill and strengthens predictions of population level ecotoxicity in the event of a future spill.

A large body of research on the ecotoxicity of oil was generated following the DHOS to answer questions about its impact. Consequently, this dissertation addressed research questions derived from those studies. This dissertation increases the understanding of oil toxicity and strengthens the ability of scientists to predict ecological effects of future spills. Given the fact that oil exploration is being driven into more remote and extreme environments, an increase in the frequency of oil spill disasters is likely.

APPENDIX A
PERMISSION TO USE PUBLISHED ARTICLE IN DISSERTATION

Charles A Brown

From:	Researcher Support <support@elsevier.com>
Sent:	Friday, December 20, 2019 7:05 AM
To:	Charles A Brown
Subject:	Re: Publishing agreement [191220-004030]

Dear Mr. Charles Brown,

Article reference: CBC8515

Thank you for your query regarding using your article in your thesis/dissertation.

I can confirm that that authors can use their articles, in full or in part, for a wide range of scholarly, non-commercial purposes one of which is inclusion in a thesis or dissertation.

See the following link for further information on this https://www.elsevier.com/about/our-business/policies/copyright/personal-use

As you will be able to see from the above link, our policy is to allow authors to use their work in their thesis or dissertation (provided that this is not to be published commercially).
Therefore, I can confirm that you can make it publicly available on your university web site/repository for noncommercial use.

If you require further clarification, please contact permissions@elsevier.com who will be able to help.

Kind regards,

Rommel Buenasflores Jallorina
Researcher Support
ELSEVIER

APPENDIX B
SUPPLEMENTAL MATERIAL FROM CHAPTER 3

Suspended Droplet Macro

```
macro "Suspended Droplet Evaluation" {
imageTitle=getTitle();
path=getDirectory("image");
run("Set Scale...", "distance=1 known=1.238 pixel=1 unit=um global");
run("8-bit");
run("Brightness/Contrast...");
setMinAndMax(21, 54);
run("Enhance Contrast", "saturated=0.35");
run("Subtract Background...", "rolling=20");
run("Despeckle");
run("Despeckle");
run("Despeckle");
run("Smooth");
run("Threshold...");
setThreshold(4, 255);
setOption("BlackBackground", true);
run("Convert to Mask");
run("Watershed");
run("Set Measurements...", "area perimeter feret's area_fraction redirect=None decimal=1");
run("Analyze Particles...", "size=1-500 circularity=0.3-1.00 show=Overlay display clear
summarize stack");
run("Labels...", "color=white font=10 show bold");
run("In [+]");
run("Summarize");
saveAs("jpg", path+imageTitle);
i=2;
run("Read and Write Excel", "sheet=Data_sheet_" + i);
run("Close All");
}
```

Adsorbed Droplet Macro

```
macro "Adsorbed Droplet Evaluation" {
imageTitle=getTitle();
path=getDirectory("image");
run("Set Scale...", "distance=1 known=1.238 pixel=1 unit=um global");
run("Remove Outliers...", "radius=5 threshold=1 which=Bright");
run("Remove Outliers...", "radius=5 threshold=1 which=Dark");
run("Enhance Contrast...", "saturated=0.35");
run("Split Channels");
selectWindow(imageTitle + " (green)");
run("Subtract Background...", "rolling=6");
run("Despeckle");
run("Smooth");
run("Threshold...");
setAutoThreshold("Default dark")
setThreshold(14, 255);
setOption("BlackBackground", true);
run("Convert to Mask");
run("Watershed");
run("Set Measurements...", "area perimeter exclude feret's area_fraction redirect=None
decimal=1");
run("Analyze Particles...", "size=1-500 circularity=0.3-1.00 show=Overlay display clear
summarize stack");
run("Labels...", "color=red font=10 show bold");
run("In [+]");
run("Summarize");
selectWindow(imageTitle+ " (green)");
saveAs("jpg", path+imageTitle);
close();
i=2;
run("Read and Write Excel", "sheet=Data_sheet_" + i);
}
```

Table B1. Ratio of attached droplet densities to suspended droplet densities in slick A HEWAF treatments from Experiments 1 and 2. Droplets (diameter; µm) were binned to discrete sizes to clearly illustrate ratios. Suspended droplet densities for Experiment 1 are provided below Experiment 2 densities for comparison.

End Point	Medium	Time	Binned Volume Diameter (µm)												
			1	2	3	4	5	6	7	8	9	10	11	12	13
Adsorbed Droplet Density	Natural	3 h	2.7	10.5	15.6	18.9	22.0	17.8	12.9	8.0	3.6	1.9	0.6	0.3	0.1
		6 h	5.0	6.2	7.1	8.6	9.4	7.1	5.3	3.1	1.8	1.1	0.5	0.3	0.1
	Cleaned	3 h	2.2	7.5	7.9	8.3	7.9	7.2	4.9	3.8	2.3	1.4	0.6	0.4	0.1
		6 h	4.3	5.6	7.7	8.7	10.7	9.1	7.2	4.8	3.7	2.3	1.6	0.9	0.4
Suspended Droplet Density	Exp 2	3 h	1.4	2.9	4.9	5.3	10.0	17.6	25.7	29.7	38.3	31.8	25.0	17.9	5.9
		6 h	2.6	5.7	7.3	11.5	16.3	22.9	35.7	42.6	42.9	31.1	30.9	17.1	4.0
	Exp 1	3 h	0.7	1.3	1.7	2.6	3.3	3.5	8.5	8.5	10.3	6.7	6.4	3.5	0.8
		6 h	1.7	2.7	5.7	6.0	9.7	14.5	22.7	30.4	30.8	29.2	24.5	12.0	5.2
Adsorption Ratio	Natural	3 h	1.9	3.5	3.2	3.5	2.2	1.0	0.5	0.3	0.1	0.1	0.02	0.02	0.02
		6 h	1.9	1.1	0.9	0.8	0.6	0.3	0.2	0.1	0.04	0.03	0.02	0.02	0.02
	Cleaned	3 h	1.5	2.5	1.6	1.6	0.8	0.4	0.2	0.1	0.1	0.04	0.02	0.02	0.02
		6 h	1.7	0.97	1.1	0.8	0.7	0.4	0.2	0.1	0.1	0.1	0.1	0.1	0.1

Table B2**.** Ratio of attached droplet densities to suspended droplet densities in slick A CEWAF treatments from Experiments 1 and 2. Droplets (diameter; µm) were binned to discrete sizes to clearly illustrate ratios. Suspended droplet densities for Experiment 1 are provided below Experiment 2 densities for comparison.

End Point	Medium	Time	Binned Volume Diameter (µm)												
			1	2	3	4	5	6	7	8	9	10	11	12	13
Adsorbed Droplet Density	Natural	3 h	0.7	1.1	1.3	1.4	1.7	1.6	0.9	0.7	0.4	0.2	0.2	0.2	0.01
		6 h	0.2	0.4	0.6	0.7	1.0	0.7	0.6	0.5	0.2	0.2	0.02	0.01	0.01
	Cleaned	3 h	0.3	0.4	0.5	0.6	0.7	0.7	0.7	0.7	0.2	0.2	0.1	0.1	0.03
		6 h	0.4	0.7	0.9	1.2	1.3	1.1	0.8	0.6	0.5	0.3	0.2	0.1	0.01
Suspended Droplet Density	Exp 2	3 h	5.2	13.3	10.2	14.7	16.2	11.1	11.6	8.1	5.9	4.9	2.7	1.0	0.4
		6 h	5.3	13.5	9.8	9.6	5.6	3.1	2.6	1.4	1.3	1.0	0.5	0.7	0.1
	Exp 1	3 h	1.4	3.5	3.5	2.5	1.7	2.5	0.5	0.7	0.0	0.0	0.1	0.0	0.0
		5 h	6.1	11.9	12.9	13.6	9.0	7.2	5.1	3.0	0.9	0.4	0.3	0.1	0.1
Adsorption Ratio	Natural	3 h	0.1	0.1	0.1	0.1	0.1	0.2	0.1	0.1	0.1	0.1	0.1	0.2	0.03
		6 h	0.04	0.03	0.1	0.1	0.2	0.2	0.2	0.4	0.1	0.2	0.04	0.02	0.1
	Cleaned	3 h	0.1	0.03	0.1	0.04	0.04	0.1	0.1	0.1	0.03	0.03	0.04	0.1	0.1
		6 h	0.1	0.1	0.1	0.1	0.2	0.4	0.3	0.5	0.4	0.3	0.4	0.2	0.1

Table B3. Ratio of attached droplet densities to suspended droplet densities in slick B HEWAF treatments from Experiments 1 and 2. Droplets (diameter; µm) were binned to discrete sizes to clearly illustrate ratios. Suspended droplet densities for Experiment 1 are provided below Experiment 2 densities for comparison.

End Point	Medium	Time	Binned Volume Diameter (µm)												
			1	2	3	4	5	6	7	8	9	10	11	12	13
Adsorbed Droplet Density	Natural	3 h	3.2	5.9	7.4	8.5	8.1	5.1	3.0	0.9	0.4	0.2	0.2	0.1	0.0
		6 h	1.3	1.7	1.9	2.3	2.3	1.5	0.9	0.6	0.3	0.2	0.1	0.1	0.0
	Cleaned	3 h	0.6	0.8	0.7	0.9	1.0	0.7	0.3	0.1	0.1	0.01	0.0	0.0	0.0
		6 h	2.5	2.8	3.2	3.8	3.9	4.0	3.0	2.3	1.4	0.9	0.7	0.3	0.0
Suspended Droplet Density	Exp 2	3 h	7.6	17.5	29.6	35.9	39.3	35.8	33.6	28.3	16.8	11.7	8.3	4.8	2.5
		6 h	6.3	17.1	22.9	33.2	40.1	46.9	55.6	49.4	36.1	29.9	23.6	14.1	7.3
	Exp 1	3 h	1.9	5.7	10.0	16.7	23.4	26.9	32.6	25.6	20.2	11.6	7.9	5.9	2.6
		6 h	1.7	5.4	7.6	9.0	13.8	16.6	18.8	19.8	14.1	10.3	5.1	1.2	0.7
Adsorption Ratio	Natural	3 h	0.4	0.3	0.3	0.2	0.2	0.1	0.1	0.03	0.03	0.02	0.02	0.01	0.0
		6 h	0.2	0.1	0.8	0.1	0.1	0.03	0.02	0.01	0.01	0.01	0.0	0.0	0.0
	Cleaned	3 h	0.1	0.04	0.03	0.03	0.0	0.02	0.01	0.0	0.0	0.0	0.0	0.0	0.0
		6 h	0.4	0.2	0.1	0.1	0.1	0.1	0.1	0.1	0.04	0.03	0.03	0.02	0.0

REFERENCES

Abdel-Raouf, M.E.-S., 2012. Factors affecting the stability of crude oil emulsions, Crude oil emulsions-Composition stability and characterization. IntechOpen.

Able, K.W., Vivian, D.N., Petruzzelli, G., Hagan, S.M., 2012. Connectivity Among Salt Marsh Subhabitats: Residency and Movements of the Mummichog (Fundulus heteroclitus). Estuaries and Coasts 35, 743-753.

ABSG Consulting Inc., 2016. 2016 Update of Occurrence Rates for Offshore Oil Spills. Prepared by ABS Consulting Inc. for USDOI, BOEM/BSEE, Arlington, VA, pp. 95. <https://www.bsee.gov/sites/bsee.gov/files/osrr-oil-spill-response-research/1086aa.pdf>

Agamy, E., 2013. Sub chronic exposure to crude oil, dispersed oil and dispersant induces histopathological alterations in the gills of the juvenile rabbit fish (Siganus canaliculatus). Ecotoxicology and Environmental Safety 92, 180-190.

Allen, P., 2015. Patrick Bayou-Deer Park, Harris County, Texas. U.S. Environmental Protection Agency. <https://semspub.epa.gov/work/06/500014750.pdf>

Armstrong, P.B., Child, J.S., 1965. Stages in the normal development of Fundulus heteroclitus. The Biological Bulletin 128, 143-168.

Atlas, R.M., Hazen, T.C., 2011. Oil biodegradation and bioremediation: A tale of the two worst spills in US history. Environmental Science & Technology 45, 6709-6715.

Aurand, D., Coelho, G., 2005. Cooperative aquatic toxicity testing of dispersed oil and the chemical response to oil spills: Ecological Effects Research Forum (CROSERF). Technical Report 07-03, Ecosystem Management and Associates, Lusby, MD, pp. 105.

Baker, R., Fry, B., Rozas, L.P., Minello, T.J., 2013. Hydrodynamic regulation of salt marsh contributions to aquatic food webs. Marine Ecology Progress Series 490, 37-52.

Baršienė, J., Rybakovas, A., Lang, T., Grygiel, W., Andreikėnaitė, L., Michailovas, A., 2012. Risk of environmental genotoxicity in the Baltic Sea over the period of 2009–2011 assessed by micronuclei frequencies in blood erythrocytes of flounder (Platichthys flesus), herring (Clupea harengus) and eelpout (Zoarces viviparus). Marine Environmental Research 77, 35-42.

Batchu, S.R., Ramirez, C.E., Gardinali, P.R., 2014. Stability of dioctyl sulfosuccinate (DOSS) towards hydrolysis and photodegradation under simulated solar conditions. Environmental Science and Technology 47, 1960-1967.

Bautista, N.M., Burggren, W.W., 2019. Parental stressor exposure simultaneously conveys both adaptive and maladaptive larval phenotypes through epigenetic inheritance in the zebrafish (Danio rerio). Journal of Experimental Biology 222, jeb208918.

Bejarano, A.C., 2018. Critical review and analysis of aquatic toxicity data on oil spill dispersants. Environmental Toxicology and Chemistry 37, 2989-3001.

Bemanian, V., Male, R., Goksøyr, A., 2004. The aryl hydrocarbon receptor-mediated disruption of vitellogenin synthesis in the fish liver: Cross-talk between AHR-and ERα-signalling pathways. Comparative Hepatology 3, 2.

Bentley, P.J., 2002. Endocrines and osmoregulation: a comparative account of the regulation of water and salt in vertebrates, Zoophysiology and Ecology Springer Science & Business Media, 1-37.

Best, C., Ikert, H., Kostyniuk, D.J., Craig, P.M., Navarro-Martin, L., Marandel, L., Mennigen, J.A., 2018. Epigenetics in teleost fish: From molecular mechanisms to physiological phenotypes. Comparative Biochemistry and Physiology Part B: Biochemistry and Molecular Biology 224, 210-244.

Beyer, J., Trannum, H.C., Bakke, T., Hodson, P.V., Collier, T.K., 2016. Environmental effects of the Deepwater Horizon oil spill: a review. Marine Pollution Bulletin 110, 28-51.

Billiard, S.M., Meyer, J.N., Wassenberg, D.M., Hodson, P.V., Di Giulio, R.T., 2007. Nonadditive effects of PAHs on early vertebrate development: mechanisms and implications for risk assessment. Toxicological Sciences 105, 5-23.

Billiard, S.M., Timme-Laragy, A.R., Wassenberg, D.M., Cockman, C., Di Giulio, R.T., 2006. The role of the aryl hydrocarbon receptor pathway in mediating synergistic developmental toxicity of polycyclic aromatic hydrocarbons to zebrafish. Toxicological Sciences 92, 526-536.

Blaber, S.J., 1975. Lipid content and condition in an estuarine teleost. Zoologica Africana 10, 63-73.

Bodinier, C., Galvez, F., Gautreaux, K., Rivera, A., Green, C.C., 2014. Toxicological and physiological effects of the surfactant dioctyl sodium sulfosuccinate at varying salinities during larval development of the Gulf killifish (Fundulus grandis). Impacts of Oil Spill Disasters on Marine Habitats and Fisheries in North America 17, 35.

Bodinier, C., Sucré, E., Lecurieux-Belfond, L., Blondeau-Bidet, E., Charmantier, G., 2010. Ontogeny of osmoregulation and salinity tolerance in the gilthead sea bream Sparus aurata. Comparative Biochemistry and Physiology Part A: Molecular & Integrative Physiology 157, 220-228.

Bowman, A.W., Azzalini, A., 1997. Applied smoothing techniques for data analysis: the kernel approach with S-Plus illustrations. Oxford University Press, Oxford, U.K., pp. 193.

Bozinovic, G., Sit, T.L., Di Giulio, R., Wills, L.F., Oleksiak, M.F., 2013. Genomic and physiological responses to strong selective pressure during late organogenesis: few gene expression changes found despite striking morphological differences. BMC Genomics 14, 779.

BP Gulf Science Data, 2014. Chemical analysis and physical properties of weathered, unweathered, and surrogate crude oils from the Deepwater Horizon accident in the Gulf of Mexico, July 2010 to January 2011. Gulf of Mexico Research Initiative Information and Data Cooperative (GRIIDC): Harte Research Institute, Texas A&M University - Corpus Christi.< https://data.gulfresearchinitiative.org/data/BP.x750.000:0003>.

BP Gulf Science Data, 2014. Chemical analysis and physical properties of weathered, unweathered, and surrogate crude oils from the Deepwater Horizon accident in the Gulf of Mexico, July 2010 to January 2011. Gulf of Mexico Research Initiative Information and Data Cooperative (GRIIDC): Harte Research Institute, Texas A&M University - Corpus Christi.< https://data.gulfresearchinitiative.org/data/BP.x750.000:0003>.

Brauner, C.J., Rombough, P.J., 2012. Ontogeny and paleophysiology of the gill: new insights from larval and air-breathing fish. Respiratory Physiology & Neurobiology 184, 293-300.

Brette, F., Machado, B., Cros, C., Incardona, J.P., Scholz, N.L., Block, B.A., 2014. Crude oil impairs cardiac excitation-contraction coupling in fish. Science 343, 772-776.

Brette, F., Shiels, H.A., Galli, G.L., Cros, C., Incardona, J.P., Scholz, N.L., Block, B.A., 2017. A novel cardiotoxic mechanism for a pervasive global pollutant. Scientific Reports 7, 41476.

Brooks, S., Tyler, C.R., Sumpter, J.P., 1997. Egg quality in fish: what makes a good egg? Reviews in Fish Biology and Fisheries 7, 387-416.

Brown, C., Williamson, K., Galvez, F., 2019. The influence of salinity on the toxicity of Corexit at multiple life stages of Gulf killifish. Comparative Biochemistry and Physiology Part C: Toxicology and Pharmacology 221, 38-48.

Brown, C.A., Gothreaux, C.T., Green, C.C., 2011. Effects of temperature and salinity during incubation on hatching and yolk utilization of Gulf killifish Fundulus grandis embryos. Aquaculture 315, 335-339.

Brown-Peterson, N.J., Krasnec, M.O., Lay, C.R., Morris, J.M., Griffitt, R.J., 2017. Responses of juvenile southern flounder exposed to Deepwater Horizon oil-contaminated sediments. Environmental Toxicology and Chemistry 36, 1067-1076.

Brummett, A.R., Dumont, J.N., 1981. A comparison of chorions from eggs of northern and southern populations of Fundulus heteroclitus. Copeia, 607-614.

Bue, B.G., Sharr, S., Moffitt, S., Craig, A.K., 1996. Effects of the Exxon Valdez oil spill on pink salmon embryos and preemergent fry, American Fisheries Society Symposium Number 18, 619-627.

Bugel, S.M., Bonventre, J.A., White, L.A., Tanguay, R.L., Cooper, K.R., 2014. Chronic exposure of killifish to a highly polluted environment desensitizes estrogen-responsive reproductive and biomarker genes. Aquatic Toxicology 152, 222-231.

Bugel, S.M., White, L.A., Cooper, K.R., 2013. Inhibition of vitellogenin gene induction by 2, 3, 7, 8-tetrachlorodibenzo-p-dioxin is mediated by aryl hydrocarbon receptor 2 (AHR2) in zebrafish (Danio rerio). Aquatic Toxicology 126, 1-8.

Burggren, W.W., 2005. Developing animals flout prominent assumptions of ecological physiology. Comparative Biochemistry and Physiology Part A: Molecular and Integrative Physiology 141, 430-439.

Calabrese, E.J., Mattson, M.P., 2017. How does hormesis impact biology, toxicology, and medicine?. NPJ Aging and Mechanisms of Disease 3, 13.

Campo, P., Venosa, A.D., Suidan, M.T., 2013. Biodegradability of Corexit 9500 and dispersed South Louisiana crude oil at 5 and 25 °C. Environmental Science and Technology 47, 1960-1967.

Carls, M.G., Holland, L., Larsen, M., Collier, T.K., Scholz, N.L., Incardona, J.P., 2008. Fish embryos are damaged by dissolved PAHs, not oil particles. Aquatic Toxicology 88, 121-127.

Carls, M.G., Hose, J.E., Thomas, R.E., Rice, S.D., 2000. Exposure of Pacific herring to weathered crude oil: Assessing effects on ova. Environmental Toxicology and Chemistry: An International Journal 19, 1649-1659.

Carr, D.L., Smith, E.E., Thiyagarajah, A., Cromie, M., Crumly, C., Davis, A., Dong, M., Garcia, C., Heintzman, L., Hopper, T., 2018. Assessment of gonadal and thyroid histology in Gulf killifish (Fundulus grandis) from Barataria Bay Louisiana one year after the Deepwater Horizon oil spill. Ecotoxicology and Environmental Safety 154, 245-254.

Chandrasekar, S., Sorial, G.A., Weaver, J.W., 2006. Dispersant effectiveness on oil spills–impact of salinity. ICES Journal of Marine Science 63, 1418-1430.

Cheshenko, K., Pakdel, F., Segner, H., Kah, O., Eggen, R.I., 2008. Interference of endocrine disrupting chemicals with aromatase CYP19 expression or activity, and consequences for reproduction of teleost fish. General and Comparative Endocrinology 155, 31-62.

Chesney, E.J., Baltz, D.M., Thomas, R.G., 2000. Louisiana estuarine and coastal fisheries and habitats: perspectives from a fish's eye view. Ecological Applications 10, 350-366.

Chollett, D., Perez, K.E., King-Heiden, T.C., 2014. Embryonic exposure to 2, 3, 7, 8-tetrachlorodibenzo-p-dioxin impairs prey capture by zebrafish larvae. Environmental Toxicology and Chemistry 33, 784-790.

Clark, B.W., Di Giulio, R.T., 2012. Fundulus heteroclitus adapted to PAHs are cross-resistant to multiple insecticides. Ecotoxicology 21, 465-474.

Clark, B.W., Matson, C.W., Jung, D., Di Giulio, R.T., 2010. AHR2 mediates cardiac teratogenesis of polycyclic aromatic hydrocarbons and PCB-126 in Atlantic killifish (Fundulus heteroclitus). Aquatic Toxicology 99, 232-240.

Clemment, T., Stone, N., 2004. Collection, removal, and quantification of eggs produced by rosy red fathead minnows in outdoor pools. North American Journal of Aquaculture 66, 75-80.

Corrales, J., Thornton, C., White, M., Willett, K.L., 2014. Multigenerational effects of benzo [a] pyrene exposure on survival and developmental deformities in zebrafish larvae. Aquatic Toxicology 148, 16-26.

Coulon, M., Gothreaux, C., Green, C., 2012. Influence of substrate and salinity on air-incubated Gulf killifish embryos. North American Journal of Aquaculture 74, 54-59.

Crawford, S.S., Balon, E.K., 1994. Alternative life histories of the genus Lucania: 3. An ecomorphological explanation of altricial (L. parva) and precocial (L. goodei) species. Environmental Biology of Fishes 41, 369-402.

Cserháti, T., Forgács, E., Oros, G., 2002. Biological activity and environmental impact of anionic surfactants. Environment International 28, 337-348.

Dasgupta, S., Choyke, S., Ferguson, P.L., McElroy, A.E., 2018. Antioxidant responses and oxidative stress in sheepshead minnow larvae exposed to Corexit 9500® or its component surfactant, DOSS. Aquatic Toxicology 194, 10-17.

Dasgupta, S., Choyke, S., Ferguson, P.L., McElroy, A.E., 2018. Antioxidant responses and oxidative stress in sheepshead minnow larvae exposed to Corexit 9500® or its component surfactant, DOSS. Aquatic Toxicology 194, 10-17.

Dasgupta, S., McElroy, A.E., 2017. Cytotoxicity and CYP1A inhibition in rainbow trout liver (RTL-W1) cell lines exposed to dispersant Corexit 9500 and its major surfactant components. Toxicology in Vitro 44, 377-381.

De Soysa, T.Y., Ulrich, A., Friedrich, T., Pite, D., Compton, S.L., Ok, D., Bernardos, R.L., Downes, G.B., Hsieh, S., Stein, R., 2012. Macondo crude oil from the Deepwater Horizon oil spill disrupts specific developmental processes during zebrafish embryogenesis. BMC Biology 10, 40.

Deepwater Horizon Natural Resource Damage Assessment Trustees, 2016. Deepwater Horizon oil spill: final programmatic damage assessment and restoration plan and final programmatic environmental impact statement. <http://www.gulfspillrestoration.noaa.gov/restoration-planning/gulf-plan>.

Denison, M.S., Nagy, S.R., 2003. Activation of the aryl hydrocarbon receptor by structurally diverse exogenous and endogenous chemicals. Annual Review of Pharmacology and Toxicology 43, 309-334.

Di Toro, D.M., McGrath, J.A., Stubblefield, W.A., 2007. Predicting the toxicity of neat and weathered crude oil: toxic potential and the toxicity of saturated mixtures. Environmental Toxicology and Chemistry: An International Journal 26, 24-36.

Dong, W., Hinton, D.E., Kullman, S.W., 2011. TCDD disrupts hypural skeletogenesis during medaka embryonic development. Toxicological Sciences 125, 91-104.

Dubansky, B., Whitehead, A., Miller, J.T., Rice, C.D., Galvez, F., 2013. Multitissue molecular, genomic, and developmental effects of the Deepwater Horizon oil spill on resident Gulf killifish (Fundulus grandis). Environmental Science and Technology 47, 5074-5082.

Duff, D.W., Fleming, W., 1972. Sodium metabolism of the freshwater cyprinodont, Fundulus catenatus. Journal of Comparative Physiology A: Neuroethology, Sensory, Neural, and Behavioral Physiology 80, 179-189.

Dupuis, A., Ucán-Marín, F., 2015. A literature review on the aquatic toxicology of petroleum oil: An overview of oil properties and effects to aquatic biota. Canadian Science Advisory Secretariat, pp. 52.

Ericson, G., Balk, L., 2000. DNA adduct formation in northern pike (Esox lucius) exposed to a mixture of benzo [a] pyrene, benzo [k] fluoranthene and 7H-dibenzo [c, g] carbazole: time-course and dose-response studies. Mutation Research/Fundamental and Molecular Mechanisms of Mutagenesis 454, 11-20.

Evans, D.H., Piermarini, P.M., Choe, K.P., 2005. The multifunctional fish gill: dominant site of gas exchange, osmoregulation, acid-base regulation, and excretion of nitrogenous waste. Physiological Reviews 85, 97-177.

Exxon Valdez Oil Spill Trustee Council, 1994. Exxon Valdez oil spill restoration plan. <http://www.evostc.state.ak.us/Universal/Documents/Restoration/1994RestorationPlan.pdf>

Fabisiak, J., Goldstein, B., 2011. Oil Dispersants and Human Health Effects, The Future of Dispersant Use in Oil Spill Response Initiative. Coastal Response Research Center and The National Oceanic Atmospheric Administration, Durham, 1– 252.

Faksness, L.-G., Grini, P.G., Daling, P.S., 2004. Partitioning of semi-soluble organic compounds between the water phase and oil droplets in produced water. Marine Pollution Bulletin 48, 731-742.

Farhoudi, A., Abedian Kenari, A., Nazari, R., Makhdoomi, C., 2011. Study of body composition, lipid and fatty acid profile during larval development in caspian sea carp (Cyprinus carpio). Journal of Fisheries and Aquatic Science 6, 417-428.

Fodrie, F.J., Heck Jr, K.L., 2011. Response of coastal fishes to the Gulf of Mexico oil disaster. PLoS One 6, e21609.

Forman, H.J., Zhang, H.Q., Rinna, A., 2009. Glutathione: Overview of its protective roles, measurement, and biosynthesis. Molecular Aspects of Medicine 30, 1-12.

Forth, H.P., Mitchelmore, C.L., Morris, J.M., Lay, C.R., Lipton, J., 2017a. Characterization of dissolved and particulate phases of water accommodated fractions used to conduct

aquatic toxicity testing in support of the Deepwater Horizon natural resource damage assessment. Environmental Toxicology and Chemistry 36, 1460-1472.

Forth, H.P., Mitchelmore, C.L., Morris, J.M., Lipton, J., 2017b. Characterization of oil and water accommodated fractions used to conduct aquatic toxicity testing in support of the Deepwater Horizon oil spill natural resource damage assessment. Environmental Toxicology and Chemistry 36, 1450-1459.

Fritz, E., Garside, E., 1974. Salinity preferences of Fundulus heteroclitus and F. diaphanus (Pisces: Cyprinodontidae): their role in geographic distribution. Canadian Journal of Zoology 52, 997-1003.

Geier, M.C., Chlebowski, A.C., Truong, L., Simonich, S.L.M., Anderson, K.A., Tanguay, R.L., 2018. Comparative developmental toxicity of a comprehensive suite of polycyclic aromatic hydrocarbons. Archives of Toxicology 92, 571-586.

George-Ares, A., Clark, J., 2000. Aquatic toxicity of two Corexit® dispersants. Chemosphere 40, 897-906.

González-Doncel, M., González, L., Fernández-Torija, C., Navas, J.M., Tarazona, J.V., 2008. Toxic effects of an oil spill on fish early life stages may not be exclusively associated to PAHs: studies with Prestige oil and medaka (Oryzias latipes). Aquatic Toxicology 87, 280-288.

Gopalan, B., Katz, J., 2010. Turbulent shearing of crude oil mixed with dispersants generates long microthreads and microdroplets. Physical Review Letters 104, 054501.

Graham, B., Reilly, W.K., Beinecke, F., Boesch, D.F., Garcia, T.D., Murray, C.A., Ulmer, F., 2011. Deep Water: The Gulf Oil Disaster And The Future Of Offshore Drilling - Report to the President. National Commission on the BP Deepwater Horizon Spill Offshore Drilling (U.S.), Washington, D.C.

Greeley Jr, M.S., Hols, H., Wallace, R.A., 1991. Changes in size, hydration and low molecular weight osmotic effectors during meiotic maturation of Fundulus oocytes in vivo. Comparative Biochemistry and Physiology Part A: Physiology 100, 639-647.

Greeley Jr, M.S., MacGregor III, R., 1983. Annual and semilunar reproductive cycles of the gulf killifish, Fundulus grandis, on the Alabama gulf coast. Copeia, 711-718.

Greeley Jr, M.S., MacGregor III, R., Marion, K.R., 1988. Changes in the ovary of the Gulf killifish, Fundulus grandis (Baird and Girard), during seasonal and semilunar spawning cycles. Journal of Fish Biology 33, 97-107.

Green, C., Gothreaux, C., Lutz, C., 2010. Reproductive output of Gulf killifish at different stocking densities in static outdoor tanks. North American Journal of Aquaculture 72, 321-331.

Greer, J.B., Pasparakis, C., Stieglitz, J.D., Benetti, D., Grosell, M., Schlenk, D., 2019. Effects of corexit 9500A and Corexit-crude oil mixtures on transcriptomic pathways and developmental toxicity in early life stage mahi-mahi (Coryphaena hippurus). Aquatic Toxicology 212, 233-240.

Guan, Y., Zhang, G.-x., Zhang, S., Domangue, B., Galvez, F., 2016. The potential role of polyamines in gill epithelial remodeling during extreme hypoosmotic challenges in the Gulf killifish, Fundulus grandis. Comparative Biochemistry and Physiology Part B: Biochemistry and Molecular Biology 194, 39-50.

Guggino, W.B., 1980. Salt balance in embryos of Fundulus heteroclitus and F. bermudae adapted to seawater. American Journal of Physiology-Regulatory, Integrative and Comparative Physiology 238, R42-R49.

Hahn, M., Hestermann, E., 2008. Receptor-mediated mechanisms of toxicity. In: The Toxicology of Fishes. CRC Press, New York, 235-272.

Hahn, M.E., 1998. The aryl hydrocarbon receptor: a comparative perspective. Comparative Biochemistry and Physiology Part C: Pharmacology, Toxicology and Endocrinology 121, 23-53.

Hamilton, P.B., Cowx, I.G., Oleksiak, M.F., Griffiths, A.M., Grahn, M., Stevens, J.R., Carvalho, G.R., Nicol, E., Tyler, C.R., 2016. Population-level consequences for wild fish exposed to sublethal concentrations of chemicals–a critical review. Fish and Fisheries 17, 545-566.

Hamilton, P.B., Rolshausen, G., Uren Webster, T.M., Tyler, C.R., 2017. Adaptive capabilities and fitness consequences associated with pollution exposure in fish. Philosophical Transactions of the Royal Society B: Biological Sciences 372, 20160042.

Hansen, B.H., Parkerton, T., Nordtug, T., Størseth, T.R., Redman, A., 2019a. Modeling the toxicity of dissolved crude oil exposures to characterize the sensitivity of cod (Gadus morhua) larvae and role of individual and unresolved hydrocarbons. Marine Pollution Bulletin 138, 286-294.

Hansen, B.H., Salaberria, I., Read, K.E., Wold, P.A., Hammer, K.M., Olsen, A.J., Altin, D., Øverjordet, I.B., Nordtug, T., Bardal, T., 2019b. Developmental effects in fish embryos exposed to oil dispersions–The impact of crude oil micro-droplets. Marine Environmental Research 150, 104753.

Hansen, B.H., Sørensen, L., Carvalho, P.A., Meier, S., Booth, A.M., Altin, D., Farkas, J., Nordtug, T., 2018. Adhesion of mechanically and chemically dispersed crude oil droplets to eggs of Atlantic cod (Gadus morhua) and haddock (Melanogrammus aeglefinus). Science of the Total Environment 640, 138-143.

Haritash, A., Kaushik, C., 2009. Biodegradation aspects of polycyclic aromatic hydrocarbons (PAHs): a review. Journal of Hazardous Materials 169, 1-15.

Hayworth, J.S., Clement, T.P., 2012. Provenance of Corexit-related chemical constituents found in nearshore and inland Gulf Coast waters. Marine Pollution Bulletin 64, 2005-2014.

He, C., Zuo, Z., Shi, X., Li, R., Chen, D., Huang, X., Chen, Y., Wang, C., 2011. Effects of benzo (a) pyrene on the skeletal development of Sebastiscus marmoratus embryos and the molecular mechanism involved. Aquatic Toxicology 101, 335-341.

Head, J.A., Dolinoy, D.C., Basu, N., 2012. Epigenetics for ecotoxicologists. Environmental Toxicology and Chemistry 31, 221-227.

Heerklotz, H., 2008. Interactions of surfactants with lipid membranes. Quarterly Reviews of Biophysics 41, 205-264.

Heintz, R.A., Rice, S.D., Wertheimer, A.C., Bradshaw, R.F., Thrower, F.P., Joyce, J.E., Short, J.W., 2000. Delayed effects on growth and marine survival of pink salmon Oncorhynchus gorbuscha after exposure to crude oil during embryonic development. Marine Ecology Progress Series 208, 205-216.

Heuer, R.M., Shiels, H.A., Galli, G.L., Cox, G.K., Stieglitz, J.D., Benetti, D.D., Grosell, M., Crossley, D.A., 2018. Crude oil impairs heart cell function in the mahi-mahi (Coryphaena hippurus). The FASEB Journal 32, 602.611-602.611.

Hicken, C.E., Linbo, T.L., Baldwin, D.H., Willis, M.L., Myers, M.S., Holland, L., Larsen, M., Stekoll, M.S., Rice, S.D., Collier, T.K., 2011. Sublethal exposure to crude oil during embryonic development alters cardiac morphology and reduces aerobic capacity in adult fish. Proceedings of the National Academy of Sciences 108, 7086-7090.

Hodson, P.V., 2017. The Toxicity to Fish Embryos of PAH in Crude and Refined Oils. Archives of Environmental Contamination and Toxicology 73, 12-18.

Hofsteen, P., Plavicki, J., Johnson, S.D., Peterson, R.E., Heideman, W., 2013. Sox9b is required for epicardium formation and plays a role in TCDD-induced heart malformation in zebrafish. Molecular Pharmacology 84, 353-360.

Houma ICP Aerial Dispersant Group, 2010. After action report deepwater horizon MC252 aerial dispersant response, pp. 80. <http://www.mdl2179trialdocs.com/releases/release201501260800005/TREX-013037.pdf>.

Hove, J.R., Köster, R.W., Forouhar, A.S., Acevedo-Bolton, G., Fraser, S.E., Gharib, M., 2003. Intracardiac fluid forces are an essential epigenetic factor for embryonic cardiogenesis. Nature 421, 172.

Hwang, P.-P., Lee, T.-H., Lin, L.-Y., 2011. Ion regulation in fish gills: recent progress in the cellular and molecular mechanisms. American Journal of Physiology-Regulatory, Integrative and Comparative Physiology 301, R28-R47.

Hylland, K., 2006. Polycyclic aromatic hydrocarbon (PAH) ecotoxicology in marine ecosystems. Journal of Toxicology and Environmental Health, Part A 69, 109-123.

Incardona, J.P., 2017. Molecular mechanisms of crude oil developmental toxicity in fish. Archives of Environmental Contamination and Toxicology 73, 19-32.

Incardona, J.P., Carls, M.G., Holland, L., Linbo, T.L., Baldwin, D.H., Myers, M.S., Peck, K.A., Tagal, M., Rice, S.D., Scholz, N.L., 2015. Very low embryonic crude oil exposures cause lasting cardiac defects in salmon and herring. Scientific Reports 5, 13499.

Incardona, J.P., Collier, T.K., Scholz, N.L., 2004. Defects in cardiac function precede morphological abnormalities in fish embryos exposed to polycyclic aromatic hydrocarbons. Toxicology and Applied Pharmacology 196, 191-205.

Incardona, J.P., Day, H.L., Collier, T.K., Scholz, N.L., 2006. Developmental toxicity of 4-ring polycyclic aromatic hydrocarbons in zebrafish is differentially dependent on AH receptor isoforms and hepatic cytochrome P4501A metabolism. Toxicology and Applied Pharmacology 217, 308-321.

Incardona, J.P., Gardner, L.D., Linbo, T.L., Brown, T.L., Esbaugh, A.J., Mager, E.M., Stieglitz, J.D., French, B.L., Labenia, J.S., Laetz, C.A., 2014. Deepwater Horizon crude oil impacts the developing hearts of large predatory pelagic fish. Proceedings of the National Academy of Sciences 111, E1510-E1518.

Incardona, J.P., Linbo, T.L., Scholz, N.L., 2011. Cardiac toxicity of 5-ring polycyclic aromatic hydrocarbons is differentially dependent on the aryl hydrocarbon receptor 2 isoform during zebrafish development. Toxicology and Applied Pharmacology 257, 242-249.

Incardona, J.P., Swarts, T.L., Edmunds, R.C., Linbo, T.L., Aquilina-Beck, A., Sloan, C.A., Gardner, L.D., Block, B.A., Scholz, N.L., 2013. Exxon Valdez to Deepwater Horizon: Comparable toxicity of both crude oils to fish early life stages. Aquatic Toxicology 142, 303-316.

International Association of Oil and Gas Producers, 2019. Global Production Report 2019, pp. 36.

Jasperse, L., Levin, M., Rogers, K., Perkins, C., Bosker, T., Griffitt, R.J., Sepúlveda, M.S., De Guise, S., 2019. Transgenerational effects of polycyclic aromatic hydrocarbon exposure on sheepshead minnows (Cyprinodon variegatus). Environmental Toxicology and Chemistry 38, 638-649.

John, V., Arnosti, C., Field, J., Kujawinski, E., McCormick, A., 2016. The role of dispersants in oil spill remediation: fundamental concepts, rationale for use, fate, and transport issues. Oceanography 29, 108-117.

John, V., Arnosti, C., Field, J., Kujawinski, E., McCormick, A., 2016. The role of dispersants in oil spill remediation: Fundamental concepts, rationale for use, fate, and transport issues. Oceanography 29, 108-117.

Jones, D.R., Braun, M.H., 2011. Design and physiology of the heart | The Outflow Tract from the Heart. Encyclopedia of Fish Physiology 2, 1015-1029.

Jones, M.N., 1992. Surfactant interactions with biomembranes and proteins. Chemical Society Reviews 21, 127-136.

Jonker, M.T., Brils, J.M., Sinke, A.J., Murk, A.J., Koelmans, A.A., 2006. Weathering and toxicity of marine sediments contaminated with oils and polycyclic aromatic hydrocarbons. Environmental Toxicology and Chemistry: An International Journal 25, 1345-1353.

Josiam, R., 2015. US Oil Recovery Superfund Site, Pasadena, Harris County, Texas. U.S. Environmental Protection Agency. < https://semspub.epa.gov/work/06/500012065.pdf>

Kamler, E., 2005. Parent–egg–progeny relationships in teleost fishes: an energetics perspective. Reviews in Fish Biology and Fisheries 15, 399.

Karchner, S.I., Powell, W.H., Hahn, M.E., 1999. Identification and Functional Characterization of Two Highly Divergent Aryl Hydrocarbon Receptors (AHR1 and AHR2) in the Teleost Fundulus heteroclitus: Evidence for a Novel Subfamily of Ligand-Binding Basic Helix Loop Helix-PER-ARNT-SIM (bHLH-PAS) Factors. Journal of Biological Chemistry 274, 33814-33824.

Kashiwada, S., Tatsuta, H., Kameshiro, M., Sugaya, Y., Sabo-Attwood, T., Chandler, G.T., Ferguson, P.L., Goka, K., 2008. Stage-dependent differences in effects of carbaryl on population growth rate in Japanese medaka (Oryzias latipes). Environmental Toxicology and Chemistry 27, 2397-2402.

Katoh, F., Shimizu, A., Uchida, K., Kaneko, T., 2000. Shift of Chloride Cell Distribution during Early Life Stages in Seawater-Adapted Killifish, Fundulus heteroclitus. Zoological Science 17, 11-18.

Kennedy, C.J., Farrell, A.P., 2005. Ion homeostasis and interrenal stress responses in juvenile Pacific herring, Clupea pallasi, exposed to the water-soluble fraction of crude oil. Journal of Experimental Marine Biology and Ecology 323, 43-56.

Khursigara, A.J., Perrichon, P., Bautista, N.M., Burggren, W.W., Esbaugh, A.J., 2017. Cardiac function and survival are affected by crude oil in larval red drum, Sciaenops ocellatus. Science of The Total Environment 579, 797-804.

Kleinow, K.M., Nichols, J.W., Hayton, W.L., McKim, J.M., Barron, M.G., 2008. Toxicokinetics in Fishes. CRC Press, Boca Raton.

Knecht, A.L., Truong, L., Marvel, S.W., Reif, D.M., Garcia, A., Lu, C., Simonich, M.T., Teeguarden, J.G., Tanguay, R.L., 2017. Transgenerational inheritance of neurobehavioral and physiological deficits from developmental exposure to benzo [a] pyrene in zebrafish. Toxicology and Applied Pharmacology 329, 148-157.

Kneib, R.T., 1997. The role of tidal marshes in the ecology of estuarine nekton. Oceanography and Marine Biology 35, 163-220.

Kuhl, A.J., Nyman, J.A., Kaller, M.D., Green, C.C., 2013. Dispersant and salinity effects on weathering and acute toxicity of South Louisiana crude oil. Environmental Toxicology and Chemistry 32, 2611-2620.

Kujawinski, E.B., Kido Soule, M.C., Valentine, D.L., Boysen, A.K., Longnecker, K., Redmond, M.C., 2011. Fate of dispersants associated with the Deepwater Horizon oil spill. Environmental Science & Technology 45, 1298-1306.

Landry, C., Steele, S., Manning, S., Cheek, A., 2007. Long term hypoxia suppresses reproductive capacity in the estuarine fish, Fundulus grandis. Comparative Biochemistry and Physiology Part A: Molecular and Integrative Physiology 148, 317-323.

Landry, M.E., Adams, E., Bejarano, A., Boufadel, M., White, H.K., 2019. The Use of Dispersants in Marine Oil Spill Response. The National Academies Press, Washington D.C., pp. 364.

Leahy, J.G., Colwell, R.R., 1990. Microbial degradation of hydrocarbons in the environment. Microbiology and Molecular Biology Reviews 54, 305-315.

Lee, J.W., Na, D.S., Chae, S.K., Kim, C., Kang, J.Y., Ju, B.K., Lee, H., Kim, S.U., Hwang, C.N., Lee, S.H., 2005. Using the chorions of fertilized zebrafish eggs as a biomaterial for the attachment and differentiation of mouse stem cells. Langmuir 21, 7615-7620.

Lee, K., Boufadel, M., Chen, B., Foght, J., Hodson, P., Swanson, S., Venosa, A., 2015. Expert Panel Report on the Behaviour and Environmental Impacts of Crude Oil Released into Aqueous Environments ISBN 978–1–928140–02–3, Royal Society of Canada.

Lehr, B., Sky, B., Possolo, A., Allen, A., Boufadel, M., Coolbaugh, T., Daling, P., Fingas, M., French McCay, D., Goodman, R., Jones, R., Khelifa, A., Lambert, P., Lee, K., Leifer, I., Mearns, A., Overton, E., Payne, J., Beegle-Krause, C.J., Farr, J., Galt, J., Hammond, S., Lasheras, J., Mabile, N., Miller, M., Svekovsky, J., Yapa, P., 2010. Oil budget calculator deepwater horizon: a report to the National Incident Command. Federal Interagency Solutions Group, Oil Budget Calculator Science and Engineering Team, 21-186.

Lewis, D.F., Ioannides, C., Parke, D.V., 1998. Cytochromes P450 and species differences in xenobiotic metabolism and activation of carcinogen. Environmental Health Perspectives 106, 633-641.

Lewis, S.S., Weber, G.J., Freeman, J.L., Sepúlveda, M.S., 2012. Molecular epigenetic changes caused by environmental pollutants. Toxicology and Epigenetics, 73-109.

Li, F.J., Duggal, R.N., Oliva, O.M., Karki, S., Surolia, R., Wang, Z., Watson, R.D., Thannickal, V.J., Powell, M., Watts, S., Kulkarni, T., Batra, H., Bolisetty, S., Agarwal, A., Antony, V.B., 2015. Heme oxygenase-1 protects corexit 9500A-induced respiratory epithelial injury across species. PloS One 10, e0122275.

Li, H., Boufadel, M.C., 2010. Long-term persistence of oil from the Exxon Valdez spill in two-layer beaches. Nature Geoscience 3, 96.

Lin, C.Y., Tjeerdema, R.S., 2008. Crude oil, oil, gasoline and petrol. In: Encyclopedia of Ecology. Academic Press, Oxford, 797−805.

Logan, D.T., 2007. Perspective on ecotoxicology of PAHs to fish. Human and Ecological Risk Assessment 13, 302-316.

Mackay, D., Chau, A., Hossain, K., Bobra, M., 1984. Measurement and prediction of the effectiveness of oil spill chemical dispersants, in: T. Allen (Ed.), Oil Spill Chemical Dispersants: Research, Experience, and Recommendations. ASTM International, West Conshohocken.

Mackay, D., Shiu, W.Y., 1977. Aqueous solubility of polynuclear aromatic hydrocarbons. Journal of Chemical and Engineering Data 22, 399-402.

Mager, E.M., Esbaugh, A.J., Stieglitz, J.D., Hoenig, R., Bodinier, C., Incardona, J.P., Scholz, N.L., Benetti, D.D., Grosell, M., 2014. Acute embryonic or juvenile exposure to Deepwater Horizon crude oil impairs the swimming performance of mahi-mahi (Coryphaena hippurus). Environmental Science and Technology 48, 7053-7061.

McGenity, T.J., 2014. Hydrocarbon biodegradation in intertidal wetland sediments. Current Opinion in Biotechnology 27, 46-54.

McNutt, M.K., Camilli, R., Crone, T.J., Guthrie, G.D., Hsieh, P.A., Ryerson, T.B., Savas, O., Shaffer, F., 2012. Review of flow rate estimates of the Deepwater Horizon oil spill. Proceedings of the National Academy of Sciences 109, 20260-20267.

Meador, J.P., Nahrgang, J., 2019. Characterizing Crude Oil Toxicity to Early-Life Stage Fish Based On a Complex Mixture: Are We Making Unsupported Assumptions? Environmental Science and Technology 53, 11080-11092.

Mendelssohn, I.A., Andersen, G.L., Baltz, D.M., Caffey, R.H., Carman, K.R., Fleeger, J.W., Joye, S.B., Lin, Q., Maltby, E., Overton, E.B., 2012. Oil impacts on coastal wetlands: implications for the Mississippi River Delta ecosystem after the Deepwater Horizon oil spill. BioScience 62, 562-574.

Michel, J., Owens, E.H., Zengel, S., Graham, A., Nixon, Z., Allard, T., Holton, W., Reimer, P.D., Lamarche, A., White, M., 2013. Extent and degree of shoreline oiling: Deepwater Horizon oil spill, Gulf of Mexico, USA. PloS One 8, e65087.

Milinkovitch, T., Kanan, R., Thomas-Guyon, H., Le Floch, S., 2011. Effects of dispersed oil exposure on the bioaccumulation of polycyclic aromatic hydrocarbons and the mortality of juvenile Liza ramada. Science of the Total Environment 409, 1643-1650.

Mohammed, A., 2013. Why are early life stages of aquatic organisms more sensitive to toxicants than adults?, in: S. Gowder (Ed.), New Insights into Toxicity and Drug Testing. InTechOpen.

Monteverdi, G.H., Giulio, R.T.D., 2000. In vitro and in vivo association of 2, 3, 7, 8-tetrachlorodibenzo-p-dioxin and benzo [a] pyrene with the yolk-precursor protein vitellogenin. Environmental Toxicology and Chemistry: An International Journal 19, 2502-2511.

Morin, R.P., Able, K.W., 1983. Patterns of geographic variation in the egg morphology of the fundulid fish, Fundulus heteroclitus. Copeia, 726-740.

Mousavi, M., Abdollahi, T., Pahlavan, F., Fini, E.H., 2016. The influence of asphaltene-resin molecular interactions on the colloidal stability of crude oil. Fuel 183, 262-271.

National Research Council, 2005. Oil spill dispersants: efficacy and effects. National Academies Press, Washington D.C., pp. 377.

Nelson, T.R., Sutton, D., DeVries, D.R., 2014. Summer movements of the Gulf Killifish (Fundulus grandis) in a northern Gulf of Mexico salt marsh. Estuaries and Coasts 37, 1295-1300.

Nilsen, E., Smalling, K.L., Ahrens, L., Gros, M., Miglioranza, K.S., Picó, Y., Schoenfuss, H.L., 2019. Critical review: Grand challenges in assessing the adverse effects of contaminants of emerging concern on aquatic food webs. Environmental Toxicology and Chemistry 38, 46-60.

Nixon, Z., Zengel, S., Baker, M., Steinhoff, M., Fricano, G., Rouhani, S., Michel, J., 2016. Shoreline oiling from the Deepwater Horizon oil spill. Marine Pollution Bulletin 107, 170-178.

Nordlie, F.G., 2000. Patterns of reproduction and development of selected resident teleosts of Florida salt marshes. Hydrobiologia 434, 165-182.

Nordlie, F.G., 2003. Fish communities of estuarine salt marshes of eastern North America, and comparisons with temperate estuaries of other continents. Reviews in Fish Biology and Fisheries 13, 281-325.

Nordlie, F.G., 2006. Physicochemical environments and tolerances of cyprinodontoid fishes found in estuaries and salt marshes of eastern North America. Reviews in Fish Biology and Fisheries 16, 51-106.

Oziolor, E.M., Apell, J.N., Winfield, Z.C., Back, J.A., Usenko, S., Matson, C.W., 2018. Polychlorinated biphenyl (PCB) contamination in Galveston Bay, Texas: Comparing concentrations and profiles in sediments, passive samplers, and fish. Environmental Pollution 236, 609-618.

Oziolor, E.M., Bigorgne, E., Aguilar, L., Usenko, S., Matson, C.W., 2014. Evolved resistance to PCB-and PAH-induced cardiac teratogenesis, and reduced CYP1A activity in Gulf killifish (Fundulus grandis) populations from the Houston Ship Channel, Texas. Aquatic Toxicology 150, 210-219.

Oziolor, E.M., Matson, C.W., 2015. Evolutionary toxicology: population adaptation in response to anthropogenic pollution, Extremophile Fishes. Springer, 247-277.

Oziolor, E.M., Reid, N.M., Yair, S., Lee, K.M., VerPloeg, S.G., Bruns, P.C., Shaw, J.R., Whitehead, A., Matson, C.W., 2019. Adaptive introgression enables evolutionary rescue from extreme environmental pollution. Science 364, 455-457.

Patterson, J., Bodinier, C., Green, C., 2012. Effects of low salinity media on growth, condition, and gill ion transporter expression in juvenile Gulf killifish, Fundulus grandis. Comparative Biochemistry and Physiology Part A: Molecular & Integrative Physiology 161, 415-421.

Patterson, J.T., Allgood, T.G., Green, C.C., 2013. Intraspecific variation in reproductive potential with maternal body size in Gulf Killifish Fundulus grandis. Aquaculture 384, 134-139.

Pelka, K.E., Henn, K., Keck, A., Sapel, B., Braunbeck, T., 2017. Size does matter–Determination of the critical molecular size for the uptake of chemicals across the chorion of zebrafish (Danio rerio) embryos. Aquatic Toxicology 185, 1-10.

Perschbacher, P.W., Aldrich, D.V., Strawn, K., 1990. Survival and growth of the early stages of Gulf killifish in various salinities. The Progressive Fish-Culturist 52, 109-111.

Petersen, G.I., Kristensen, P., 1998. Bioaccumulation of lipophilic substances in fish early life stages. Environmental Toxicology and Chemistry: An International Journal 17, 1385-1395.

Peterson, R., Martin-Robichaud, D., 1986. Perivitelline and vitelline potentials in teleost eggs as influenced by ambient ionic strength, natal salinity, and electrode electrolyte; and the influence of these potentials on cadmium dynamics within the egg. Canadian Journal of Fisheries and Aquatic Sciences 43, 1445-1450.

Petitjean, Q., Jean, S., Gandar, A., Côte, J., Laffaille, P., Jacquin, L., 2019. Stress responses in fish: From molecular to evolutionary processes. Science of the Total Environment 684, 371-380.

Pfeiler, E., Luna, A., 1984. Changes in biochemical composition and energy utilization during metamorphosis of leptocephalous larvae of the bonefish (Albula). Environmental Biology of Fishes 10, 243-251.

Philibert, D.A., Lyons, D., Philibert, C., Tierney, K.B., 2019. Field-collected crude oil, weathered oil and dispersants differentially affect the early life stages of freshwater and saltwater fishes. Science of the Total Environment 647, 1148-1157.

Pilcher, W., Miles, S., Tang, S., Mayer, G., Whitehead, A., 2014. Genomic and genotoxic responses to controlled weathered-oil exposures confirm and extend field studies on impacts of the Deepwater Horizon oil spill on native killifish. PLoS One 9, e106351.

Place, B.J., Perkins, M.J., Sinclair, E., Barsamian, A.L., Blakemore, P.R., Field, J.A., 2016. Trace analysis of surfactants in Corexit oil dispersant formulations and seawater. Deep Sea Research Part II: Topical Studies in Oceanography 129, 273-281.

Post, J.R., Lee, J.A., 1996. Metabolic ontogeny of teleost fishes. Canadian Journal of Fisheries and Aquatic Sciences 53, 910-923.

Post, J.R., Parkinson, E., 2001. Energy allocation strategy in young fish: allometry and survival. Ecology 82, 1040-1051

Powers, S.P., Grabowski, J.H., Roman, H., Geggel, A., Rouhani, S., Oehrig, J., Baker, M., 2017. Consequences of large-scale salinity alteration during the Deepwater Horizon oil spill on subtidal oyster populations. Marine Ecology Progress Series 576, 175-187.

Prodocimo, V., Galvez, F., Freire, C.A., Wood, C.M., 2007. Unidirectional Na+ and Ca 2+ fluxes in two euryhaline teleost fishes, Fundulus heteroclitus and Oncorhynchus mykiss, acutely submitted to a progressive salinity increase. Journal of Comparative Physiology B: Biochemical, Systems, and Environmental Physiology 177, 519-528.

Ramachandran, S.D., Sweezey, M.J., Hodson, P.V., Boudreau, M., Courtenay, S.C., Lee, K., King, T., Dixon, J.A., 2006. Influence of salinity and fish species on PAH uptake from dispersed crude oil. Marine Pollution Bulletin 52, 1182-1189.

Ramee, S., Green, C., Allen, P.J., 2016. Effects of low salinities on osmoregulation, growth, and survival of juvenile Gulf Killifish. North American Journal of Aquaculture 78, 8-19.

Rawson, D., Zhang, T., Kalicharan, D., Jongebloed, W., 2000. Field emission scanning electron microscopy and transmission electron microscopy studies of the chorion, plasma membrane and syncytial layers of the gastrula-stage embryo of the zebrafish Brachydanio rerio: a consideration of the structural and functional relationships with respect to cryoprotectant penetration. Aquaculture Research 31, 325-336.

Reddy, C.M., Arey, J.S., Seewald, J.S., Sylva, S.P., Lemkau, K.L., Nelson, R.K., Carmichael, C.A., McIntyre, C.P., Fenwick, J., Ventura, G.T., 2012. Composition and fate of gas and oil released to the water column during the Deepwater Horizon oil spill. Proceedings of the National Academy of Sciences 109, 20229-20234.

Redman, A.D., Butler, J.D., Letinski, D.J., Parkerton, T.F., 2017. Investigating the role of dissolved and droplet oil in aquatic toxicity using dispersed and passive dosing systems. Environmental Toxicology and Chemistry 36, 1020-1028.

Redman, A.D., McGrath, J.A., Stubblefield, W.A., Maki, A.W., Di Toro, D.M., 2012. Quantifying the concentration of crude oil microdroplets in oil–water preparations. Environmental Toxicology and Chemistry 31, 1814-1822.

Riehl, R., Patzner, R.A., 1998. Minireview: the modes of egg attachment in teleost fishes. Italian Journal of Zoology 65, 415-420.

Riis-Vestergaard, J., 1982. Water and salt balance of halibut eggs and larvae (Hippoglossus hippoglossus). Marine Biology 70, 135-139.

Rizzo, E., Moura, T.F., Sato, Y., Bazzoli, N., 1998. Oocyte surface in four teleost fish species postspawning and fertilization. Brazilian Archives of Biology and Technology 41, 37-48.

Rombough, P., 2007. The functional ontogeny of the teleost gill: Which comes first, gas or ion exchange? Comparative Biochemistry and Physiology Part A: Molecular & Integrative Physiology 148, 732-742.

Romero, I.C., Sutton, T., Carr, B., Quintana-Rizzo, E., Ross, S.W., Hollander, D.J., Torres, J.J., 2018. Decadal Assessment of Polycyclic Aromatic Hydrocarbons in Mesopelagic Fishes from the Gulf of Mexico Reveals Exposure to Oil-Derived Sources. Environmental Science and Technology 52, 10985-10996.

Rooker, J.R., Kitchens, L.L., Dance, M.A., Wells, R.D., Falterman, B., Cornic, M., 2013. Spatial, temporal, and habitat-related variation in abundance of pelagic fishes in the Gulf of Mexico: potential implications of the Deepwater Horizon oil spill. PloS One 8, e76080.

Rosety-Rodríguez, M., Ordoñez, F., Rosety, M., Rosety, J., Rosety, I., Ribelles, A., Carrasco, C., 2002. Morpho-histochemical changes in the gills of turbot, Scophthalmus maximus L., induced by sodium dodecyl sulfate. Ecotoxicology and Environmental Safety 51, 223-228.

Rotchell, J., Miller, M., Hinton, D., Di Giulio, R., Ostrander, G., 2008. Chemical carcinogenesis in fishes. The Toxicology of Fishes. CRC Press, New York, 531-596.

Roth, A.-M.F., Baltz, D.M., 2009. Short-term effects of an oil spill on marsh-edge fishes and decapod crustaceans. Estuaries and Coasts 32, 565–572.

Rountree, R.A., Able, K.W., 2007. Spatial and temporal habitat use patterns for salt marsh nekton: implications for ecological functions. Aquatic Ecology 41, 25-45.

Sandoval, K., Ding, Y., Gardinali, P., 2017. Characterization and environmental relevance of oil water preparations of fresh and weathered MC-252 Macondo oils used in toxicology testing. Science of the Total Environment 576, 118-128.

Schaefer, J., Frazier, N., Barr, J., 2016. Dynamics of near-coastal fish assemblages following the Deepwater Horizon oil spill in the northern Gulf of Mexico. Transactions of the American Fisheries Society 145, 108-119.

Schindelin, J., Arganda-Carreras, I., Frise, E., Kaynig, V., Longair, M., Pietzsch, T., Preibisch, S., Rueden, C., Saalfeld, S., Schmid, B. and Tinevez, J.Y., 2012. Fiji: an open-source platform for biological-image analysis. Nature Methods 9, 676.

Schreier, S., Malheiros, S.V.P., de Paula, E., 2000. Surface active drugs: self-association and interaction with membranes and surfactants. Physicochemical and biological aspects. Biochimica et Biophysica Acta (BBA) - Biomembranes 1508, 210-234.

Scornaienchi, M.L., Thornton, C., Willett, K.L., Wilson, J.Y., 2010. Cytochrome P450-mediated 17b-estradiol metabolism in zebrafish (Danio rerio). Journal of Endocrinology 206, 317-325.

Scott, J.A., Incardona, J.P., Pelkki, K., Shepardson, S., Hodson, P.V., 2011. AhR2-mediated, CYP1A-independent cardiovascular toxicity in zebrafish (Danio rerio) embryos exposed to retene. Aquatic Toxicology 101, 165-174.

Seemann, F., Peterson, D.R., Witten, P.E., Guo, B.-S., Shanthanagouda, A.H., Rui, R.Y., Zhang, G., Au, D.W., 2015. Insight into the transgenerational effect of benzo [a] pyrene on bone formation in a teleost fish (Oryzias latipes). Comparative Biochemistry and Physiology Part C: Toxicology and Pharmacology 178, 60-67.

Shearer, K.D., 1984. Changes in elemental composition of hatchery-reared rainbow trout, Salmo gairdneri, associated with growth and reproduction. Canadian Journal of Fisheries and Aquatic Sciences 41, 1592-1600.

Shi, C., Xie, L., Zhang, L., Lu, X., Zeng, H., 2019. Probing the Interaction Mechanism between Oil Droplets with Asphaltenes and Solid Surfaces Using AFM. Journal of Colloid and Interface Science 558, 173-181.

Short, J.W., 2017. Advances in understanding the fate and effects of oil from accidental spills in the United States beginning with the Exxon Valdez. Archives of Environmental Contamination and Toxicology 73, 5-11.

Short, J.W., Irvine, G.V., Mann, D.H., Maselko, J.M., Pella, J.J., Lindeberg, M.R., Payne, J.R., Driskell, W.B., Rice, S.D., 2007. Slightly weathered Exxon Valdez oil persists in Gulf of Alaska beach sediments after 16 years. Environmental Science & Technology 41, 1245-1250.

Shu, L., Suter, M.J.F., Räsänen, K., 2015. Evolution of egg coats: linking molecular biology and ecology. Molecular Ecology 24, 4052-4073.

Silliman, B.R., van de Koppel, J., McCoy, M.W., Diller, J., Kasozi, G.N., Earl, K., Adams, P.N., Zimmerman, A.R., 2012. Degradation and resilience in Louisiana salt marshes after the BP–Deepwater Horizon oil spill. Proceedings of the National Academy of Sciences 109, 11234-11239.

Silliman, B.R., Zieman, J.C., 2001. Top-down control of Spartina alterniflora production by periwinkle grazing in a Virginia salt marsh. Ecology 82, 2830-2845.

Simpson, D.G., Gunter, G., 1956. Notes on habitats, systematic characters and life histories of Texas salt water cyprinodonts. Tulane Studies in Zoology 4, 115-134.

Sklar, F.H., Browder, J.A., 1998. Coastal environmental impacts brought about by alterations to freshwater flow in the Gulf of Mexico. Environmental Management 22, 547-562.

Sklar, F.H., Browder, J.A., 1998. Coastal environmental impacts brought about by alterations to freshwater flow in the Gulf of Mexico. Environmental Management 22, 547-562.

Song, S., Zhang, H., Sun, L., Shi, J., Cao, X., Yuan, S., 2018. Molecular Dynamics Study on Aggregating Behavior of Asphaltene and Resin in Emulsified Heavy Oil Droplets with Sodium Dodecyl Sulfate. Energy and Fuels 32, 12383-12393.

Sørensen, L., Melbye, A.G., Booth, A.M., 2014. Oil droplet interaction with suspended sediment in the seawater column: Influence of physical parameters and chemical dispersants. Marine Pollution Bulletin 78, 146-152.

Sørensen, L., Sørhus, E., Nordtug, T., Incardona, J.P., Linbo, T.L., Giovanetti, L., Karlsen, Ø., Meier, S., 2017. Oil droplet fouling and differential toxicokinetics of polycyclic aromatic hydrocarbons in embryos of Atlantic haddock and cod. PloS One 12, e0180048.

Sørhus, E., Edvardsen, R.B., Karlsen, Ø., Nordtug, T., van der Meeren, T., Thorsen, A., Harman, C., Jentoft, S., Meier, S., 2015. Unexpected interaction with dispersed crude oil droplets drives severe toxicity in atlantic haddock embryos. PloS One 10, e0124376.

Sørhus, E., Incardona, J.P., Karlsen, Ø., Linbo, T., Sørensen, L., Nordtug, T., Van Der Meeren, T., Thorsen, A., Thorbjørnsen, M., Jentoft, S., 2016. Crude oil exposures reveal roles for intracellular calcium cycling in haddock craniofacial and cardiac development. Scientific Reports 6, 31058.

Speight, J.G., El-Gendy, N.S., 2017. Introduction to petroleum biotechnology. Gulf Professional Publishing, Houston, TX, pp. 566.

Sterling Jr, M.C., Bonner, J.S., Ernest, A.N., Page, C.A., Autenrieth, R., 2004. Chemical dispersant effectiveness testing: influence of droplet coalescence. Marine Pollution Bulletin 48, 969-977.

Strzyzewska, E., Szarek, J., Babinska, I., 2016. Morphologic evaluation of the gills as a tool in the diagnostics of pathological conditions in fish and pollution in the aquatic environment: a review. Veterinární Medicína 61, 123–132.

Sundt, R.C., Björkblom, C., 2011. Effects of produced water on reproductive parameters in prespawning Atlantic cod (Gadus morhua). Journal of Toxicology and Environmental Health, Part A 74, 543-554.

Sverdrup, L.E., Nielsen, T., Krogh, P.H., 2002. Soil ecotoxicity of polycyclic aromatic hydrocarbons in relation to soil sorption, lipophilicity, and water solubility. Environmental Science and Technology 36, 2429-2435.

Tadros, T.F., 2013. Emulsion formation, stability, and rheology. Emulsion Formation and Stability 1, 1-75.

Teal, J., Pendleton, E., Kitchens, W., Young, M.W., 1986. The ecology of regularly flooded salt marshes of New England: A community profile. U.S. Fish and Wildlife Service, Washington D.C., pp. 61.

Teal, J., Pendleton, E., Kitchens, W., Young, M.W., 1986. The ecology of regularly flooded salt marshes of New England: A community profile. U.S. Fish and Wildlife Service, Washington, D.C., 61.

Thorson, T.B., 1961. The Partitioning of Body Water in Osteichthyes: Phylogenetic and Ecological Implications in Aquatic Vertebrates. The Biological Bulletin 120, 238-254.

Tissot, B.P., Welte, D.H., 1984. Geochemical fossils and their significance in petroleum formation, Petroleum Formation and Occurrence. Springer, 93-130.

Tummons, E.N., Hejase, C.A., Yang, Z., Chew, J.W., Bruening, M.L., Tarabara, V.V., 2019. Oil droplet behavior on model nanofiltration membrane surfaces under conditions of hydrodynamic shear and salinity. Journal of Colloid and Interface Science 560, 247-259.

Turner, R.E., Overton, E.B., Meyer, B.M., Miles, M.S., McClenachan, G., Hooper-Bui, L., Engel, A.S., Swenson, E.M., Lee, J.M., Milan, C.S., 2014. Distribution and recovery trajectory of Macondo (Mississippi Canyon 252) oil in Louisiana coastal wetlands. Marine Pollution Bulletin 87, 57-67.

U.S. Department of Justice, 2015. Statement by Attorney General Loretta E. Lynch on the agreement in principle with BP to settle civil claims for the Deepwater Horizon oil spill (Press AAT Submission 14871 19 Release).

Varsamos, S., Nebel, C., Charmantier, G., 2005. Ontogeny of osmoregulation in postembryonic fish: a review. Comparative Biochemistry and Physiology Part A: Molecular & Integrative Physiology 141, 401-429.

Verdouw, H., Van Echteld, C., Dekkers, E., 1978. Ammonia determination based on indophenol formation with sodium salicylate. Water Research 12, 399-402.

Villalobos, S.A., Hamm, J.T., Teh, S.J., Hinton, D.E., 2000. Thiobencarb-induced embryotoxicity in medaka (Oryzias latipes): stage-specific toxicity and the protective role of chorion. Aquatic Toxicology 48, 309-326.

Waring, G.T., Josephson, E., Maze-Foley, K., Rosel, P.E., 2009. US Atlantic and Gulf of Mexico marine mammal stock assessments 2009. NOAA Technical Memorandum NMFS-NE-213, pp. 528.

Weatherley, A., Gill, H., Rogers, S., 1979. Growth dynamics of muscle fibres, dry weight, and condition in relation to somatic growth rate in yearling rainbow trout (Salmo gairdneri). Canadian Journal of Zoology 57, 2385-2392.

White, H.K., Lyons, S.L., Harrison, S.J., Findley, D.M., Liu, Y., Kujawinski, E.B., 2014. Long-term persistence of dispersants following the Deepwater Horizon oil spill. Environmental Science & Technology Letters 1, 295-299.

Whitehead, A., Clark, B.W., Reid, N.M., Hahn, M.E., Nacci, D., 2017. When evolution is the solution to pollution: Key principles, and lessons from rapid repeated adaptation of killifish (Fundulus heteroclitus) populations. Evolutionary Applications 10, 762-783.

Whitehead, A., Dubansky, B., Bodinier, C., Garcia, T.I., Miles, S., Pilley, C., Raghunathan, V., Roach, J.L., Walker, N., Walter, R.B., 2012. Genomic and physiological footprint of the Deepwater Horizon oil spill on resident marsh fishes. Proceedings of the National Academy of Sciences 109, 20298-20302.

Whitehead, A., Pilcher, W., Champlin, D., Nacci, D., 2011. Common mechanism underlies repeated evolution of extreme pollution tolerance. Proceedings of the Royal Society B: Biological Sciences 279, 427-433.

Whitehead, A., Triant, D.A., Champlin, D., Nacci, D., 2010. Comparative transcriptomics implicates mechanisms of evolved pollution tolerance in a killifish population. Molecular Ecology 19, 5186-5203.

Williams, D.A., Brown, S.D., Crawford, D.L., 2008. Contemporary and historical influences on the genetic structure of the estuarine-dependent Gulf killifish Fundulus grandis. Marine Ecology Progress Series 373, 111-121.

Wills, L.P., Matson, C.W., Landon, C.D., Di Giulio, R.T., 2010. Characterization of the recalcitrant CYP1 phenotype found in Atlantic killifish (Fundulus heteroclitus) inhabiting a Superfund site on the Elizabeth River, VA. Aquatic Toxicology 99, 33-41.

Wills, L.P., Zhu, S., Willett, K.L., Di Giulio, R.T., 2009. Effect of CYP1A inhibition on the biotransformation of benzo [a] pyrene in two populations of Fundulus heteroclitus with different exposure histories. Aquatic Toxicology 92, 195-201.

Wilson, K.W., 1977. Acute toxicity of oil dispersants to marine fish larvae. Marine Biology 40, 65-74.

Wong, S., Lim, J., Dol, S., 2015. Crude oil emulsion: A review on formation, classification and stability of water-in-oil emulsions. Journal of Petroleum Science and Engineering 135, 498-504.

Wood, C.M., Laurent, P., 2003. Na+ versus Cl− transport in the intact killifish after rapid salinity transfer. Biochimica et Biophysica Acta (BBA)-Biomembranes 1618, 106-119.

Wuenschel, M.J., Jugovich, A.R., Hare, J.A., 2006. Estimating the energy density of fish: the importance of ontogeny. Transactions of the American Fisheries Society 135, 379-385.

Xiong, K.M., Peterson, R.E., Heideman, W., 2008. Aryl hydrocarbon receptor-mediated down-regulation of sox9b causes jaw malformation in zebrafish embryos. Molecular Pharmacology 74, 1544-1553.

Yelick, P.C., Schilling, T.F., 2002. Molecular dissection of craniofacial development using zebrafish. Critical Reviews in Oral Biology and Medicine 13, 308-322.

VITA

Charles A. Brown grew up Augusta, Georgia, exploring the creeks and woods behind his house. After graduating Evans High School in 2002, he attended Augusta State University. Charles graduated from Augusta State University in 2008 with a Bachelor of Science in biology and a minor in chemistry. Charles began his pursuit of his Master of Science degree in fisheries and aquaculture at Louisiana State University in the summer of 2008 under Dr. Christopher Green and graduated spring of 2011. After completion of his Masters of Science, he began working with Dr. Fernando Galvez in the Department of Biological Sciences at Louisiana State University. Charles plans to graduate Spring of 2020 to begin the next chapter of his life.